RECEIVED
-11- 1995
LIBRARY
STANDARDS DEVELOPMENT BRANCH OMOE
3693600009079
DE — MOE820403 GROUP

LARGE SUBSURFACE SEWAGE DISPOSAL SYSTEMS

Research Publication No. 89

April 1982

Ministry of the Environment
Ontario

The Honourable
Keith C. Norton, Q.C.,
Minister

Gérard J. M. Raymond
Deputy Minister

Copyright Provisions and Restrictions on Copying:

This Ontario Ministry of the Environment work is protected by Crown copyright (unless otherwise indicated), which is held by the Queen's Printer for Ontario. It may be reproduced for non-commercial purposes if credit is given and Crown copyright is acknowledged.

It may not be reproduced, in all or in part, for any commercial purpose except under a licence from the Queen's Printer for Ontario.

For information on reproducing Government of Ontario works, please contact ServiceOntario Publications at copyright@ontario.ca

LARGE SUBSURFACE

SEWAGE DISPOSAL SYSTEMS

by:

M. M. Ali, P. Eng., M.S.C.E.

and

H. T. Chan, Ph.D., P. Eng.

Applied Sciences Section
Pollution Control Branch
Research Publication No. 89

April 1982

Ministry of the Environment
135 St. Clair Avenue, West
Toronto, Ontario M4V 1P5

© 1982 Her Majesty the Queen in Right of Ontario

ABSTRACT

A field investigation was conducted to determine the impact of a large (0.54 ha) subsurface sewage disposal system on groundwater.

Groundwater mounding, influenced by the soil conditions, hydraulic loading rate, climatic and natural environmental factors, can be predicted by either of two mathematical models (Hantush and Sykes).

Nitrate, chloride, sodium, calcium, sulphate, hardness and conductivity were measured to study the magnitude and extent of the groundwater contamination. A modified version of the 'Langmuir Equation', was used to determine the adsorption capacity of the soil.

PROJECT STAFF

The following staff of the Applied Sciences Section of the Ministry of the Environment were instrumental in the soil testing, installation, and operation of the system:

H. R. Foggett

J. McGrachan

M. U. Roberts

F. C. Rodrigues

J. McGrahan, senior project technician, was responsible for data collection and for preparation of the charts and tables used in this report.

ACKNOWLEDGEMENT

N. G. Ehlert, Project Engineer, helped in the site selection during the initial stages of the project.

The staff members of the Hydrology and Monitoring Section of the Water Resources Branch assisted in the geophysical explorations.

The analysis of the water table mounding by the finite-element model was provided by Professor J. F. Sykes, Department of Civil Engineering, University of Waterloo.

TABLE OF CONTENTS

Table of Contents (cont'd.)

LIST OF TABLES

List of Tables (cont'd.)

LIST OF FIGURES

List of Figures (cont'd.)

List of Figures (cont'd.)

List of Figures (cont'd.)

List of Figures (cont'd.) Page No.

List of Figures (cont'd.)

LIST OF PLATES

INTRODUCTION

1.0 INTRODUCTION

Large leaching beds are being proposed with greater frequency by developers as a means of disposal for the effluent from package sewage treatment plants serving small subdivisions.

Large beds offer the economic benefits of scale as compared to individual septic tank - leaching bed installations, and the operational benefits of year-round use and low energy input compared to spray irrigation.

Possible limitations of effluent discharge into these beds may be imposed by excessive groundwater mounding causing surface flooding (2, 29) and extensive migration of contaminants, especially nitrates, into potable water supplies (2, 3, 12, 26). Because of this, there was reluctance on the part of regulatory agencies such as the Ministry of the Environment and Ministry of Health, to approve such systems. Since few field data were available on the performance of large leaching beds, there was a need to determine the environmental impact of subsurface sewage effluent disposal from these systems, under actual field conditions.

The purpose of this study was to determine the environmental impact of such large subsurface sewage effluent disposal systems from two main points of view.

1. To determine the effect of hydraulic loading on the level of groundwater under the leaching bed.

2. To determine the impact of subsurface sewage effluent disposal on the natural quality of the groundwater.

In order to achieve these objectives, a suitable site was selected adjacent to the Norwood Sewage Treatment Plant in Peterborough County, Ontario. A large leaching bed, 84 m x 64 m in size with 2,440 metres of trenched pipe was installed in the study area in

accordance with the local and provincial regulations. The leaching bed was dosed with effluent from the Norwood Extended Aeration Sewage Treatment Plant.

Fluctuations in the groundwater level and the movement of selected contaminants were monitored by 36 piezometers/single level sampling wells* and 6 multiple level sampling wells installed within and outside the perimeter of the leaching bed. Pertinent data were collected during a 146 week study period.

In the analyses of the collected data, two mathematical models ('Hantush' and 'Sykes') were investigated for predicting the mounding of the groundwater under the leaching bed. A modified version of the 'Langmuir Equation' was used to determine the adsorption capacity of the soil. Contaminant concentration plumes were developed to study the magnitude and extent of the groundwater contamination.

After a description of the selected site and effluent disposal system, the analyses results of the collected data, based on the study objectives, are grouped and presented in two parts:

- Groundwater Mounding;
- Groundwater Contamination.

The discussion, summary and conclusions on each of the above parts are then dealt with separately, followed by the recommendations.

From this extensive and relatively long-term groundwater monitoring program, valuable field data were obtained which provided a good insight on the impact of a large subsurface sewage disposal system on a groundwater regime.

---

* The terms piezometer and sampling well are used interchangeably in this report.

SITE AND DISPOSAL SYSTEM

2.0 SITE AND DISPOSAL SYSTEM

2.1 Site Selection

Seven sites adjacent to existing sewage treatment plants were evaluated. The location adjoining the Norwood Sewage Treatment Plant was selected on the basis of the availability of an adequate area of land for the construction of the disposal system, the quality of the plant effluent, preliminary soil conditions, topography, year-round accessibility to the site and distance from the Applied Sciences Laboratories of the Ministry of the Environment.

2.2 Site Location

Norwood is situated on the Trans-Canada Highway, central Ontario route, twenty-seven kilometres east of the City of Peterborough and ten kilometres north of the Town of Hastings, at the junction of Highway 7 and Highway 45.

The project site was located south of the Sewage Treatment Plant in the southwest quadrant of the Town of Norwood and is shown in Figure 1.

The Norwood Sewage Treatment Plant uses the extended aeration process (oxidation ditch) and is equipped with facility for phosphorus removal. The design capacity of the plant is 730,000 L/d, with an effluent low in Biochemical Oxygen Demand and Suspended Solids and high in Nitrates, typical of a small package plant. The treated effluent is discharged into the Ouse River, which flows through the Town of Norwood on the northeast side of the plant and enters the Trent Canal System at the north end of Rice Lake.

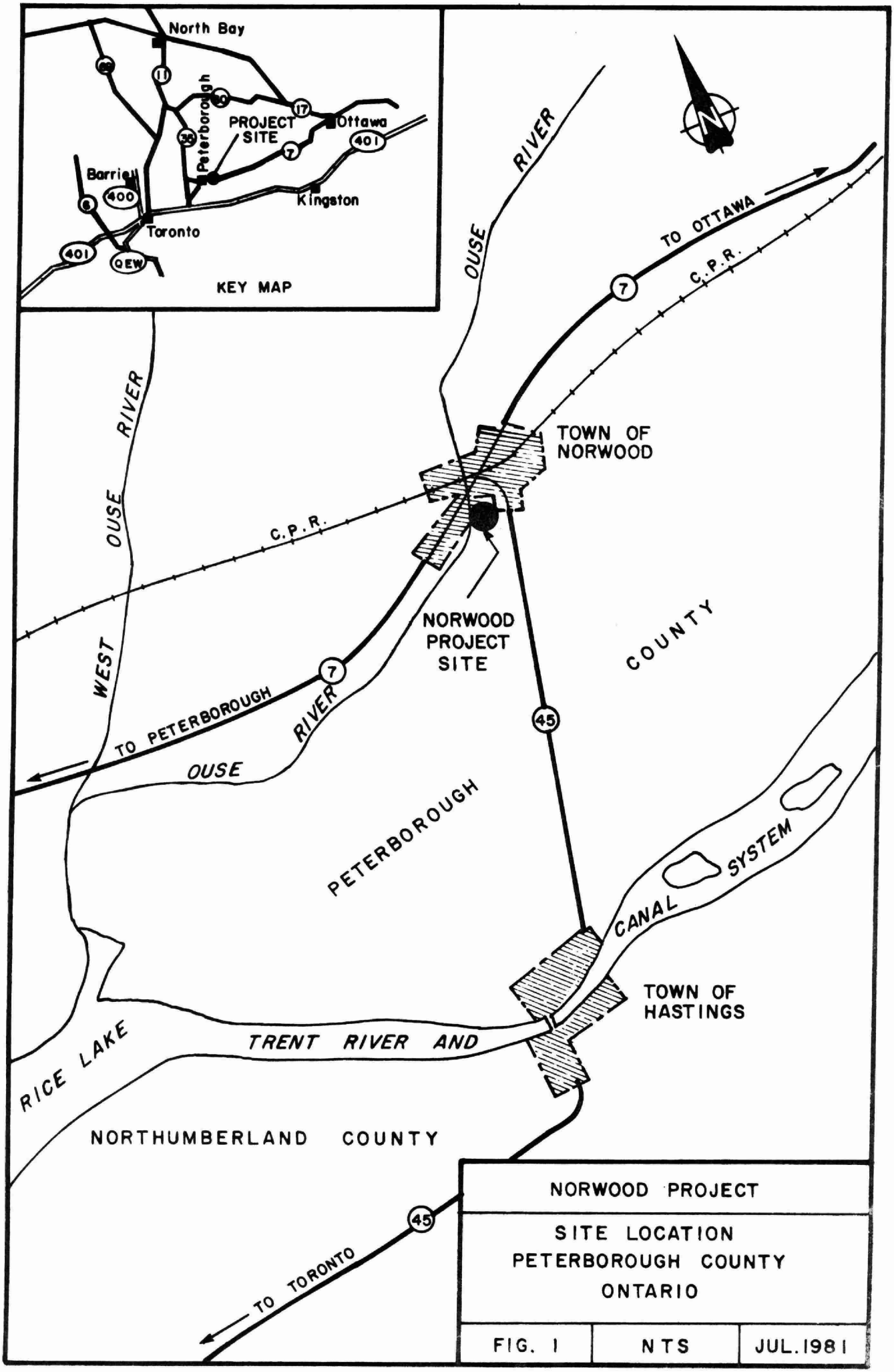
North Bay
Peterborough
PROJECT SITE
Ottawa
Barrie
Toronto
Kingston
KEY MAP
OUSE RIVER
TO OTTAWA
C.P.R.
TOWN OF NORWOOD
NORWOOD PROJECT SITE
WEST OUSE RIVER
TO PETERBOROUGH
OUSE RIVER
PETERBOROUGH COUNTY
CANAL SYSTEM
TOWN OF HASTINGS
TRENT RIVER AND
RICE LAKE
NORTHUMBERLAND COUNTY
TO TORONTO
NORWOOD PROJECT
SITE LOCATION
PETERBOROUGH COUNTY
ONTARIO
FIG. 1
NTS
JUL. 1981

2.3 Construction of the Disposal System

The sewage effluent disposal system used in this study, comprised mainly :

(a) A distribution box to give equal flow to all sections of the leaching bed.

(b) Trenched perforated pipe, 2,440 metres in total length, for spreading sewage effluent into the soil.

(c) A storage tank and a double loop syphon system capable of feeding a known quantity of sewage effluent to the leaching bed.

2.3.1 Distribution Box

The distribution box was constructed in situ with 'ready-mix' concrete and was located in the centre of the proposed leaching bed at the appropriate elevation. Figure A on plate I shows the inside arrangement of the constructed distribution box. The position and design of the distribution box is shown in Figures 2 and 3.

The box was 1.2 m long, 1.07 m wide and 1.2 m deep. The walls of the box were 150 mm thick and there was provision for four holes on two opposite sides for eight 100 mm diameter headers placed lower than and at right angle to the axis of 150 mm diameter main feed-pipe.

A steel baffle plate was secured close to the feed inlet to decrease any turbulence and surge during the loading period. Eight 90^{o} elbows were attached to the header pipes inside the box and cut to the same elevation to ensure equal distribution of feed for all the headers. Each header provided feed for ten rows of tiles in each of the eight bays of the leaching bed.

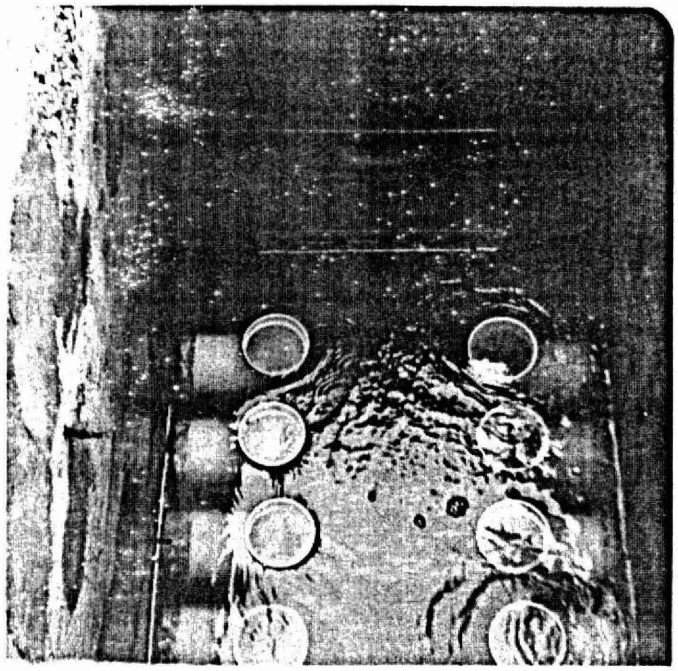

A. DISTRIBUTION BOX CONSTRUCTION

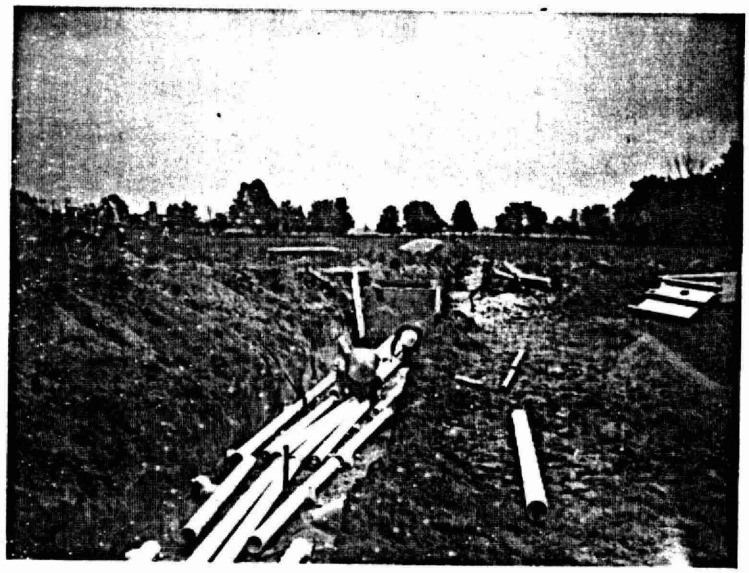

B. TRENCH CONSTRUCTION

PLATE 1

2.3.2 Leaching Bed

The leaching bed area was 84 m long and 64 m wide and was divided into eight equal bays: A, B, C, D, E, F, G, and H. Each bay was 19.2 m long, 30.5 m wide and comprised of ten rows 100 mm diameter perforated PVC pipes, 30.5 m in length laid parallel 2.1 m apart in 0.45 m wide trenches, about 0.15 m above the bottom of the trench.

Each trench bottom was filled with crushed stone or gravel around the pipe and backfilled with top soil in accordance with the existing Regulation 229 of the Ministry of the Environment. Figure B in plate I shows the site during the construction phase. The layout and design of the leaching bed is shown in Figure 2.

The ground elevation ranged from 30.1 m to 29.3 m (Figure 4) giving a surface slope of 0.8 m over the length of the leaching bed. Because of this slope, the trenches were 0.51 m deep at the north end and 1.36 m deep at the south end of the bed. Each bay of tiles was fed by a 100 mm diameter solid pipe from the distribution box. The headers receiving feed in all the bays were kept level for an equal distribution of effluent.

The crown elevation of the perforated pipes varied throughout the bed from 29.07 m to 28.80 m. The pipes were provided with a 0.10 m slope along their 30.5 m length for gravity flow. The end of each row was capped and a 13 mm diameter hole was drilled in the centre of the cap. A plastic 90° elbow was cemented into the hole and a length of tygon tubing from the elbow was extended above ground level, as a vent, to prevent the development of airlock during the loading cycle.

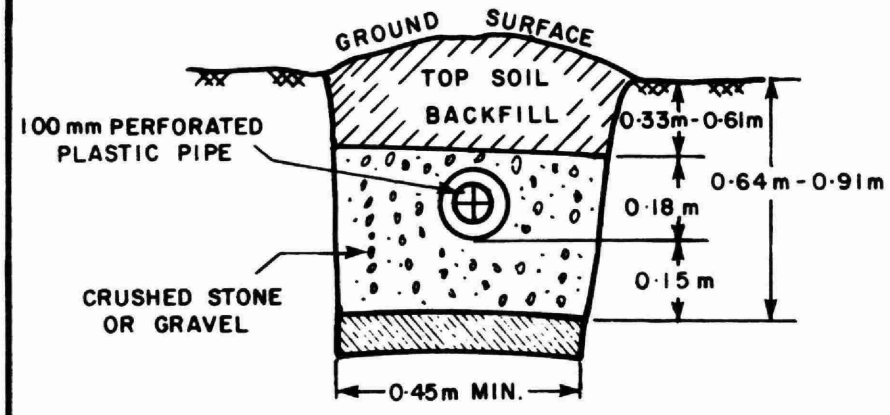

ABSORPTION TRENCH CROSS SECTION

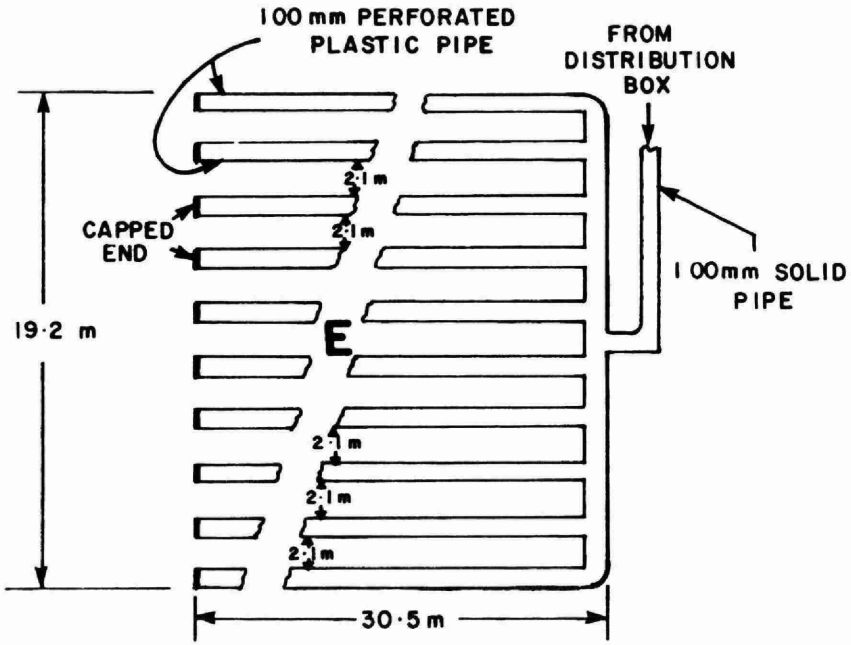

LAYOUT OF BED 'E'

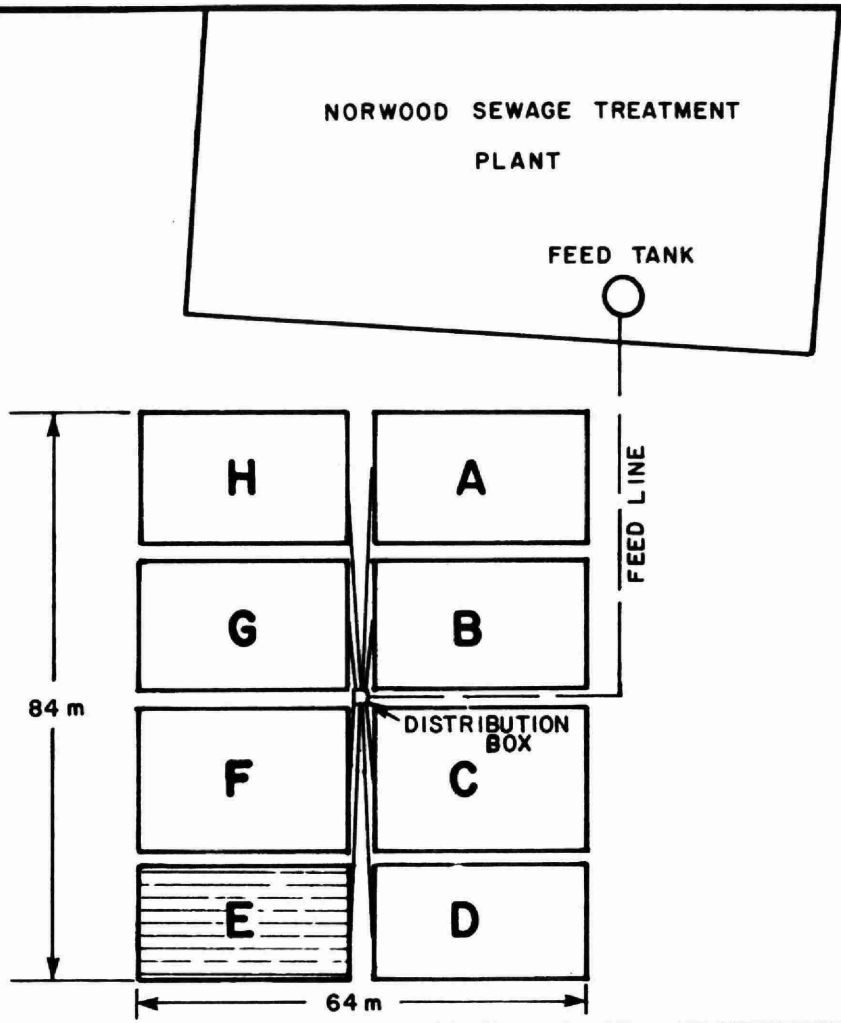

PLAN

NORWOOD PROJECT		
LAYOUT AND DESIGN OF LEACHING BED		
FIG. 2	NTS	JUL. 1981

2.3.3 Feed Tank and Syphon System

The feed tank was an insulated, fiberglass, cylindrical shaped tank, 6.1 m in height, 3.2 m in diameter and had a capacity of 45,000 L. It was positioned inside the Sewage Treatment Plant boundary, over a levelled sand pad, close to the final clarifier. A submersible pump rated at 205 L/min was connected to a 24 hour timer, with 15 minute increments and used to fill the tank. It took about 210 minutes for the submersible pump to fill the feed tank to the point when the syphon was activated. Figure A in plate II shows the feed tank at the time of installation. Figure 3 shows the layout and design of the feed and distribution system.

In order to feed the large leaching bed, so that 75% of the volume of the tiles are filled with effluent (equivalent to about 15,000 L), a special system was developed which comprised a double loop syphon of 150 mm diameter plastic pipe utilizing an initial 5.5 m head in the feed tank. The syphon was activated when the liquid in the feed tank reached a level of 0.61 m below the top of the tank.

The pipe carrying the discharge from the tank to the distribution box was buried in a trench and had a slope of 0.10 m per 30.5 m length, for gravity flow. The flow during the first minute was approximately 2,400 L/min and decreased to 1,350 L/min after 20 minutes. The tank drained 40,900 L in 30 minutes. The submersible pump remained activated for 10 minutes after the feed cycle started to ensure complete working of the system.

2.4 Site Exploration

A detailed exploration of the test site was undertaken including: (i) the determination of the soil types and stratigraphy, (ii) the flow characteristics of the natural soil deposit.

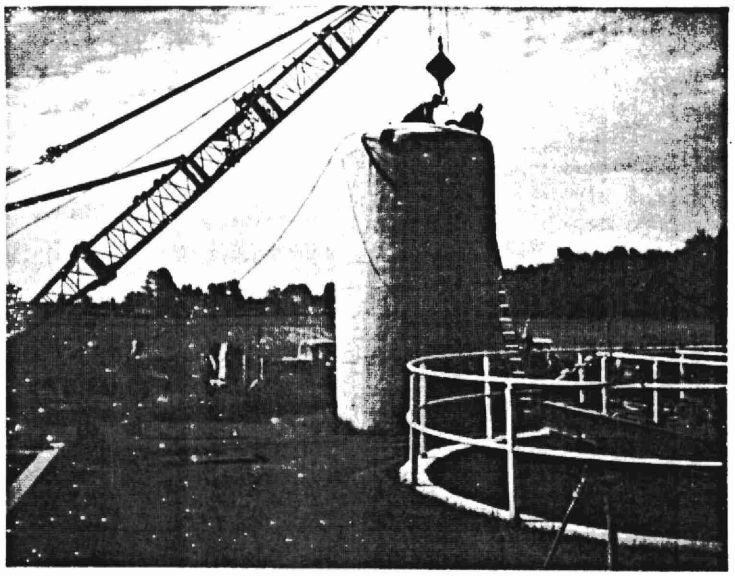

A. FEED TANK INSTALLATION

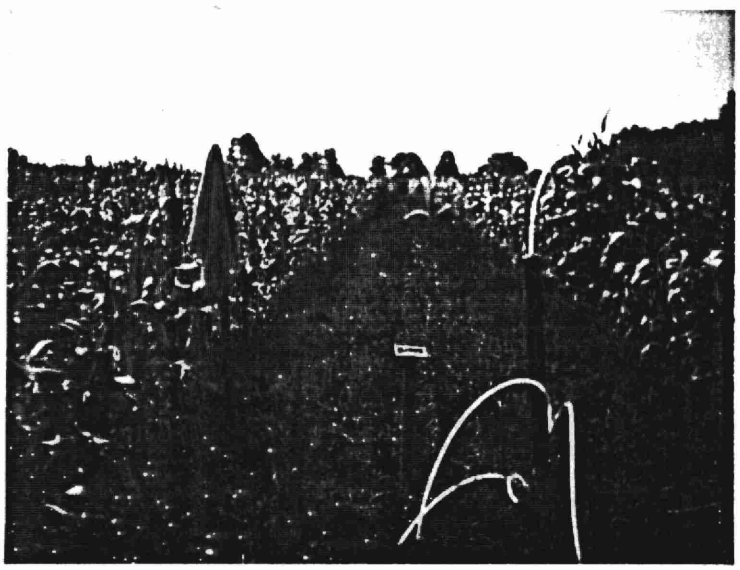

B. SAMPLE POINT INSTALLATION

PLATE II

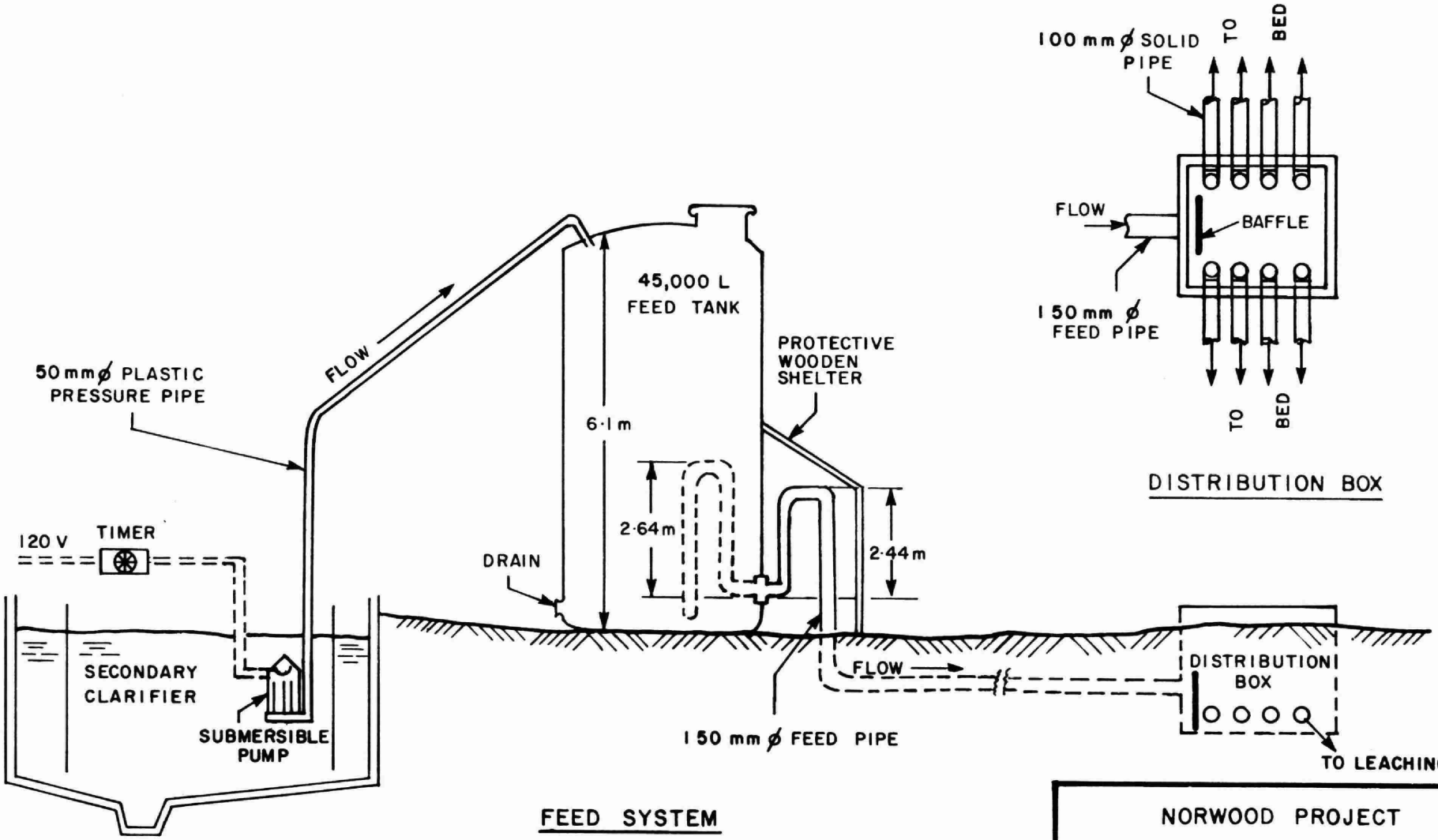

FEED SYSTEM

DISTRIBUTION BOX

NORWOOD PROJECT		
FEED AND DISTRIBUTION SYSTEM		
FIG. 3	NTS	JUL. 1981

2.4.1 Percolation Test

The percolation tests ('perc tests') were performed at one metre depth according to the Ministry of the Environment standard procedure. The test results are presented in Table 1 and the test locations are shown in Figure 4.

TABLE 1

PERCOLATION TEST RESULTS

Test Location	Percolation Time (min/cm)
1	0.17
2	0.23
3	0.25
4	0.21
Average	0.22

The percolation or 't' time varied from 0.17 to 0.25 min/cm which indicates a very permeable sandy soil near the ground surface. However, results obtained from other soil tests at the site showed that the soil became less permeable with increasing depth. It is reasonable to expect a larger 't' time in the soil below the 1 m depth.

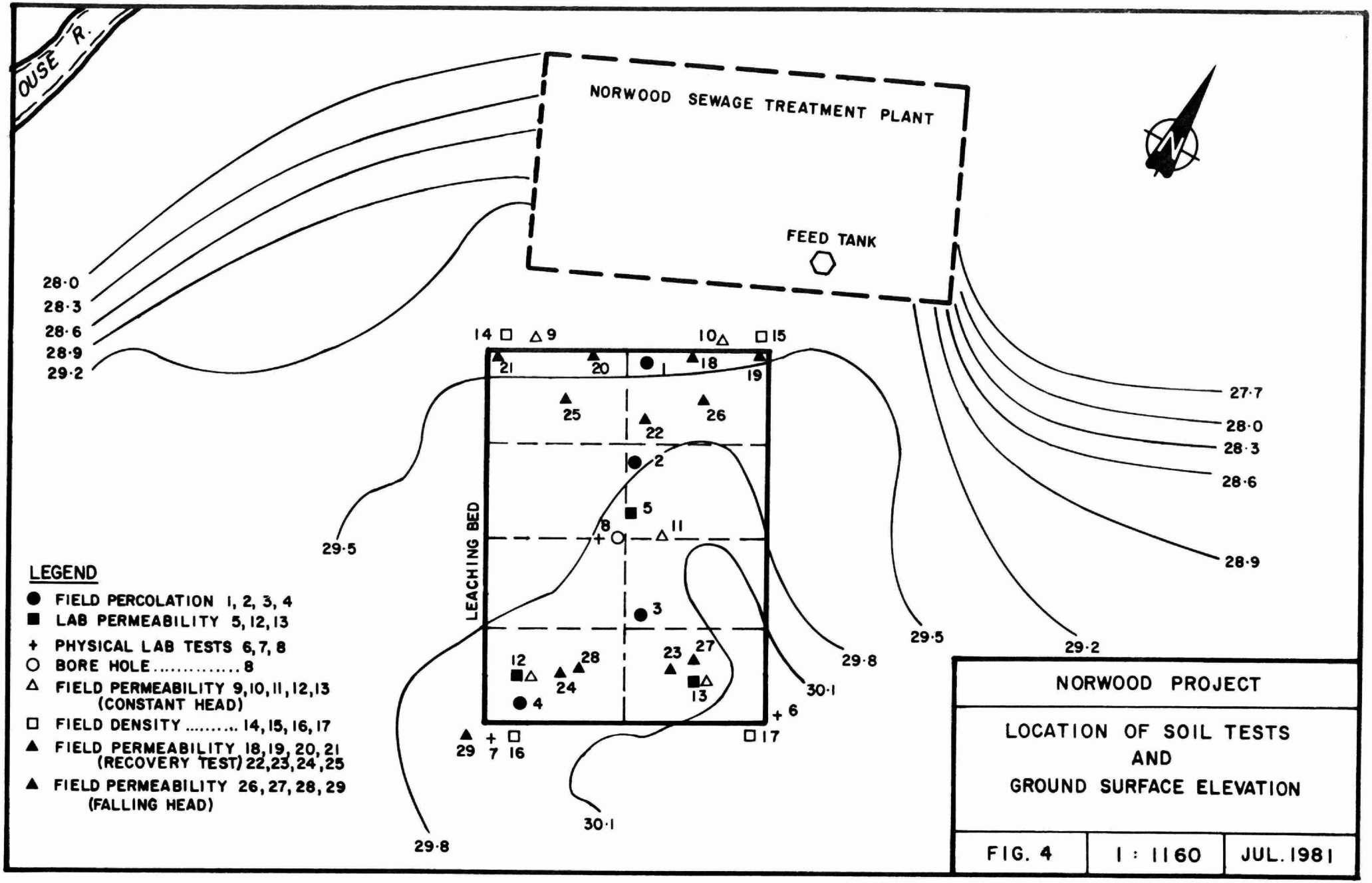

NORWOOD PROJECT

LOCATION OF SOIL TESTS AND GROUND SURFACE ELEVATION

FIG. 4	1 : 1160	JUL. 1981

2.4.2 Soil Classification and Identification

A number of boreholes were made at the site to recover soil samples for identification and testing. In addition, the soil stratigraphy was determined on the basis of the information obtained from the boreholes. In Figure 4, the borehole locations and ground surface elevation contours are indicated. In the laboratory, grain size distribution tests were done for most of the soil samples and the Atterberg limits (the liquid and plastic limits) were performed on the slightly cohesive and cohesive soil samples.

The classification of the soil samples, the grain size test data, the liquid limit and plastic limit results are summarized in Table 2.

2.4.3 Geophysical Exploration and Soil Stratigraphy

The depth of the bedrock from the ground surface was established by resistivity and seismic techniques, which was undertaken by the Hydrology and Monitoring Section of the Ministry of the Environment. The results are shown in Figure 5. The geophysical test results indicated that the bedrock sloped downward approximately in a northwesterly direction toward the Ouse River. The depth to bedrock under the leaching bed ranged from about 9 m in the southeast corner of the bed to 15 m in the northwest corner of the bed and then to about 18 m near the river.

Based on the information obtained during the field investigation from the boreholes, the laboratory test data and the results of the geophysical exploration, a soil stratigraphy along the centre line of the leaching bed, in the north to south direction, is presented in Figure 6.

TABLE 2

GRAIN SIZE DISTRIBUTION AND CLASSIFICATION OF SOILS

Test Location	Elevation (m)	Sand %	Silt %	Clay %	Coefficient of Uniformity (Cu)	Liquid Limit (Wl)	Plastic Limit (Wp)	Plasticity Index (Ip)	Soil Type *
5	27.1 - 28.8	41	54	5	9.25	-	-	-	Silty Sand
6	26.7 - 27.0	7	84	9	8.64	24.6	20.5	4.1	Silt
7	26.7 - 27.0	3	79	18	4.67	32.5	18.8	13.7	Clayey Silt
8	26.8	5	86	9	8.90	-	-	-	Silt
	25.3	25	75	-	6.40	-	-	-	Sandy Silt
	23.8	25	75	-	-	23.6	19.7	3.9	Sandy Silt
	20.7	-	85	15	-	24.1	20.1	4.0	Silt
Northeast	27.6	91	8	0	2.31	-	-	-	Silty Sand
Corner	26.7	-	-	-	-	-	-	-	" "
	23.0	30	68	2	4.33	-	-	-	Sandy Silt
Northwest	27.5	-	-	-	-	-	-	-	Silty Sand
Corner	26.6	-	-	-	-	-	-	-	" "
	25.6	-	-	-	-	-	-	-	" "
	24.7	66	34	0	2.20	-	-	-	Fine Silty Sand
	23.8	-	-	-	-	-	-	-	" " "
Southwest	28.3	23	70	7	11.14	-	-	-	Sandy Silt
Corner									(slightly cohesive)
	27.4	0	92	8	7.70	-	-	-	Clayey Silt
	26.4	-	-	-	-	-	-	-	Silt (slightly cohesive)
	25.5	0	85	15	8.85	-	-	-	Clayey Silt
	24.6	(Hole terminated, refusal)			-	-	-	-	Silt, Sand and Gravel
Southeast	28.3	-	-	-	-	-	-	-	Silt (slightly cohesive)
corner	27.4	52	62	5	13.3	-	-	-	Sandy Silt
									(slightly cohesive)
	26.4	-	-	-	-	-	-	-	" "
	25.8	(Hole terminated, refusal)			-	-	-	-	Silt with Sand and Gravel
50 m South	28.6	-	-	-	-	-	-	-	Silt (slightly cohesive)
of Bed	27.7	-	-	-	-	-	-	-	" " "
	26.7	(Hole terminated, refusal)			-	-	-	-	Silt (cohesive), Sand and Gravel

* According to the Unified Soil Classification System.

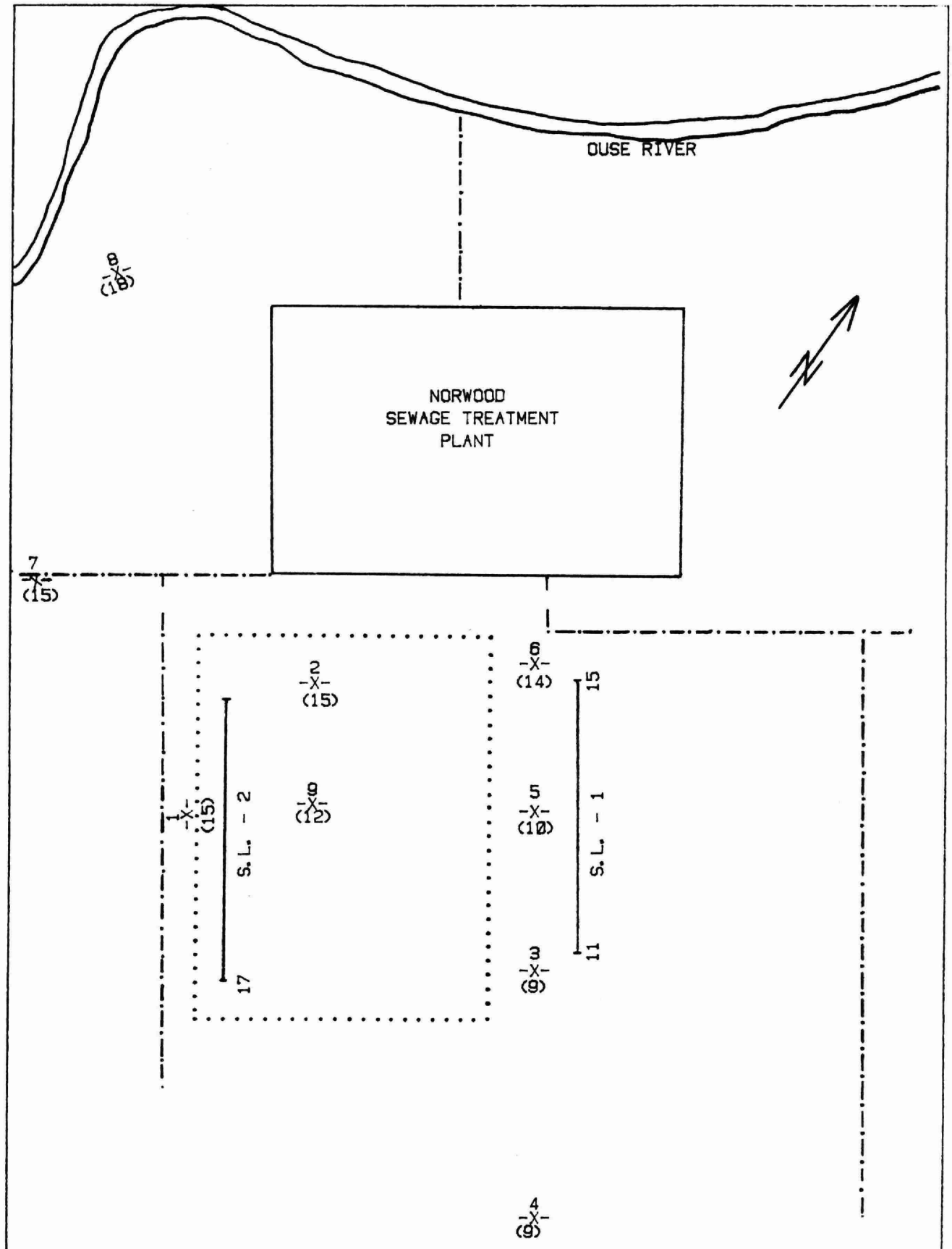

LEGEND

8 (15) — VERTICAL ELECTRIC SOUNDING; DEPTH TO BEDROCK IN METRES

FENCE LINE

SEISMIC LINE

NORWOOD

DEPTH OF BEDROCK BY GEOPHYSICAL SURVEY

FIG. 5	1 : 1200	JUL. 1981

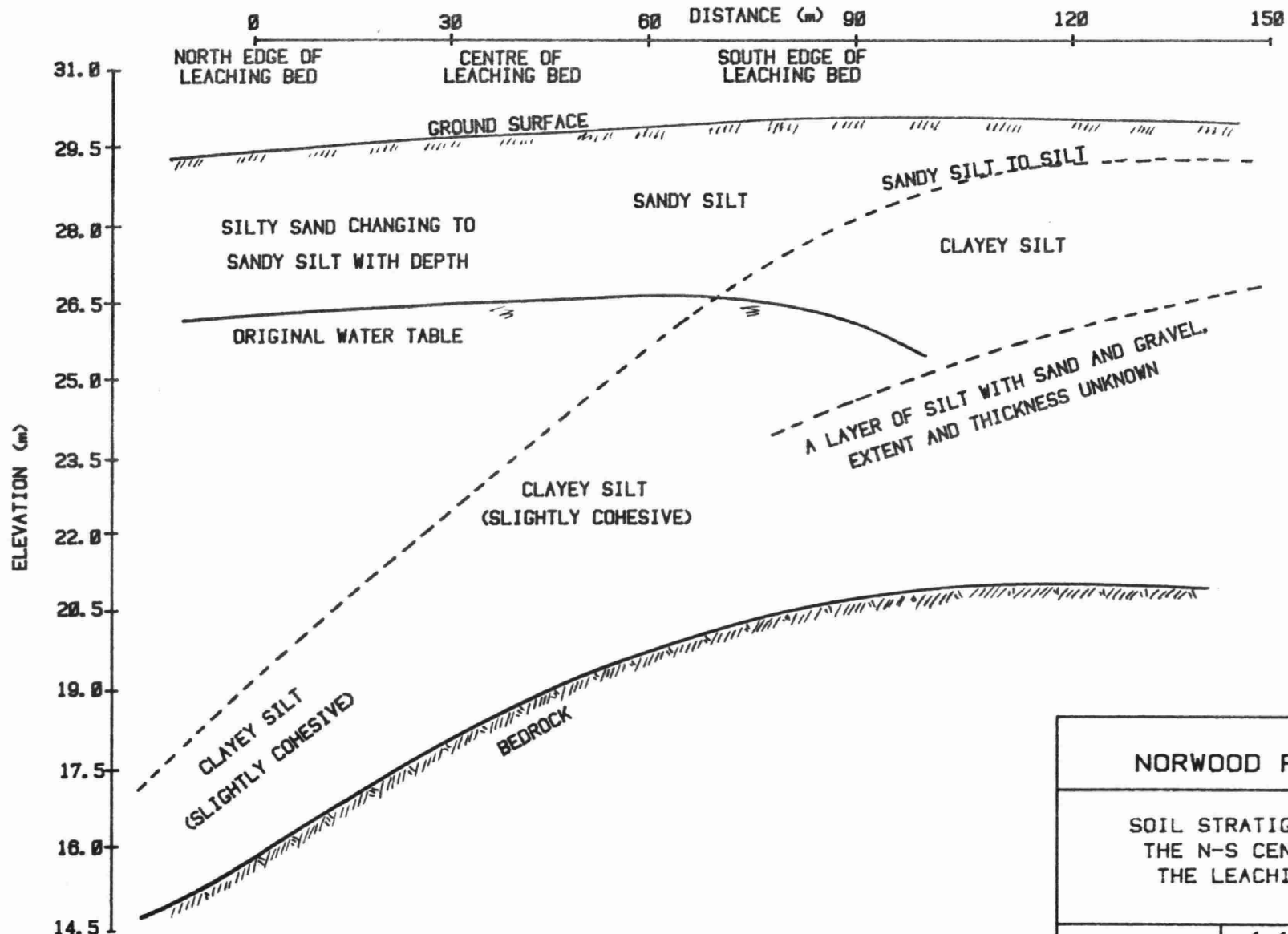

NORWOOD PROJECT		
SOIL STRATIGRAPHY THROUGH THE N-S CENTRE LINE OF THE LEACHING BED		
FIG. 6	1:117 V 1:890 H	JULY 1981

2.4.4 Permeability Tests

The permeability (hydraulic conductivity)* of the soil was an important factor for this study as it affects the groundwater mounding and the movement of contaminants in the groundwater. Three methods were used to measure the permeability of the soils.

(1) Laboratory 'Constant-Head' Permeability Tests

(a) For sandy soil samples, the testing technique can be found in many soil mechanics text books (23). The collected soil sample was disturbed and was compacted in a small container to a density similar to the in situ value.

(b) For the clayey soil samples, the permeability was measured in a 'constant-head' permeameter designed by Chan and Kenney (11). 'Undisturbed' Shelby tube soil samples were used for the tests. The test results are presented in Table 3. It should be pointed out that the laboratory permeability values were measured on small soil samples, and generally, the laboratory values would be smaller than the actual field values for a large volume of soil.

(2) Field 'Constant-Head' Permeability Tests

The field permeability apparatus used at the site consisted of constant pressure and flow measuring units. The design of the apparatus was similar to that described by Wilkinson (37). The constant water pressure was maintained by a water reservoir connected to the plastic tube of a piezometer which had been driven into the soil. The type used for this permeability test was the Geonor Piezometer. Because the dimensions of the porous section of the piezometer were small (length 0.31 m, diameter 25 mm), the permeability of only a small volume of the soil could be measured.

---

* The terms 'permeability' and 'hydraulic conductivity' are used interchangeably in this report.

TABLE 3

SOIL PERMEABILITY TEST RESULTS

Test Location	Elevation	Lab. Permeability (cm/s)
5	28.8 - 27.1	1.6×10^{-4}
12	25.5	6.0×10^{-6}
13	26.4	3.0×10^{-6}
	25.8	0.3×10^{-6}

Test Location	Elevation (m)	Field Permeability (cm/s) ('Constant-Head' Test)
9	27.5	6.6×10^{-5}
	26.6	3.6×10^{-5}
	24.7	2.8×10^{-5}
10	27.6	5.1×10^{-5}
	26.7	3.4×10^{-5}
	24.9	2.1×10^{-5}
11	28.0	2.0×10^{-5}
	27.0	2.0×10^{-5}
	25.8	0.8×10^{-6}
12	27.3	4.1×10^{-5}
	26.4	1.0×10^{-5}
	25.2	1.7×10^{-4}
13	28.3	2.3×10^{-5}
	27.3	5.0×10^{-5}

Test Location	Elevation (m)	Field Permeability (cm/s) ('Falling Head' Test)	('Recovery' Test)
18	25.6	1.2×10^{-4}	0.6×10^{-4}
19	25.6	4.5×10^{-4}	12.0×10^{-4}
20	24.9	2.5×10^{-4}	7.0×10^{-4}
21	24.7	3.7×10^{-4}	8.0×10^{-4}
22	24.9	1.3×10^{-4}	3.1×10^{-4}
23	25.3	1.2×10^{-4}	0.1×10^{-4}
24	26.1	1.5×10^{-4}	0.4×10^{-4}
25	25.6	0.7×10^{-4}	0.1×10^{-4}
26	24.8	2.8×10^{-4}	-
27	25.5	-	0.2×10^{-4}
28	25.4	1.2×10^{-4}	2.5×10^{-4}
29	25.6	1.0×10^{-4}	0.5×10^{-4}

(3) Field Variable-Head Permeability Tests

The permeability tests were done in piezometers which were also used for the regular groundwater level monitoring and sampling.

Two methods were used to conduct the tests. In the 'falling-head' test, water was put in the pipe of a piezometer and the rate of the lowering of the water level was recorded. The field permeability of the soil can be calculated by the formula suggested by Hvorslev (19). In the 'recovery' (or infiltration) test, water was taken out from the pipe of a piezometer, and the rate of the rise of the water level in the pipe was measured. The equation suggested by Schmid (30) was used to calculate the field permeability. Results obtained in a number of piezometers are tabulated in Table 3.

2.4.5 Soil Porosity

The porosity of the soil was determined at locations 14 to 17 (Figure 4), by measuring the bulk density of the soil and the soil water content. At these locations, the bulk density of the soil was measured by the in situ 'sand cone' method in a small excavation, 1 m below the ground surface. The porosity of the soil could be computed by assuming the specific gravity of the soil particles being equal to 2.67.

At several other locations, the bulk density and the water content of the soil samples taken with Shelby tubes were measured and the porosity of the soil could then be calculated.

Table 4 summarizes the test results, which were later used to estimate the specific yield of the soil at the site.

TABLE 4

SOIL DENSITY AND POROSITY TEST RESULTS

Test Location	Elevation (m)	Soil Type	Water Content %	Dry Density (g/cm^3)	% Saturation	Porosity
14	28.33	Silty Sand	12.0	1.52	42	0.42
15	28.50	" "	6.9	1.56	26	0.42
16	29.13	" "	8.4	1.78	45	0.32
17	29.00	" "	9.8	1.63	41	0.40
24	28.06	Silt	22.8	1.48	76	0.44
24	28.06	"	20.9	1.65	91	0.38
24	27.56	"	22.1	1.66	97	0.37
24	27.56	"	21.8	1.65	93	0.38
24	26.56	"	27.6	1.52	100	0.40
25	27.54	Silty Sand	11.8	1.67	40	0.44
25	27.54	" "	7.5	1.72	30	0.40
25	25.74	Sandy Silt	18.7	1.82	100	0.34
25	25.74	" "	18.2	1.85	100	0.34

2.5 Groundwater Monitoring System

In order to monitor the level of the water table and sub-surface movement of the contaminants, a network of piezometers/sampling wells was installed inside and around the perimeter of the leaching bed. The location and arrangement of the wells were based on the direction of the groundwater flow and anticipated movement of the groundwater contaminants. Two types of wells were used which are shown in Figure 7.

Type 'A' wells comprised a wellpoint with three rows of 13 mm diameter holes down its 0.45 m in length, wrapped with No. 60 mesh screen and had a tapered end. Galvanized metal pipe sections, 30 mm in diameter and 1.5 m long were joined to the well points by galvanized couplings to the desired length for the intake of groundwater.

Type 'B' wells were provided with sample intakes at three levels and comprised 0.6 m long, 76 mm diameter PVC pipe sections, joined together with plastic couplings. No. 14 rubber stoppers were used to separate the sections and provide a watertight seal from each other. An end cap sealed the bottom section of the well. A number of 10 mm diamter holes were drilled into the sides of each section for a length of 0.2 m and then covered by No. 270 nylon mesh. A 10 mm diameter polyethylene sampling tube was inserted through the side wall at the lower end of the section and a 10 mm diameter polyethylene vent tube was inserted at the upper end of each sealed section. The top section was extended above the ground surface with a sample tube running down the centre of the pipe, and being open to the atmosphere did not need a vent tube. Figure 'B' in plate II shows an installation of Type 'A' (left) and Type 'B' (right) sampling wells.

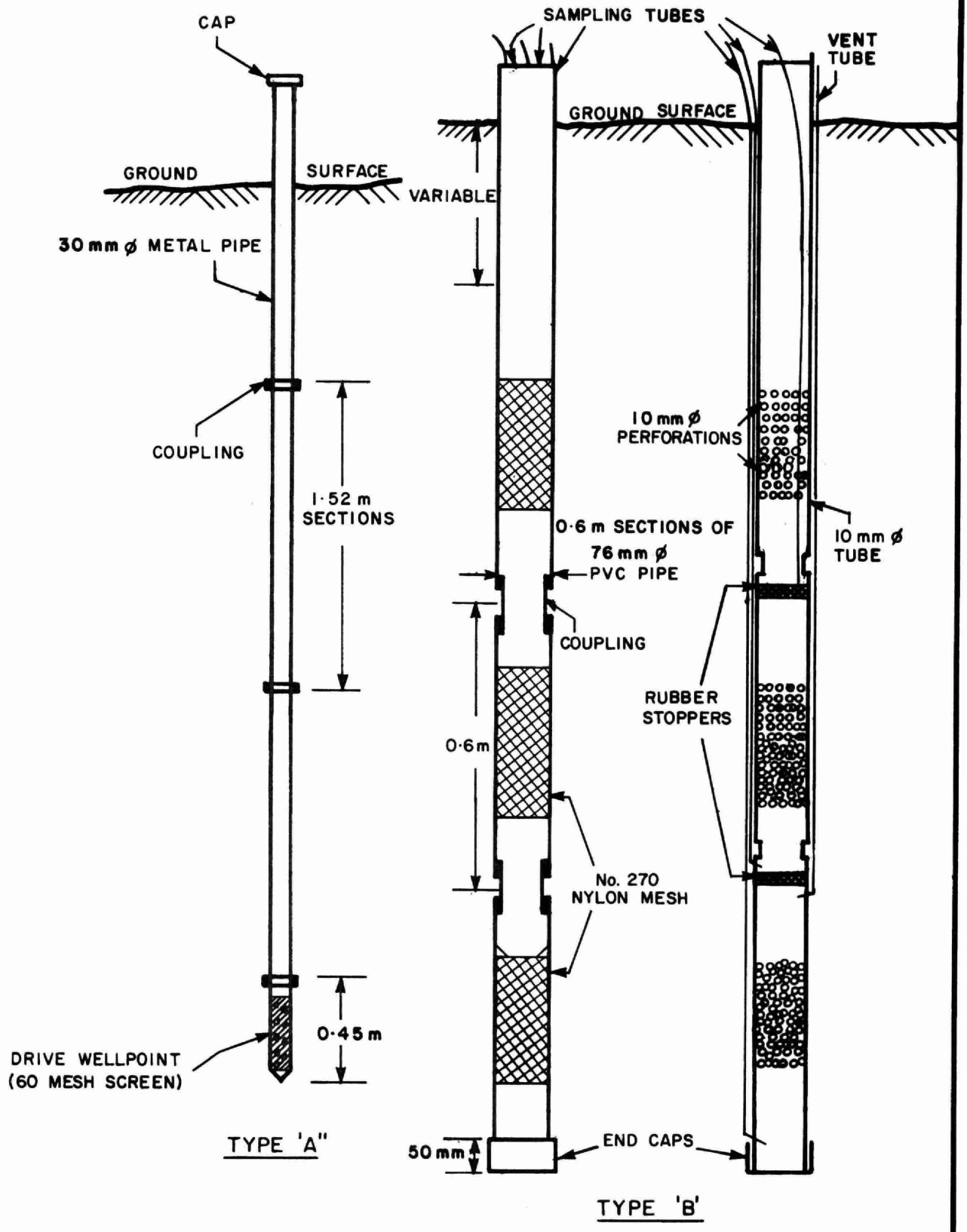

NORWOOD PROJECT		
TYPES OF SAMPLING WELLS		
FIG. 7	NTS	JUL. 1981

Both types of wells were installed in auger holes which were refilled with the native soil. Table 5 shows elevation at the middle of the sample intake for the single and multi-level piezometers/ sampling wells, in relation to the ground surface and lowest initial water table.

Initially, in June 1976, there were eight wells installed within and six wells installed around the perimeter of the leaching bed. Later, a network of wells was established on the east side, 10 to 60 metres away from the bed. By December 1976, three rows at 30, 60 and 90 metres were added on the west side of the bed. In May 1977, the series of wells in the east side had to be removed at the request of the land-owner. On May 17, 1977, six multiple level sampling wells (Type 'B') were installed adjacent to the existing wells in the bays A, B, D, E, F, and G, inside the perimeter of the leaching bed. A total number of 36 Type 'A' piezometers/wells and 6 Type 'B' piezometers/wells were finally used to monitor the level of groundwater table and contaminants movement. The network of piezometers and sampling wells is shown in Figure 8.

Water from the wells was aspirated into one-litre glass bottles, using a hand operated vacuum pump. A battery operated depth probe was used to monitor the depth of groundwater table in the wells.

A weekly monitoring and sampling program from July 13 to September 28, 1976, established the background data for the project. Fluctuations of the water table before subsurface disposal were plotted from this background information. The background chemical concentration in the groundwater was also established by these data.

TABLE 5

ELEVATIONS OF PIEZOMETER/SAMPLING WELL INTAKES

Piezometer Location	Ground Surface (m)	Initial Water Table (m)	Mid-Point Intake Elevation of Single Level Piezometer/Well (m)
1	29.13	26.21	25.78
2	29.46	26.10	25.75
3	29.59	26.00	26.00
4	29.71	26.04	25.91
5	29.15	26.30	25.74
6	28.88	26.27	25.19
7	29.19	26.31	25.62
8	28.17	25.76	24.41
9	29.52	25.83	25.78
10	29.71	26.34	25.88
11	29.66	26.48	25.97
12	29.42	26.48	25.77
13	29.30	26.40	25.61
14	28.95	26.02	25.23
15	27.77	25.44	24.45
16	29.90	26.00	26.00
17	30.09	25.71	25.64
18	29.70	26.43	26.05
19	29.29	26.35	25.18
20	29.26	26.39	25.60
21	29.21	26.24	25.55
22	28.00	25.84	24.75
23	30.06	26.42	25.36
24	29.79	26.55	25.15
25	29.64	26.41	24.88
26	29.54	26.39	24.79
27	30.14	25.55	25.64
28	30.08	26.44	25.49
29	30.14	26.50	25.45
30	29,98	26.46	25.30
31	29.60	26.37	24.80
32	29.44	26.43	25.11
33	29.50	26.49	25.85
34	29.41	26.44	25.80
35	29.11	26.42	26.06
36	27.66	26.33	25.33

MID-POINT INTAKE ELEVATIONS OF MULTI-LEVEL PIEZOMETER/SAMPLING WELL

	Ground Surface	Level 1	Level 2	Level 3
A	29.55	26.81	26.18	25.61
B	29.92	26.82	26.26	25.65
C	30.07	27.02	26.41	**
D	30.04	26.99	26.36	25.77
E	30.08	26.93	26.30	25.74
F	29.85	28.30	27.69	27.11
G	29.63	27.62	27.04	26.43

2.6 Initial Water Table

The elevation of the water table, before subsurface disposal, was established by measuring the depth of the groundwater level in the piezometers from the ground surface. The water table contours are shown in Figure 8.

These contours indicate the presence of a slight water table mounding below the leaching bed at the beginning of the field testing program. On the south side of the bed, a slight depression of the water table was noted. This anomaly could have been due to the presence of a layer of sand, gravel and clayey silt mixture at the piezometer tip elevation, and a downward flow of groundwater at this location.

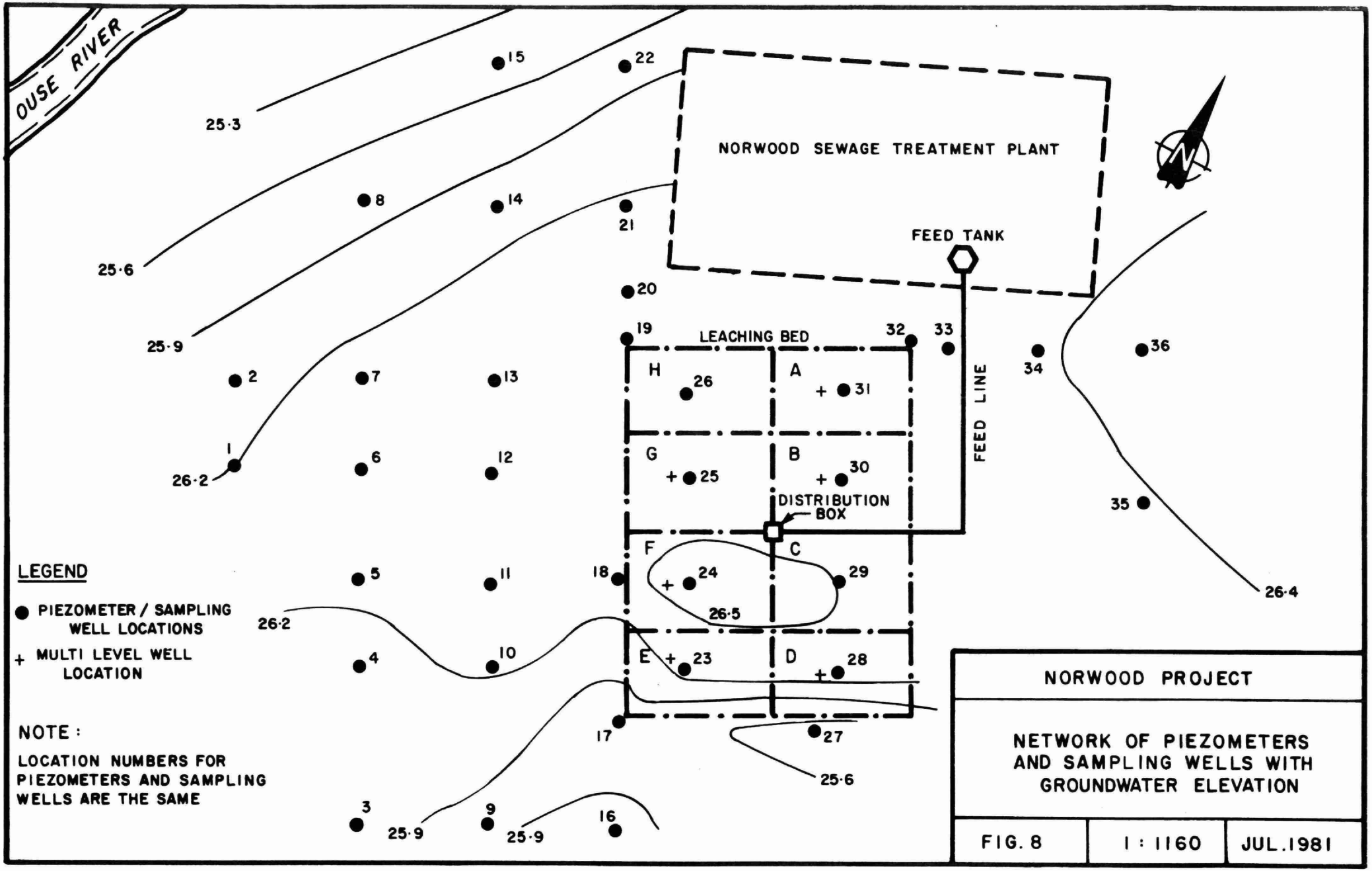
OUSE RIVER
NORWOOD SEWAGE TREATMENT PLANT
FEED TANK
FEED LINE
LEACHING BED
DISTRIBUTION BOX
H
A
G
B
F
C
E
D
25·3
25·6
25·9
26·2
26·5
26·4
LEGEND
PIEZOMETER / SAMPLING WELL LOCATIONS
MULTI LEVEL WELL LOCATION
NOTE :
LOCATION NUMBERS FOR PIEZOMETERS AND SAMPLING WELLS ARE THE SAME
NORWOOD PROJECT
NETWORK OF PIEZOMETERS AND SAMPLING WELLS WITH GROUNDWATER ELEVATION
FIG. 8
1 : 1160
JUL. 1981

GROUNDWATER MOUNDING

3.0 GROUNDWATER MOUNDING

3.1 Precipitation, Evapotranspiration and Water Table Fluctuation

Groundwater levels fluctuate naturally from season to season within the yearly climatic cycle. The geographical location, the hydrogeology of the site, climatological influences such as, precipitation and evapotranspiration all combine to determine the maximum height of the water table. Disposal of sewage effluent into the soil through a leaching bed is an additional source of influence.

3.1.1 Precipitation

Precipitation falls as rain for most of the year and as snow or rain mixed with freezing rain during the winter months. The amount of precipitation varies from year to year and for the period studied, (July 1976 to April 1979), the precipitation total was 2360 mm, giving an annual average of 809 mm, at the Norwood site, (13). Although, snowfall is measured in centimetres, it is recorded as equivalent millimetres of water. The effect of rainfall on groundwater levels is dependent on the intensity and duration of the individual event, but the single most significant factor affecting the level of the water table is the spring thaw period. In winter, when the mean air temperature falls below $0^{o}C$, moisture and free water freezes in the upper soil layers while snow accumulates on the ground surface. As long as the frozen layer remains in the soil, the melting surface snow would not percolate to the water table. Only at the moment of final melting of the frost layer does any free standing surface water seep through the soil to the water table. The thawing of the frozen soil may take several weeks to complete and by itself, causes an increase in the groundwater levels. During a mild early spring, most of the surface snow melts quickly while the frost in the soil thaws more slowly. This enables much of the snow melt to 'run off' before it has a chance

to infiltrate into the soil. During a cool late spring, the surface snow cover remains longer on the ground allowing the underlying frost layer more time to thaw. In other words, the thawing of the frost layer occurs at the interface of the frozen upper soil layer and the subsoil which is at above freezing temperatures. This produces a gradual upward thawing of the frost layer toward the ground surface. Cool climatic conditions leave a greater quantity of snow remaining on the ground surface and available to percolate to the water table as snow melt when the soil is free of frost. Therefore, in general, a cold spring tends to give a greater rise of water table than a mild spring.

In the spring time, the maximum load to the leaching bed was equal to the actual hydraulic load plus the quantity of frost and snow melt released into the soil from the start of the thaw until the groundwater attained its maximum level. The duration of the spring thaw at Norwood varied from 4 to 6 weeks. After the spring water level peak, the water table declined until the mound reached equilibrium. Minor fluctuations in groundwater levels, which occurred throughout the summer and fall seasons, were caused by precipitation and evapotranspiration.

Table 6 shows the pertinent weather data for the winter and spring seasons during the study period. As will be seen in subsection 3.1.3, the maximum rise of the water table during the spring thaw period could be correlated to the weather conditions, such as, mean monthly temperature, snow cover at the start of the spring thaw, etc.

TABLE 6

PERTINENT WINTER WEATHER DATA AT NORWOOD

Weather Data	YEAR		
	1976/1977	1977/1978	1978/1979
November (Mean Monthly Temperature (°C))	- 0.7	2.9	1.6
December	- 9.9	- 7.3	- 4.6
January	- 12.8	- 11.1	- 9.0
February	- 7.3	- 12.0	- 13.5
March	1.6	- 5.2	0.9
April	7.2	3.0	5.7
Freezing Degree (°C) day	908	1071	800
Recorded Winter Snow (cm)	127.0	210.0	145.0
Snow Cover at Start of Thaw (cm)	5.0	41.0	20.0

3.1.2 Evapotranspiration

Evapotranspiration (evaporation and transpiration) is a difficult parameter to measure accurately and in this study could only be estimated. From his study (32), Solomon concluded that the potential evapotranspiration is a percentage of pan evaporation. Pan evaporation is defined as the gross measurement of evaporation from an open pan measured during the frost free period from April to October. The pan evaporation values for the Lindsay area (part of Simcoe and Kawartha lake region) 70 km west of Norwood, for the three year study period was 2928 mm of water giving a yearly average of 976 mm (13). The mean annual potential evapotranspiration for the Simcoe and Kawartha lake region was 580 mm (8), which was approximately 60% of the measured pan evaporation.

TABLE 7

MEAN MONTHLY TEMPERATURE, PRECIPITATION, AND PAN EVAPORATION AT NORWOOD FROM 1976 TO 1979 (STUDY PERIOD ONLY)

Month	Mean Temperature (°C)				Precipitation (mm)				Pan Evaporation (mm)			
	1976	1977	1978	1979	1976	1977	1978	1979	1976	1977	1978	1979
January	-	-12.8	-11.1	- 9.0	-	49.5	108.7	78.5	-	-	-	-
February	-	- 7.3	-12.0	-13.5	-	40.1	6.0	58.6	-	-	-	-
March	-	1.6	- 5.2	0.9	-	71.6	56.1	52.6	-	-	-	-
April	-	7.2	3.0	5.7	-	53.1	56.0	77.0	63.0	107.0	115.0	70.5
May	-	14.4	13.7	-	-	57.4	98.3	-	73.0	178.0	141.0	-
June	19.2	16.3	16.7	-	86.9	58.9	26.4	-	164.8	171.0	186.0	-
July	19.1	20.5	20.2	-	110.5	70.4	50.2	-	173.0	182.0	212.0	-
August	18.1	18.1	19.1	-	42.4	124.0	83.1	-	150.0	164.0	170.0	-
September	13.8	14.5	13.4	-	79.8	102.1	84.8	-	165.0	82.0	136.0	-
October	5.3	7.4	7.4	-	49.0	65.8	61.6	-	64.0	61.0	58.0	-
November	- 0.7	2.9	1.6	-	22.1	114.0	62.0	-	-	-	-	-
December	- 9.9	- 7.3	- 4.6	-	33.5	114.3	53.6	-	-	-	-	-

Brandes (7) calculated that the annual evapotranspiration in Orillia (same general area as Norwood) was 526 mm. This would indicate that the annual evpotranspiration for Norwood is in a range between 50% - 60% of the annual pan evaporation. If it is assumed that at Norwood the evapotranspiration was equal to 55% of the pan evaporation, then the amount of evapotranspiration can be estimated. Table 7 summarizes the monthly temperature, precipitation and pan evaporation data for the study period at Norwood. Table 8 shows the daily average precipitation and the estimated evapotranspiration. It can be seen that at some periods of time the amount of precipitation was exceeded by the amount of evapotranspiration. This natural 'deficit' influenced the effective net hydraulic loading rate in the leaching bed which in turn caused minor fluctuations in the water table.

TABLE 8

COMPARISON OF PRECIPITATION WITH ESTIMATED EVAPOTRANSPIRATION

YEAR	Precipitation mm/day	Est'd Evapotranspiration mm/day	Precipitation mm/day	Est'd Evapotranspiration mm/day	Precipitation mm/day	Est'd Evapotranspiration mm/day
April	1.04	2.10 (d)*	1.77	1.96 (d)	1.96	2.11 (d)
May	3.30	2.37 (s)	1.85	3.61 (d)	3.17	2.50 (s)
June	2.90	3.02 (d)	1.96	3.13 (d)	0.88	3.41 (d)
July	3.56	3.07 (s)	2.27	3.23 (d)	1.62	3.76 (d)
Aug.	1.37	2.66 (d)	4.00	2.91 (s)	2.68	3.02 (d)
Sept.	2.66	3.03 (d)	3.40	1.50 (s)	2.83	2.49 (s)
Oct.	1.58	1.14 (s)	2.12	1.12 (s)	1.98	1.03 (s)

* (d) = deficit
(s) = surplus

3.1.3 Water Table Fluctuation

Typical water table fluctuations are presented in Figure 9. Two groups of results are presented: one from piezometers installed inside the leaching bed and the other from piezometers installed at varying distances from the bed. The water table below the leaching bed was influenced by the hydraulic loading from the leaching bed plus the natural environmental factors such as, precipitation and evapotranspiration. The water table fluctuations at a certain distance from the centre of the bed were less influenced by the hydraulic loading. To explain the groundwater fluctuation data, the results for piezometers 30 and 2 are shown in Figure 10. Piezometer 30 (solid line) was located within the leaching bed area while piezometer 2 (dotted line) was situated about 90 m from the perimeter of the bed and least influenced by the hydraulic loading. In Figure 10, the significant water table fluctuations are numbered for piezometer 30 and the following notes with the corresponding numbers outline some details and explanation of the fluctuations.

1. Week 0 to Week 12

A weekly monitoring program was initiated on July 14, 1976. The natural water table declined slowly after the construction of the leaching bed. The depth of the water table below the ground surface at week 11 (elevation = 26.46 m) was used as the base value for the calculation of the subsequent net groundwater levels.

2. Week 12 to Week 17

Hydraulic loading (Feed) to the leaching bed was started on October 5, 1976, at a rate of 122,700 L/d which is equivalent to 22.8 L/m^2 of leaching bed area. Within the first week of loading, there was a significant increase in the groundwater levels beneath the bed, although, this increase was not even throughout the tiled area. At the

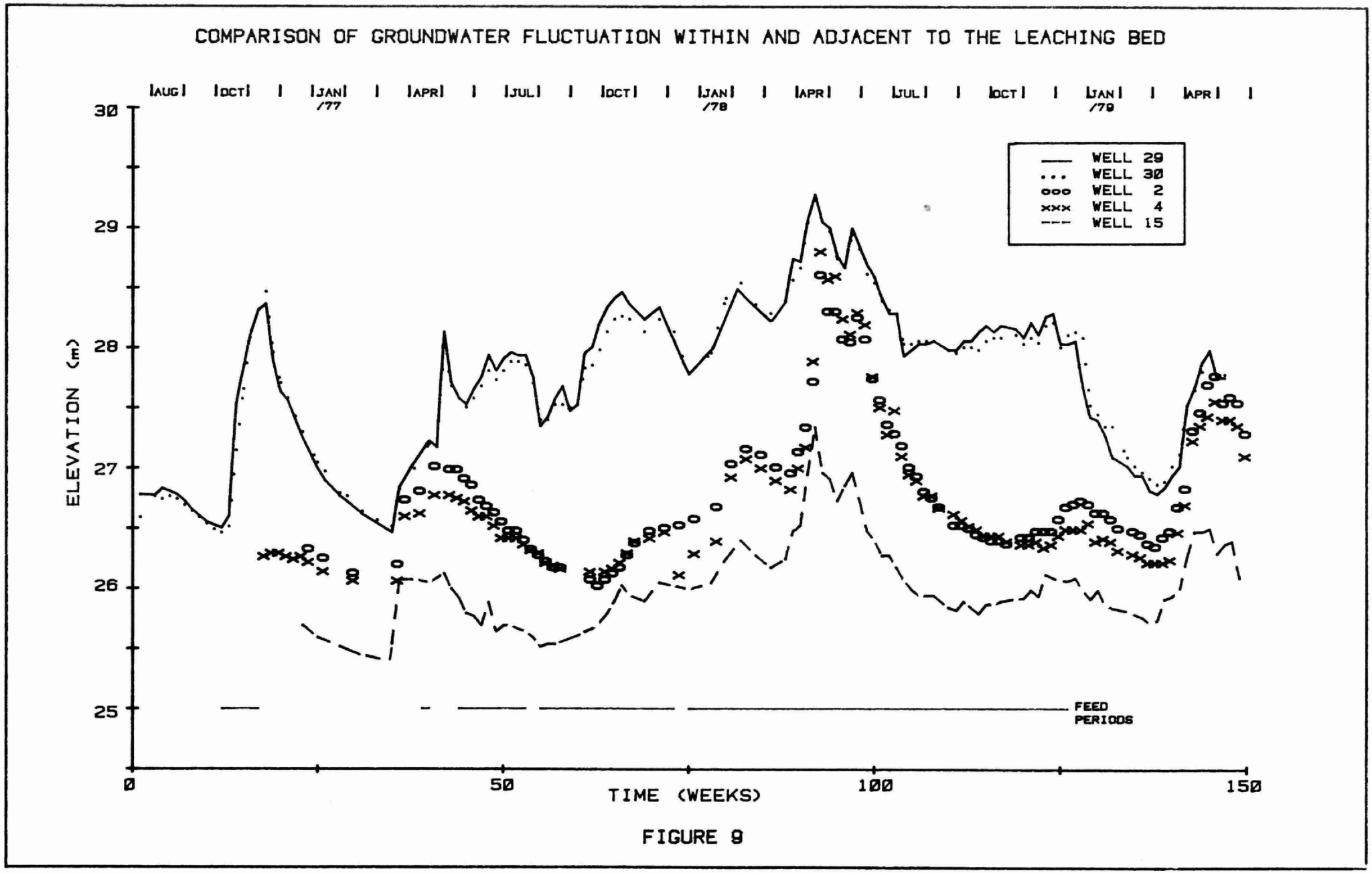
COMPARISON OF GROUNDWATER FLUCTUATION WITHIN AND ADJACENT TO THE LEACHING BED
AUG
OCT
JAN /77
APR
JUL
OCT
JAN /78
APR
JUL
OCT
JAN /79
APR
ELEVATION (m)
30
29
28
27
26
25
WELL 29
WELL 30
WELL 2
WELL 4
WELL 15
FEED PERIODS
0
50
100
150
TIME (WEEKS)

FIGURE 9

EXPLANATION AND COMPARISON OF GROUNDWATER FLUCTUATIONS AT CENTRE OF THE LEACHING BED AND AT 90 METRES FROM THE BED PERIMETER

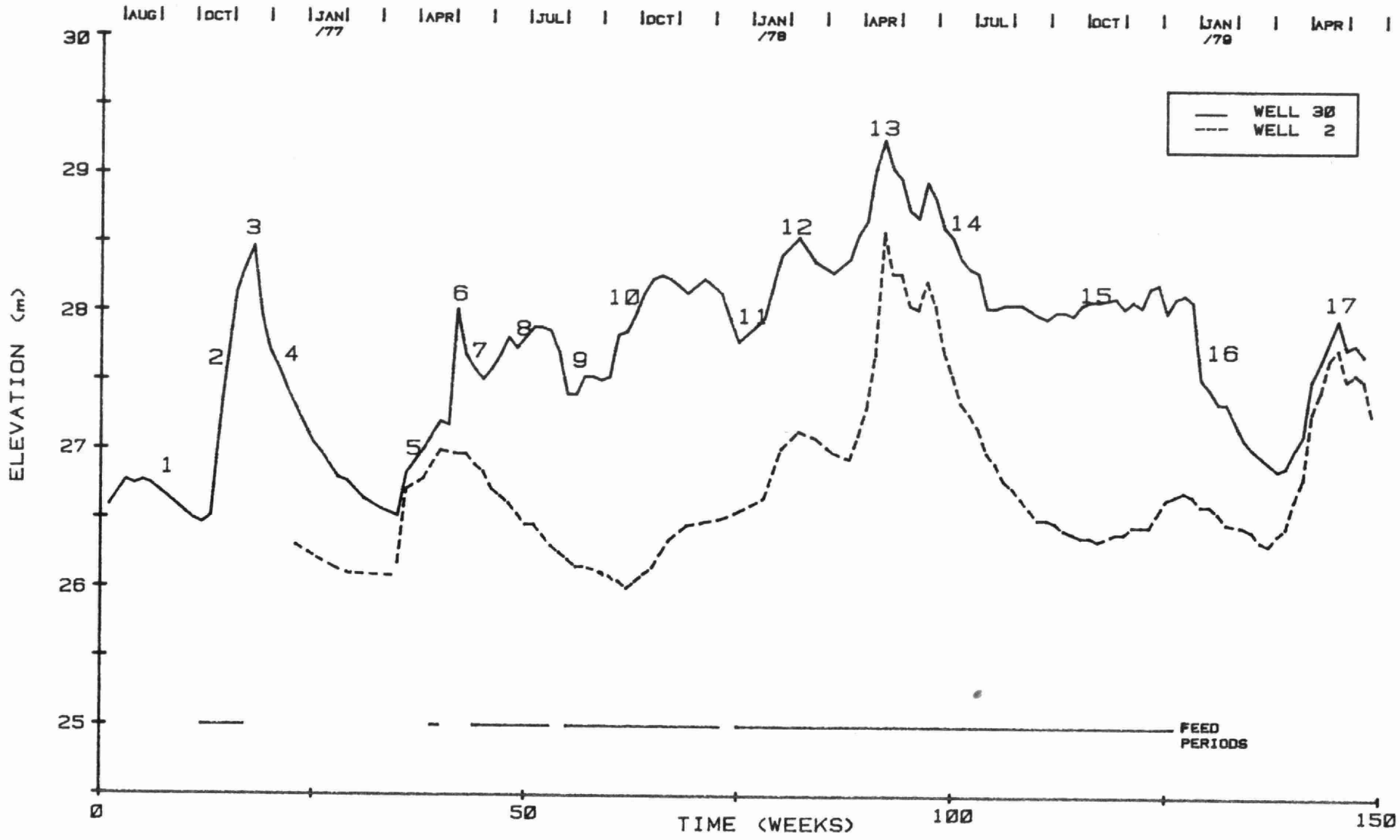

FIGURE 10

south end of the bed, the water table rise was 1.64 m in one week then continued increasing slowly over the next four weeks by an additional 0.46 m. The water table rose at a more even rate at the north end of the leaching bed, increasing by 0.43 m, 0.49 m, 0.46 m, 0.49 m, and 0.2 m during this five week loading cycle.

3. November 10, 1976

On this date, liquid was observed bubbling through the top soil and ponding on the ground surface above the bed. The system was hydraulically overloaded (i.e. in a state of failure) and loading was terminated. (See plate III). The average water table rise below the centre of the bed was 1.99 m. The total volume of feed injected into the leaching bed was 4.296×10^6 litres.

4. Week 17 to Week 34

The artificial groundwater mound declined between November 10, 1976 and March 8, 1977. This was a rest period (i.e. no feed). The response of the water table at the south end of the bed was initially different from that at the north end. The water level fell 0.82 m in the south and 0.55 m in the north during the first week of the rest period then continued to decline slowly until the water table was at pre-injection levels.

5. Week 34 to Week 40

A sharp rise in the water table was noted between March 8, 1977 and April 19, 1977, although, there was no feed to the leaching bed. This was the natural increase in water levels caused by the spring thaw period and was general over all the monitored area. The average increase caused by spring thaw was 0.76 m.

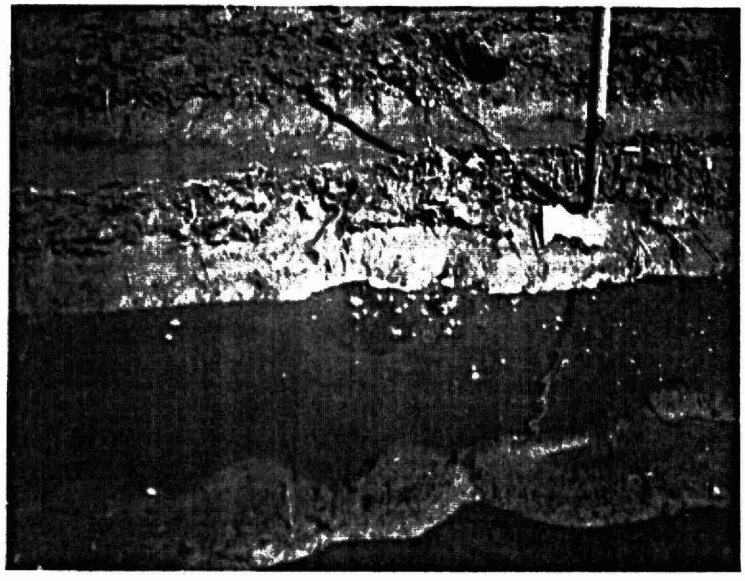

A. BED FAILURE

B. BED FAILURE

PLATE III

6. Week 40 to Week 41

Feed to the leaching bed was re-started on April 21, 1977, at 40,900 L/d. Unfortunately, an electrical malfunction developed in the timer allowing the feed pump to operate continuously. A total of 1.06×10^6 litres of secondary effluent was injected in a four-day period. The response of the water table to the massive load was an increase of 1.37 m at the south end of the bed and 0.64 m rise at the north end. The average increase was 0.98 m within the bed and 0.52 m at the perimeter. There was very little or no increase away from the tiled area because of the short duration of the loading period.

7. Week 41 to Week 44

This was a short rest period to allow the groundwater mound to decline.

8. Week 44 to Week 53

Hydraulic loading was resumed on May 17, 1977, at a rate of 40,900 L/d. The groundwater level was 1.01 m above the base elevation at the bed centre and a subsequent rise in the water table was noted below the leaching bed area.

9. Week 53 to Week 54

The system was shutdown for one week on July 19, 1977, at the request of the Water Resources Branch of the Ministry of the Environment which was conducting a river survey downstream from the treatment plant. Consequently, the water table declined at this time.

10. Week 54 to Week 73

The feed was continued at 40,900 L/d from July 25, 1977, to December 9, 1977, with an increase in the water table.

11. Week 73 to Week 74

An ice blockage in the line from the pump to the feed tank caused the system to be shutdown for one week on December 9, 1977, while repairs and modifications were made. The groundwater mound declined.

12. Week 74 to Week 87

Loading was resumed December 16, 1977. The feed was maintained at 40,900 L/d with a corresponding mound in the groundwater levels. From week 44 to week 87, including 2 one-week shutdown periods, the water table rose 1.86 m below the bed centre. The overall trend from week 44 through 87 was an increase in the height of the water table. A feed rate of 40,900 L/d was adequate to sustain an average 1.42 m rise above the base groundwater level, (i.e. elevation = 26.46 m). Volume of feed applied to the system from week 44 to 87 was 12.025×10^6 litres.

13. Week 87 to Week 91

On March 14, 1978, the water levels increased over all the monitored area due to the spring thaw. The artificial mound under the leaching bed disappeared as the spring thaw reached its peak. Excluding the centre of the bed which already contained the artificial mound, the average increase in the water table during the spring thaw was 1.69 m. Between April 12 and April 18, 1976, water was observed bubbling up through the soil onto the ground surface. (See plate III). However, the feed was continued since it was felt that the flooded condition would last for only a very short time. When the groundwater levels peaked on April 18, 1978, the average height above the base level over all the monitored area was 2.73 m. The rise of the water table during the spring thaw in 1978 was greater than that in 1977. This observation is in agreement with the weather data in Table 6. In 1978, the

freezing degree days, the recorded winter snow and the amount of snow cover at the start of the thaw were all greater than those in 1977.

14. Week 91 to Week 100

This was a period of decline and stabilization of the water table after the spring peak levels had occurred. The feed to the leaching bed was maintained at 40,900 L/d. The decrease over all the field excluding the centre of the leaching bed during this 10 week period was 1.44 m. Within the area of the bed the decline in the water table was only 0.98 m, due mainly to the continuing influence of the hydraulic loading. On May 16, 1978, liquid was again noticed breaking out from the ground surface. (There had been a prolonged period of steady rainfall at this time combined with subsoil still partly saturated from the spring thaw). The surface area remained very moist for some time after the flooding and breakout of liquid. The rise in groundwater levels from the base value on June 14, 1978, was 1.77 m at the bed centre. Total volume applied to system from week 87 to week 100 was 3.722×10^6 litres.

15. Week 100 to Week 126

This was a continuous loading period of 40,900 L/d from June 14, 1978, until the final shutdown of the system on December 13, 1978. The groundwater levels below the leaching bed remained relatively steady with minor fluctuations due to sporadic rainfall and evapotranspiration. The water table rise above the base elevation (i.e. 26.46 m) at week 126 was 1.54 metres at the centre of the leaching bed. Total volume of liquid injected into the bed for 26 weeks was 7.157×10^6 litres.

16. Week 126 to Week 138

The feed to the leaching bed was stopped on December 13, 1978. The groundwater levels immediately began to decrease and continued to drop throughout the winter until the spring thaw of 1979.

17. Week 138 to Week 144

This was the annual spring thaw period. The natural water levels increased during six weeks and peaked on April 18, 1979, at 1.54 m above the base elevation. The average increase caused by the thaw period over all the monitored area was 1.15 m. The water table rise for the 1979 spring thaw was smaller than that in 1978 as the recorded winter snow and the snow cover was less in 1979. (See Table 6). The natural water levels were declining again by week 146 of the study.

In Table 9, a summary of the net fluctuations of the groundwater table with respect to the initial base elevation is presented. The quantity of liquid applied to the leaching bed throughout the study totalled 28.26×10^6 litres.

3.2 Mathematical Techniques for Predicting Mounding

A number of mathematical models in various forms are available today for the prediction of the rise and fall of groundwater mounds under recharge areas subject to percolation including some early research (5, 15, 17). In the last decade, additional models were developed (18, 24, 25, 29, 31, 36).

Generally, in the models, an aquifer system is represented by a set of partial differential equations. With given governing boundary conditions and aquifer parameters, the differential equations can be solved both exactly and numerically. In the Norwood Project, Hantush's closed-formed solutions and Sykes' finite-element numerical model were

TABLE 9

SUMMARY OF GROUNDWATER FLUCTUATIONS (IN METRES) IN DIFFERENT GROUPS OF TEST LOCATIONS AT VARYING DISTANCES FROM THE LEACHING BED

Week No.	Comment	GROUP 1 (center)		GROUP 2 (Perimeter)		GROUP 3 (30 metres)		GROUP 4 (60 metres)		GROUP 5 (90 metres)	
		Net	Cumulative	Net	Cumulative	Net	Cumulative	Net	Cumulative	Net	Cumulative
0 - 12	Pre start-up (Base)	0.00	0.00	0.00	0.00	0.00	0.00	0.00	0.00	0.00	0.00
12 - 17	High loading rate	+1.99	1.99	+1.48	1.48	+0.84	0.84	+0.40	0.40	*	*
17 - 34	Rest period	-2.04	-0.05	-1.44	0.14	-0.80	0.04	-0.40	0.00	*	*
34 - 40	Spring thaw 1977	+0.72	0.67	+0.73	0.77	+0.70	0.74	+0.81	0.81	+0.86	0.86
40 - 41	Overload 1 week	+0.98	1.65	+0.52	1.29	+0.09	0.83	+0.12	0.83	-0.01	0.85
41 - 44	Rest period	-0.64	1.01	-4.6	0.83	-0.20	0.63	-0.19	0.64	-0.18	0.67
44 - 87	Low loading rate	+0.85	1.86	+0.50	1.33	+0.48	1.11	+0.23	0.87	+0.15	0.82
87 - 91	Spring thaw 1978 (+ low load rate)	+0.89	2.75	+1.67	3.00	+1.63	2.74	+1.83	2.70	+1.62	2.44
91 - 100	Decline (stabilize) (+ low load rate)	-0.98	1.77	-1.58	1.42	-1.44	1.30	-1.50	1.20	-1.23	1.21
100 - 126	Summer period (low loading rate)	-0.23	1.54	-0.42	1.00	-0.41	0.89	-0.57	0.63	-0.65	0.56
126 - 138	Rest period	-1.16	0.38	-0.56	0.44	-0.51	0.38	-0.26	0.37	-0.20	0.36
138 - 144	Spring thaw 1979	+1.11	1.49	+1.14	1.58	+1.12	1.50	+1.17	1.54	+1.22	1.58

used to analyse the field data. The main reason for selecting the Hantush model was the relative simplicity of its solutions which would make it easier to use for more routine design problems. Sykes' model is flexible in many ways. This model represents the more recent numerical approach to the groundwater mounding problem.

In this section, some details of Hantush's solutions are presented and in the appendix, the mathematical treatment of Sykes' model is given.

The equations developed by Hantush can be used to estimate the rise and fall of a groundwater mound in response to a uniform vertically downward rate of percolation for both rectangular and circular recharging areas. The solutions were developed from the Laplace equation in terms of the head averaged over the depth of saturation.

The following simplifying assumptions are made in the model:-

1. The aquifer is homogeneous, isotropic, infinite in areal extent and resting on a horizontal impermeable base.

2. The formation coefficients and the rate of percolation are constant in time and space.

3. The constant rate of deep percolation, relative to the horizontal flux, is so small that the groundwater flow lines are almost completely refracted in the direction of the tilt of the water table.

4. The water table is initially horizontal and remains below the bottom of the recharge area.

5. The relative rise of the water table to the initial water table depth is less than 50%.

6. The Dupuit-Forschheimer assumptions are valid.

The flow problem can be approximated by the following boundary-value problem, (see Figure 11 for co-ordinate system).

$$\frac{\partial^2 Z}{\partial X^2} + \frac{\partial^2 Z}{\partial Y^2} + \left(\frac{2W}{k}\right) f(x, y) = \left(\frac{1}{V}\right) \frac{\partial Z}{\partial t} \quad \text{.....(1)}$$

subject to the following initial and boundary conditions:

$$Z(x, y, 0) = 0 \quad \text{.....(1a)}$$

$$\frac{\partial Z(0, y, t)}{\partial x} = \frac{\partial Z(x, 0, t)}{\partial y} = 0 \quad \text{.....(1b)}$$

$$\frac{\partial Z(\infty, y, t)}{\partial x} = \frac{\partial Z(x, \infty, t)}{\partial y} = 0 \quad \text{.....(1c)}$$

$$W = \begin{cases} W & 0 < x < a, \quad 0 < y < b, \ t > 0 \quad \text{.....(1d)} \\ 0 & x > a, \quad y > b, \ t > 0 \quad \text{.....(1e)} \end{cases}$$

where $v = k\bar{b}/s$

$\bar{b} = 0.5 \left[h_i (0) + h(t_1)\right]$

$=$ constant of linearization

$Z = h^2 - h_i^2$

$k =$ permeability (hydraulic conductivity)

$s =$ specific yield

$W =$ constant rate of percolation

$t =$ time since incidence of percolation at water table

$a =$ dimension of basin in x direction

$b =$ dimension of basin in y direction

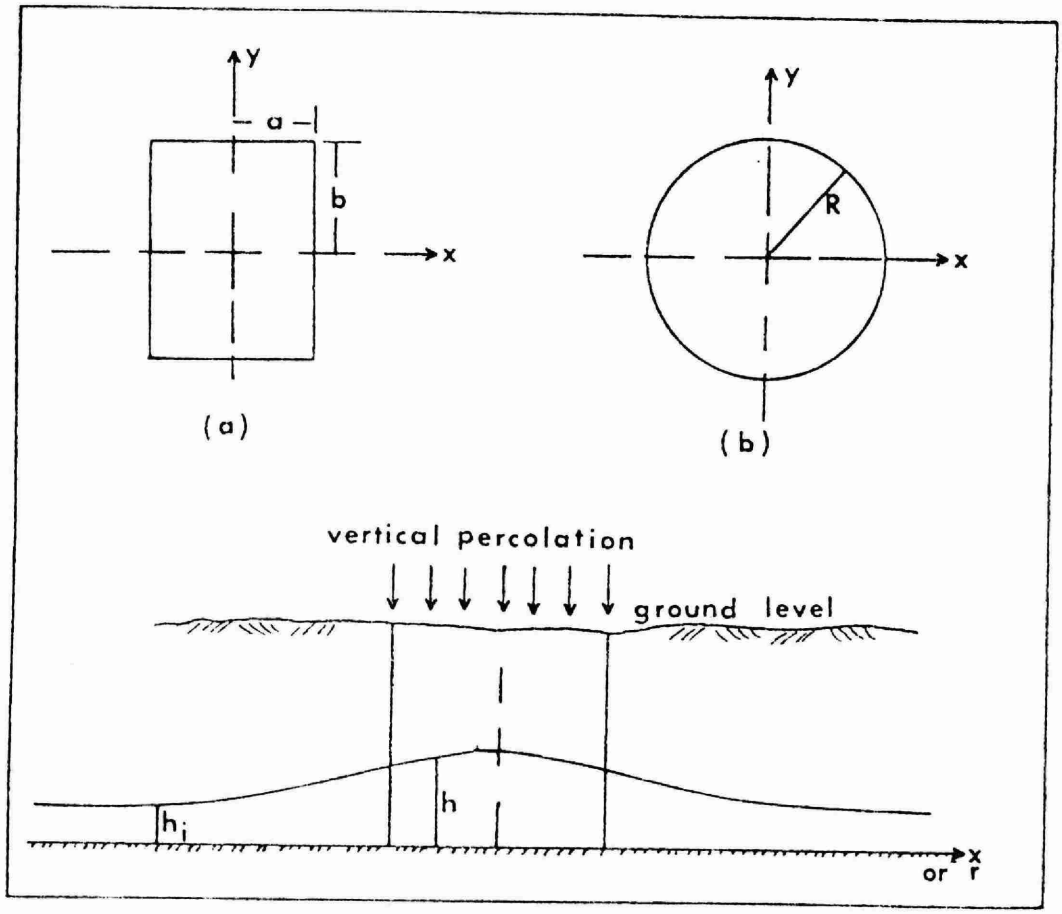

FIGURE 11

Geometry and Symbols for Rectangular and Circular Infiltration Areas and Underlying Groundwater Mound in Unconfined Aquifer (17)

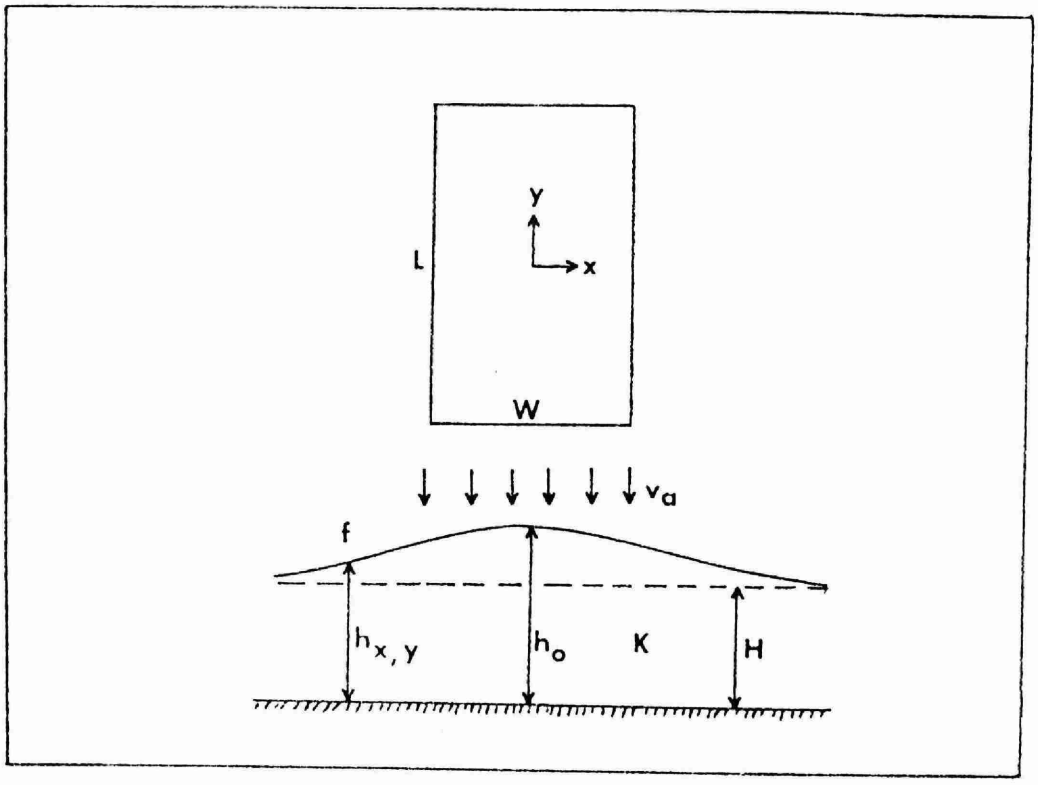

FIGURE 12

Geometry and Symbols for Rectangular Infiltration Area and Underlying Groundwater Mound in Unconfined Aquifer (6)

Successive applications of Laplace and Fourier transforms and the respective inversion formulas yields the following for the first quartile. Due to symmetry, this result is applicable to other quartiles.

$$Z(x, y, t) = \frac{vA}{2} \int_0^t \left[\operatorname{erf}\left(\frac{b + x}{\sqrt{4v\,\tau}}\right) + \operatorname{erf}\left(\frac{b - x}{\sqrt{4v\,\tau}}\right)\right] \cdot \left[\operatorname{erf}\left(\frac{a + y}{\sqrt{4v\,\tau}}\right) + \operatorname{erf}\left(\frac{a - y}{\sqrt{4v\,\tau}}\right)\right] d\tau$$

where $A = 2w/k$ .....(2)

After changing the variable of integration from τ to $t\tau$ the rise of the water table can be expressed as:

$$h^2 - h_i^2 = \frac{wvt}{2k}\left\{s^*\left(\frac{a + x}{D}, \frac{b + y}{D}\right) + s^*\left(\frac{a + x}{D}, \frac{b - y}{D}\right) + s^*\left(\frac{a - x}{D}, \frac{b + y}{D}\right) + s^*\left(\frac{a - x}{D}, \frac{b - y}{D}\right)\right\}$$

.....(3)

where $D = \sqrt{4vt}$

$$s^*(\alpha, \beta) = \int_0^1 \operatorname{erf}\left(\frac{\alpha}{\sqrt{\tau}}\right) \cdot \operatorname{erf}\left(\frac{\beta}{\sqrt{\tau}}\right) d\tau$$

Values of the above function are tabulated by Hantush. The corresponding equation for the decline of the water table if percolation ceases is:

$$h^2 - h_i^2 = Z(x, y, t) - Z(x, y, t - t_o) \quad .....(4)$$

where t_o is the time when water ceased to arrive at the water table and $Z(x, y, t)$ and $Z(x, y, t - t_o)$ are the right-hand side of equation (3) with t and $t - t_o$ as time factors, respectively. This solution of hypothetically superposing on the flow system a discharge equal to the uniform rate of percolation at $t = t_o$ is possible since the differential equation is linear in h^2.

For a circular recharge basin, Hantush based his solution on a Laplace equation of the form,

$$\frac{\partial^2 Z}{\partial r^2} + \frac{1}{r}\frac{\partial Z}{\partial r} + \frac{2W}{k} \cdot f(r) = \frac{1}{r}\frac{\partial Z}{\partial t} \qquad \text{.....(5)}$$

with the following initial and boundary conditions:

$$Z(r, 0) = 0 \qquad \text{.....(5a)}$$

$$\frac{\partial Z(0, t)}{\partial r} = 0 \qquad \text{.....(5b)}$$

$$\frac{\partial Z(\infty, t)}{\partial r} = 0 \qquad \text{.....(5c)}$$

$$W = \begin{cases} W & 0 < r < R \qquad \text{.....(5d)} \\ 0 & r > R \qquad \text{.....(5e)} \end{cases}$$

where R = radius of circular recharge area.

The problem was solved using the Laplace and zero order Hankel transformations to produce the final equation.

$$h^2 - h_i^2 = (2V/\pi k) \quad f \quad (q, p) \qquad \text{.....(6)}$$

where $V = w\pi R^2$

$$q = \frac{vt}{R^2}$$

$$p = \frac{r}{R}$$

As for the case of a rectangular recharge area, the decay of the water table for a circular area after cessation of infiltration is similarly given by,

$$h^2 - h_i^2 = Z(r, t) - Z(r, t - t_o) \qquad \text{.....(7)}$$

Hantush's equation for the rise of the mound below a rectangular recharge basin can be written in a simpler form (6) and is easier to use than Hantush's equation in its original form.

The equation for the rise of the mound in unconfined aquifers below rectangular basins is:

$$h_{x,\,y,\,t}{}^{-H} = \frac{V_a t}{4f}\Big\{ F\{(W/2 + x)n, (L/2 + y)n\} + F\{(W/2 + x)n, (L/2 - y)n\} + F\{(W/2 - x)n, (L/2 + y)n\} + F\{(W/2 - x)n, (L/2 - y)n\}\Big\} \quad \ldots\ldots\ldots(8)$$

where $h_{x,\,y,\,t}$ = height of water table above impermeable layer at x, y and time t (see Figure 12)

H = original height of water table above impermeable layer

V_a = arrival rate at water table of water from infiltration basin

t = time since start of recharge

f = fillable porosity ($1 > f > 0$) = specific yield = **s**

L = length of recharge basin (in y direction)

W = width of recharge basin (in x direction)

$n = (4.t.T/f)^{-\frac{1}{2}}$

$$F(\alpha, \beta) = \int_0^1 \operatorname{erf}(\alpha\tau^{-\frac{1}{2}}) \cdot \operatorname{erf}(\beta\tau^{-\frac{1}{2}})\,d\tau$$ {which was tabulated by Hantush}

The equation for the decay of the groundwater mound after cessation of infiltration is,

$$h_{x,\,y,\,t}{}^{-H} = Z(x, y, t) - Z(x, y, t - t_s) \quad \ldots\ldots\ldots\ldots(9)$$

where t = time since water began to arrive at the water table

t_s = time since water ceased to arrive at the water table

$Z(x, y, t)$ and $Z(x, y, t - t_s)$ = right-hand part of equation (8) with t and $(t - t_s)$ as time factors.

3.3 Analysis of Groundwater Mounding by Hantush's Method

In this section, the selection of the values of the soil (or aquifer) parameters used in the calculation of the magnitude of the groundwater mounding by Hantush's equations will be briefly discussed. The calculated results will then be compared with the field experimental data obtained in the periods when the hydraulic loading rates were 122,700 L/d and 40,900 L/d.

3.3.1 Selection of the Soil Parameter Values

As noted in 3.2, the values of the fillable porosity, 'f', (specific yield, 's'), the permeability, 'k', (hydraulic conductivity) and the thickness of the aquifer, 'H', are required in Hantush's equations to compute the amount of the groundwater mounding beneath a recharge area. These values were measured in the field exploration program which was described in detail in Chapter 2. Because the natural soil conditions were quite variable and the thickness of the aquifer was not constant, some engineering judgement was required in the selection of the values of the parameters used in the calculations.

(1) Fillable Porosity, 'f', (Specific Yield, 's')

A value of 0.2 was chosen for the fillable porosity, 'f'. The selection was based on literature data which are presented in Figure 13. In addition, the results of measurements on the porosity and the degree of saturation of the soil samples (see Table 4) obtained at the test site were used as a guide.

(2) Permeability, 'k', (Hydraulic Conductivity)

The test results are summarized in Table 3. It can be noted that the test results vary significantly, depending on the testing methods and the soil types. As shown in Figure 6, the sandy silt on the north side of the leaching bed is more permeable than the clayey

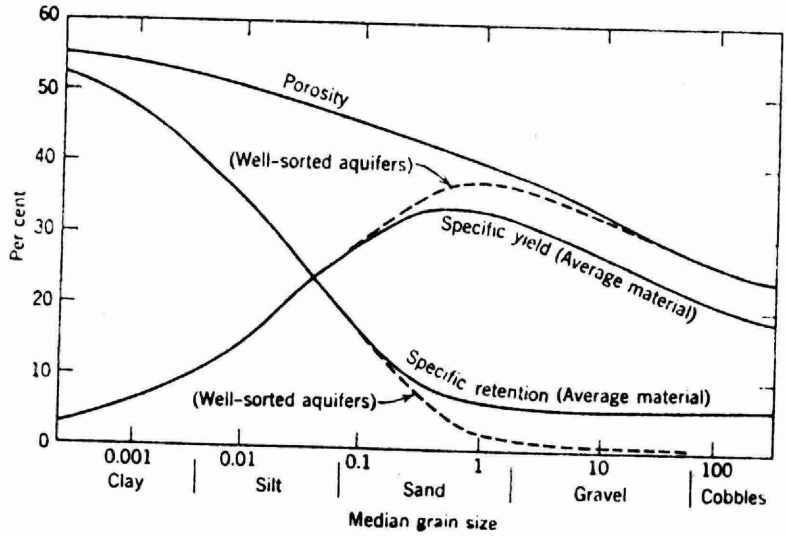

FIGURE 13

RELATION BETWEEN MEDIAN GRAIN SIZE AND WATER-STORAGE PROPERTIES OF ALLUVIUM FROM LARGE VALLEYS. (REF. P.394 IN 'HYDROLOGY' BY STANLEY N. DAVIS AND ROGER J. M. DeWIEST, JOHN WILEY & SONS, INC. 1966)

silt on the south side of the leaching bed. Table 10 is a summary of the averaged 'k' results for the sandy silt material obtained by various types of field tests.

TABLE 10

Averaged 'k' Results for Sandy Silt

k (cm/s)	Type of Field Test
2.3×10^{-4}	'Falling head'
5.1×10^{-4}	'Recovery'
3.7×10^{-4}	'Falling head' and 'Recovery'
3.5×10^{-5}	'Constant head'

It should be pointed out that in a near-horinzontal groundwater flow from a groundwater mound at the test site, the more permeable soil (i.e. the sandy silt material), under the leaching bed would have more important influence on the mounding. Therefore, the 'k' results of the more permeable soil were used in the calculations of the mounding.

(3) Thickness of the Aquifer 'H'

It is noted in Figure 5 that the thickness of the aquifer, 'H', increases in the direction towards the river. However, only a constant 'H' can be used in Hantush's equations. Therefore, the value of 'H' was assumed to be equal to 12 m. This assumption was made from geophysical data recorded in the area from the leaching bed to the Ouse River. The thickness of the aquifer was equal to the difference in elevations of the bedrock and the water table at the outset of the study. In the groundwater mounding calculations, a value of 8 m was also used and this value was approximately equal to the thickness of the sandy silt beneath and in the vicinity of the leaching bed.

3.3.2 Comparison of Experimental and Theoretical Groundwater Mounding (Hydraulic Load = 122,700 L/day) and Decline

With the values of 'k', 'H' and 'f' (or 's') presented and discussed in subsection 3.3.1, the magnitude of the groundwater mounding was computed for several combinations of permeability ('k') and aquifer thickness ('H'). The calculated results were compared with the experimental data of three groups of piezometers. The first group of piezometers are: 24, 25, 29 and 30, which were located within the leaching bed and were closest to the distribution box. The second group of piezometers are: 26 and 31, which were located on the north side of the distribution box, and the third group are: 23 and 28, which were located on the south side of the distribution box (see Figure 8). In the calculations, the field-determined 'k' values (i.e. 3.7×10^{-4} cm/s and 3.5×10^{-5} cm/s) were used, and in addition, a 'back-calculated' 'k' value was also used. This 'back-calculated' permeability value was obtained by comparing the field data at piezometers 24, 25, 29 and 30 with the theoretical results for a number of 'k' values. By the trial-and-error procedure, a 'back-calculated' 'k' value of about 5×10^{-4} cm/s was obtained for the case in which $H = 12$ m and $f = 0.2$. This 'back-calculated' 'k' value was later used with the field-determined 'k' values to predict the long-term groundwater mound under the bed.

The calculated results for a number of combinations are summarized in Tables 11a and b and are presented in Figures 14a, b and c for comparisons with the field data. As shown by Figure 14a, the average data of piezometers 24, 25, 29 and 30 compare quite well with the theoretical data for the 'k' value of 3.7×10^{-4} cm/s. However, the mounding for the 'k' value of 3.5×10^{-5} cm/s is greater than the actual measurement.

TABLE 11a

COMPARISON OF HANTUSH CALCULATED GROUNDWATER MOUND WITH FIELD DATA

Loading Rate = 122,700 L/d: f = 0.2: H = 12 m

Location From Bed Centre = 16.0 m East or West; 10.7 m North or South

Days	FIELD DATA (m) Average of 24, 25, 29, 30	'k' (m/d) (cm/s)	0.43 5.0×10^{-4}	0.32 3.7×10^{-4}	0.03 3.5×10^{-5}
3	0.38		0.34	0.34	0.35
7	0.84		0.73	0.73	0.80
10	1.10		0.98	1.00	1.15
14	1.28		1.27	1.31	1.60
16	1.46		1.40	1.46	1.83
21	1.70		1.68	1.78	2.39
24	1.78		1.83	1.96	2.72

Loading Rate = 122,700 L/d: f = 0.2: H = 8 m

Location From Bed Centre = 16.0 m East or West; 10.7 m North or South

Days	FIELD DATA (m) Average of 24, 25, 29, 30	'k' (m/d) (cm/s)	0.43 5.0×10^{-4}	0.32 3.7×10^{-4}	0.03 3.5×10^{-5}
3	0.38		0.34	0.34	0.35
7	0.84		0.77	0.76	0.81
10	1.10		1.05	1.05	1.15
14	1.28		1.38	1.40	1.61
16	1.46		1.53	1.57	1.84
21	1.70		1.87	1.95	2.40
24	1.78		2.06	2.10	2.74

TABLE 11b

COMPARISON OF HANTUSH CALCULATED GROUNDWATER MOUND WITH FIELD DATA

Loading Rate = 122,700 L/d: f = 0.2: H = 12 m

Location From Bed Centre = 16.0 m East or West; 31.0 m North or South

Days	FIELD DATA (m) Average of 26, 31	'k' (m/d) (cm/s)	0.43 5.0×10^{-4}	0.32 3.7×10^{-4}	0.03 3.5×10^{-5}	FIELD DATA (m) Average of 23, 28
3	0.13		0.20	0.20	0.25	1.23
7	0.49		0.43	0.44	0.54	1.54
10	0.73		0.59	0.61	0.74	1.64
14	0.96		0.78	0.82	1.00	1.65
16	1.18		0.88	0.95	1.13	1.70
21	1.51		1.09	1.15	1.45	1.76
24	1.65		1.21	1.29	1.64	1.79

Loading Rate = 122,700 L/d: f = 0.2: H = 8 m

Location From Bed Centre = 16.0 m East or West; 31.0 m North or South

Days	FIELD DATE (m) Average of 26, 31	'k' (m/d) (cm/s)	0.43 5.0×10^{-4}	0.32 3.7×10^{-4}	0.03 3.5×10^{-5}	FIELD DATA (m) Average of 23, 28
3	0.13		0.20	0.21	0.27	1.23
7	0.49		0.44	0.45	0.56	1.54
10	0.73		0.61	0.63	0.77	1.64
14	0.96		0.83	0.85	1.04	1.65
16	1.18		0.93	0.96	1.17	1.70
21	1.51		1.17	1.22	1.50	1.76
24	1.65		1.30	1.37	1.69	1.79

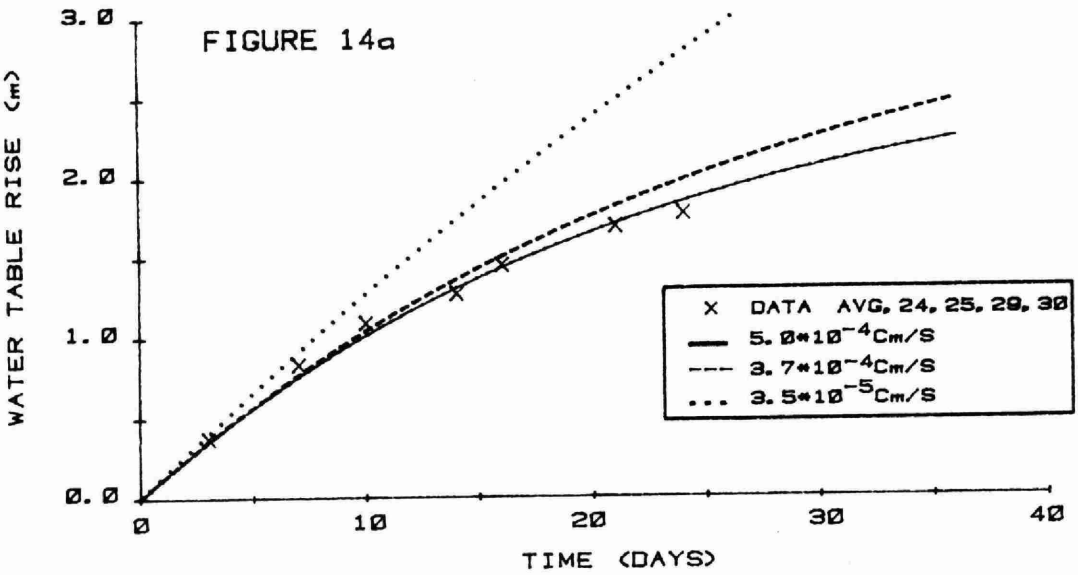

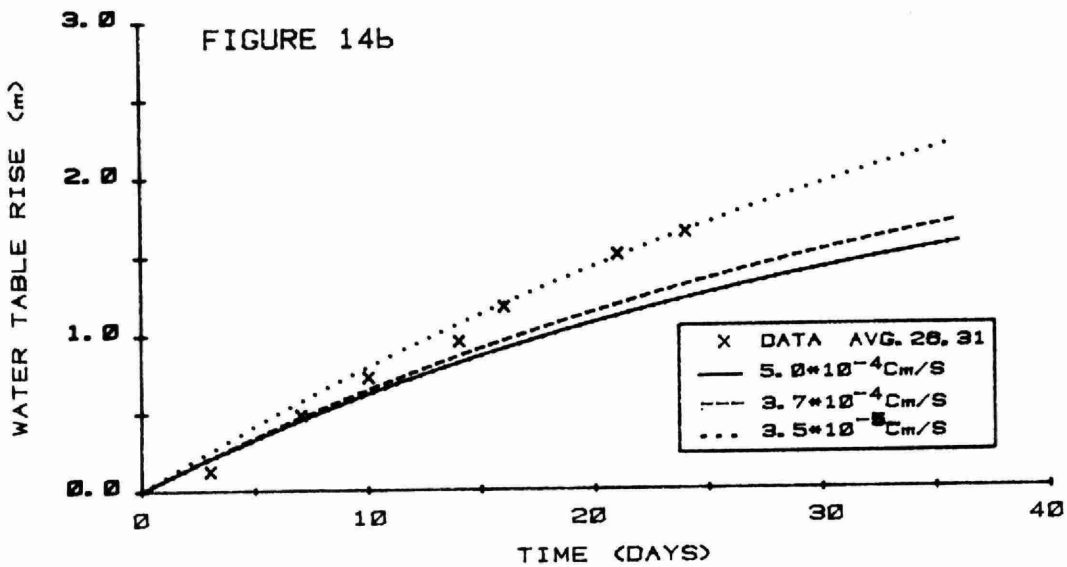

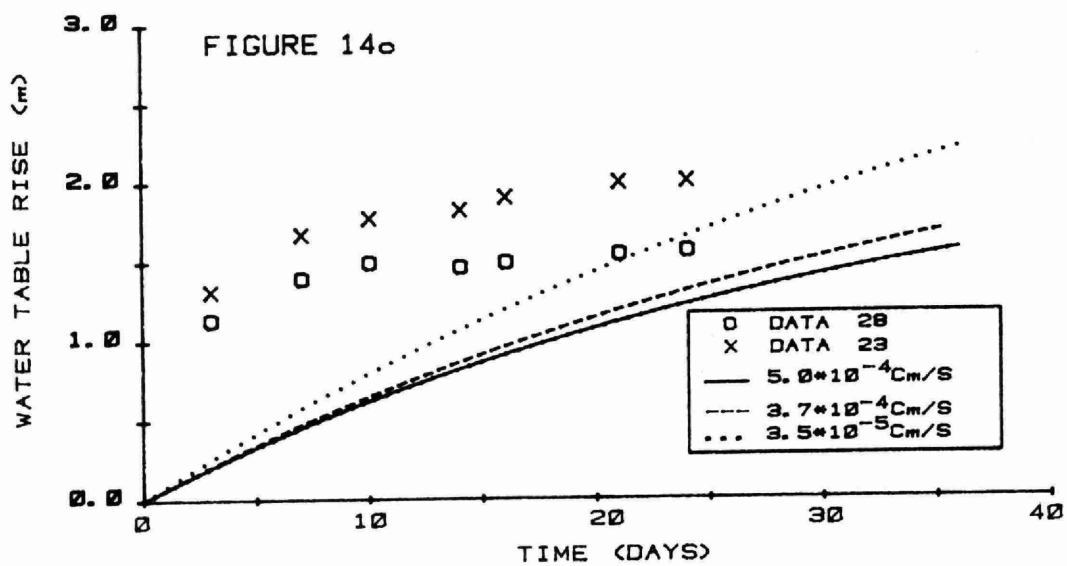

COMPARISON OF THEORETICAL AND EXPERIMENTAL GROUNDWATER MOUNDING DATA (LOADING RATE 122700 L/day)

In Figure 14b, the comparison of the experimental curve with the theoretical curves is reasonably good even though the 'k' values are quite different. The better comparison could be attributed to the short period of the hydraulic loading and the distance of the piezometers from the centre of the bed, (i.e. smaller mound at larger distance from the centre of the bed). For piezometers 23 and 28, the theoretical and experimental results compare poorly (see Figure 14c). This could be due to:

(i) different soil conditions on the south part and the north part of the leaching bed, and

(ii) the 'k' values were for the soil below the north part of the leaching bed.

In Tables 11a and b, the results for H = 12 m and 8 m are both presented. As would be expected, groundwater mound would be higher if the 'H' is 8 m instead of 12 m, 'k' and 'f' values being equal.

Figures 15a, b and c, show comparisons of the experimental and theoretical data for the decline of the water table after the hydraulic loading of 122,700 L/d was stopped. In the calculations, 'k' values of 3.5×10^{-5} cm/s, 3.7×10^{-4} cm/s and 5×10^{-4} cm/s were used to obtain the theoretical results, 'H' and 'f' being 12 m and 0.2, respectively. For different permeability values, the initial elevation of the water table before the decline would be different because a smaller 'k' value would yield a higher groundwater mound. Therefore, in comparing the theoretical and experimental data in Figures 15a, b and c, only the rate of the decline is of interest. Two comments may be made on the results in Figure 15:

(i) For the ranges of the 'k' values (10^{-4} to 10^{-5} cm/s) used, the rate in the lowering of the groundwater mound does not seem to differ significantly, and

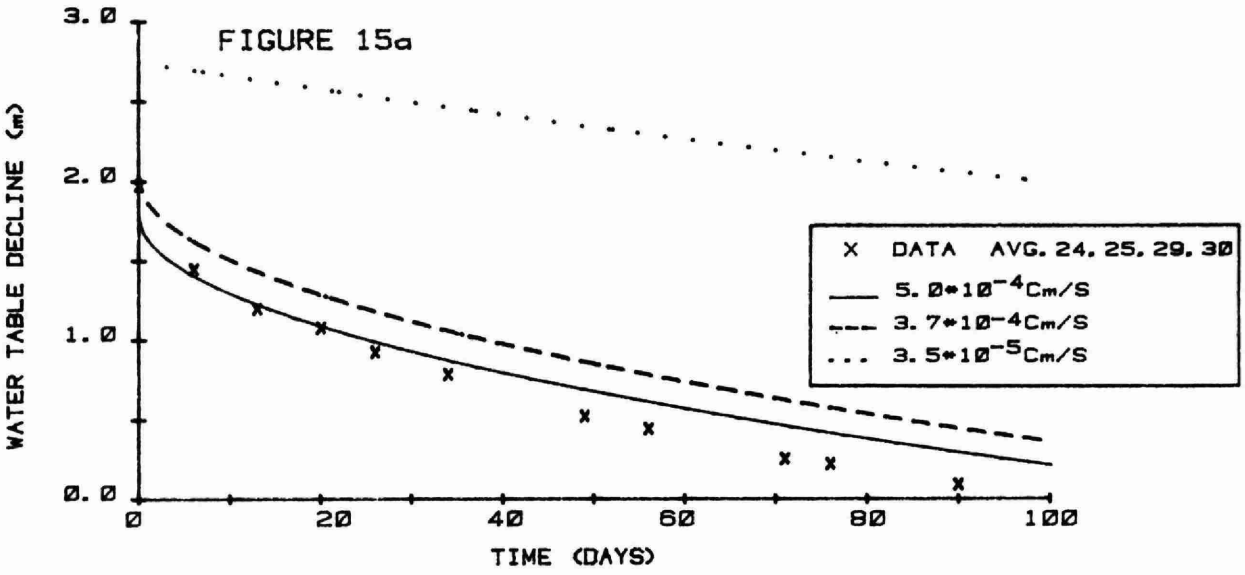

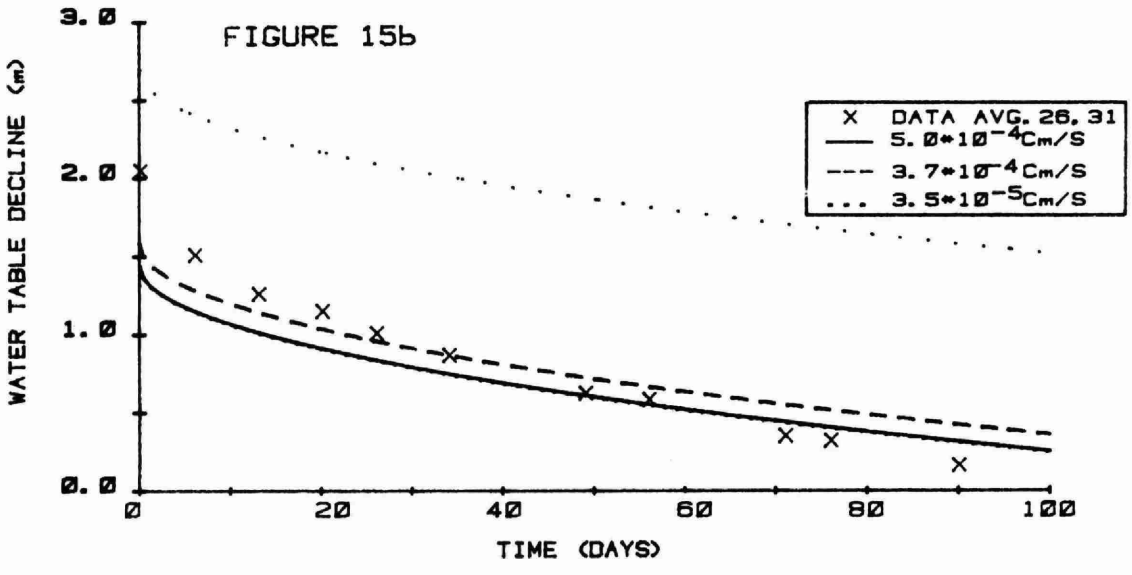

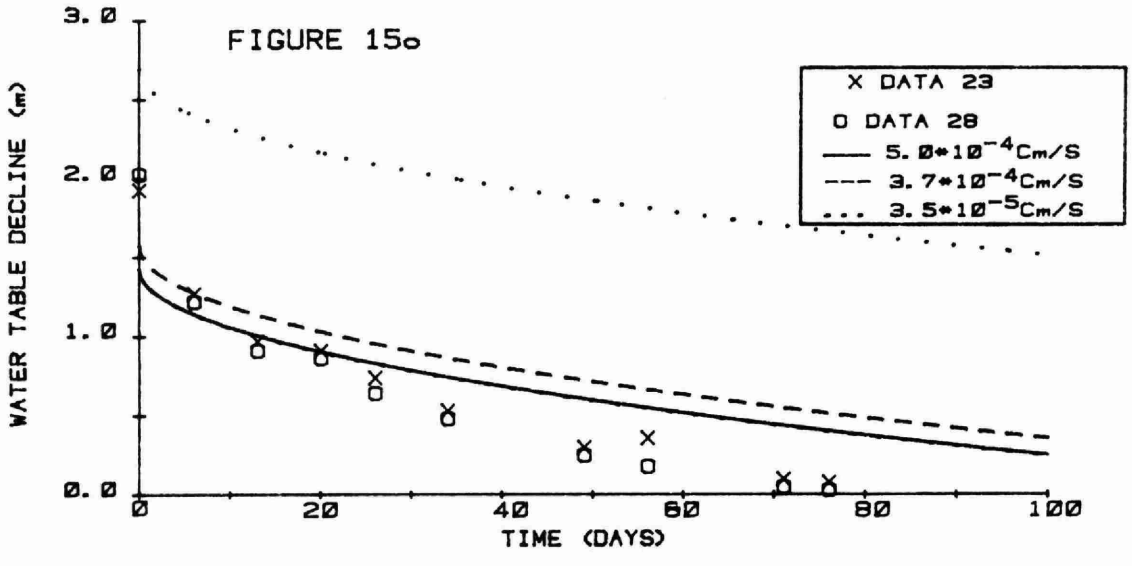

COMPARISON OF THEORETICAL AND EXPERIMENTAL GROUNDWATER DECLINE DATA

(ii) The measured rate of the decline was somewhat faster than what is predicted.

3.3.3 Groundwater Mounding During Week 44 to Week 126

During this period, with the exception of a few short durations, the hydraulic loading rate was 40,900 L/d. The fluctuations of the water table beneath and adjacent to the leaching bed are presented in Figure 9. As explained in section 3.1, the movement of the water table beneath the bed was influenced by two factors:

(i) the hydraulic loading from the bed, and

(ii) precipitation and evapotranspiration at the site. Because Hantush's method does not take into account the effect of evapotranspiration and it also assumes a constant hydraulic loading rate during the loading period, it becomes quite difficult to compare the short-term minor fluctuations of the water table with the theoretical curve. Fortunately, in design, it is the maximum rise of the water table which is of practical significance. Therefore, the comparison of the calculated maximum rise of the groundwater mound with what was measured in the field would be of prime interest. The theoretical rise of the water table at piezometer 30 was calculated by Hantush's equation for several cases and the results are tabulated in Table 12. According to the theory, the initial rise of the water table is fast at the beginning of the hydraulic loading then the rise slows down with time. Referring to the data of piezometer 30 in Figure 10, the water table elevation 26.46 m at week 12 could be considered as the 'base line' for the measurement of the net groundwater mound. Therefore, in April 1978, the maximum increase of the water table was 2.75 m. This large increase was the result of the combined effect of the hydraulic loading to the leaching bed and the infiltration of surface water from the 1978 spring thaw. From week 100 to week 126, the net rise of the water table was maintained at 1.5 m and

TABLE 12

COMPARISON OF HANTUSH CALCULATED GROUNDWATER MOUND WITH FIELD DATA

Loading Rate = 40,900 L/d: f = 0.2: H = 12 m

Location From Bed Centre = 16.0 m East or West; 10.7 m North or South

Days	FIELD DATA (m) Average of 23, 24, 25, 26, 28, 29, 30, 31	'k' (m/d)	0.43	0.32	0.03
		(cm/s)	5.0×10^{-4}	3.7×10^{-4}	3.5×10^{-5}
100	For 26 weeks		1.30	1.53	3.43
200	(week 100 to		1.67	2.00	5.77
300	week 126 of		1.89	2.29	7.44
400	study)		2.04	2.49	8.71
500	1.54		2.17	2.64	9.71

Loading Rate = 40,900 L/d: f = 0.2: H = 8 m

Location From Bed Centre = 16.0 m East or West; 10.7 m North or South

Days	FIELD DATA (m) Average of 23 24, 25, 26, 28, 29, 30, 31	'k' (m/d)	0.43	0.32	0.03
		(cm/s)	5.0×10^{-4}	3.7×10^{-4}	3.5×10^{-5}
100	For 26 weeks		1.59	1.84	3.59
200	(week 100 to		2.09	2.47	6.23
300	week 126 of		2.39	2.85	8.16
400	Study)		2.59	3.12	9.62
500	1.54		2.79	3.32	10.78

There was very little fluctuation in the elevation of the water table. However, for piezometer 2, the elevation of the water table during the same period was approximately at the same elevation before the hydraulic loading of 40,900 L/d was applied to the bed. As pointed out before, piezometer 2 was not affected significantly by the hydraulic loading in the bed. That is to say, the fluctuation of the water table at this location was mainly due to precipitation and evapotranspiration. Because piezometers 30 and 2 were located not more than 150 m apart, it may be assumed that the climatic influence on the water table at these locations was about equal. Therefore, if the water table at piezometer 30 had not been affected by the many weeks of hydraulic loading, the water table would have returned close to elevation 26.46 m. However, the net rise of the water level in piezometer 30 with respect to elevation 26.46 m was 1.54 m. Therefore, it can be inferred that this groundwater mound was the result of many weeks of hydraulic loading in the leaching bed.

The measured net rise (1.54 m) in the water in day 500 was smaller than the predicted values summarized in Table 12. The main reasons could be:

(i) the average effective hydraulic loading was less than 40,900 L/day;

(ii) the field-determined and the 'back-calculated' 'k' values were too small, and

(iii) the effective thickness of the aquifer was greater than the assumed 12 m.

3.4 Groundwater Mounding Analysis by Sykes' Finite-Element Model

The extent of the groundwater mounding under the leaching bed at the site was also calculated by Sykes' computerized model, which is described in the appendix. In using the finite-element computer model, the test site area is first divided into many small areas (elements) each of which has four corners (nodes) (Figure 16). To facilitate the comparison of the computer and experimental results, some of the nodes were placed at the piezometer locations.

In Figures 17 and 18, the computed results by Sykes' model for two loading rates are compared with those of Hantush for a constant H = 12 m and the field data.

Because Sykes' finite-element model has the flexibility of varying the input data (e.g. 'f', 'k', 'H' and hydraulic loading rate, etc.) in each element, it was decided not to use a constant aquifer thickness in the additional analyses. Instead, the thickness of the aquifer was calculated by subtracting the elevation of the water table prior to the testing program from the elevation of the bedrock as determined by geophysical techniques. In Figures 19 and 20, the computed results are compared with results obtained by the Hantush analyses, in which the thickness of the aquifer was assumed to be 12 m.

As can be seen in Figures 17, 18, 19 and 20, good comparison of results was observed between Sykes' and the Hantush model.

3.5 Discussion on Groundwater Mounding

From the extensive groundwater monitoring study conducted at Norwood, Ontario, experience and knowledge can be gained in two areas:

(i) the fluctuations of the water table beneath a large leaching bed including the relative important influence of precipitation and evaporation on groundwater mounding, and

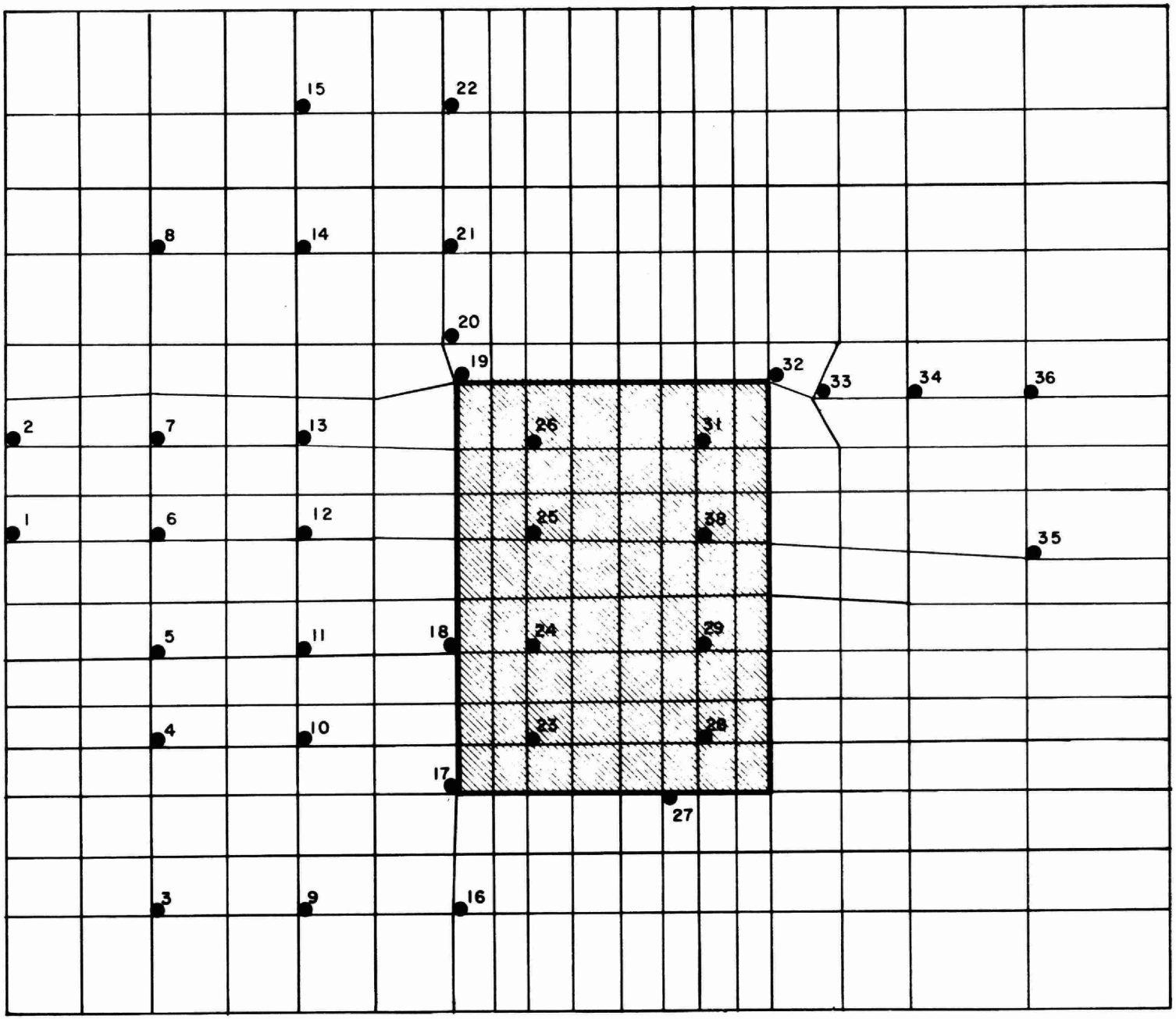

Figure 16 : Finite Elements and Nodes Used in the Sykes Model for the Study Area

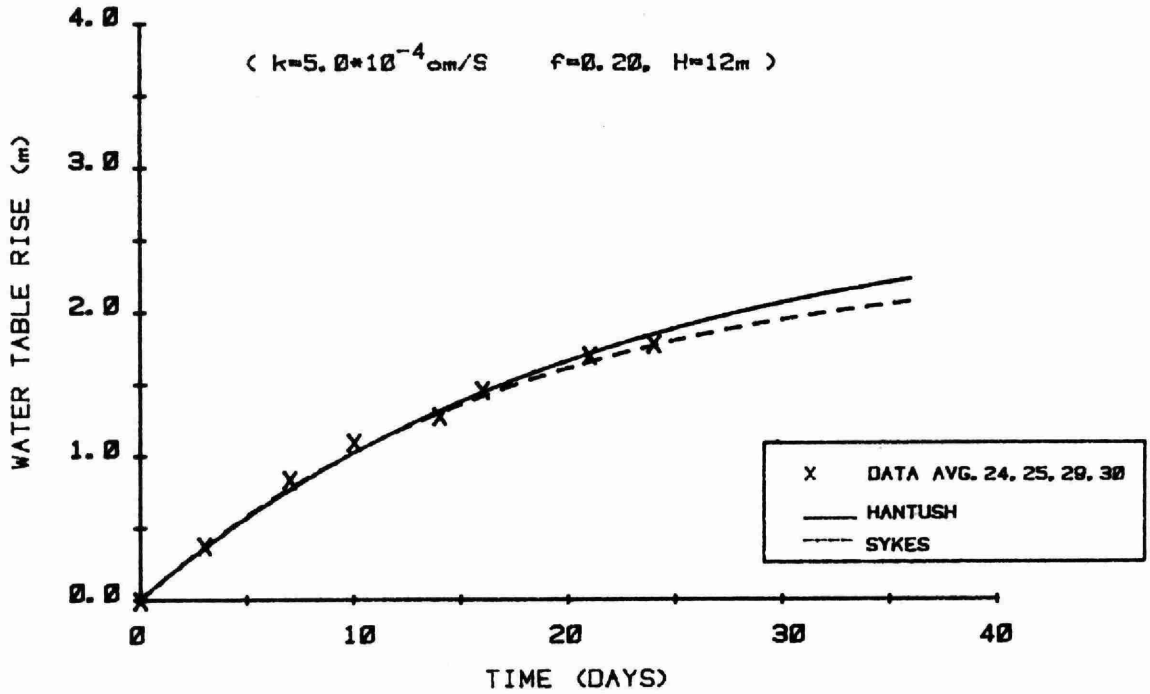

FIGURE 17 SYKES' COMPUTED RESULTS COMPARED TO HANTUSH (LOADING RATE 122700 L/day)

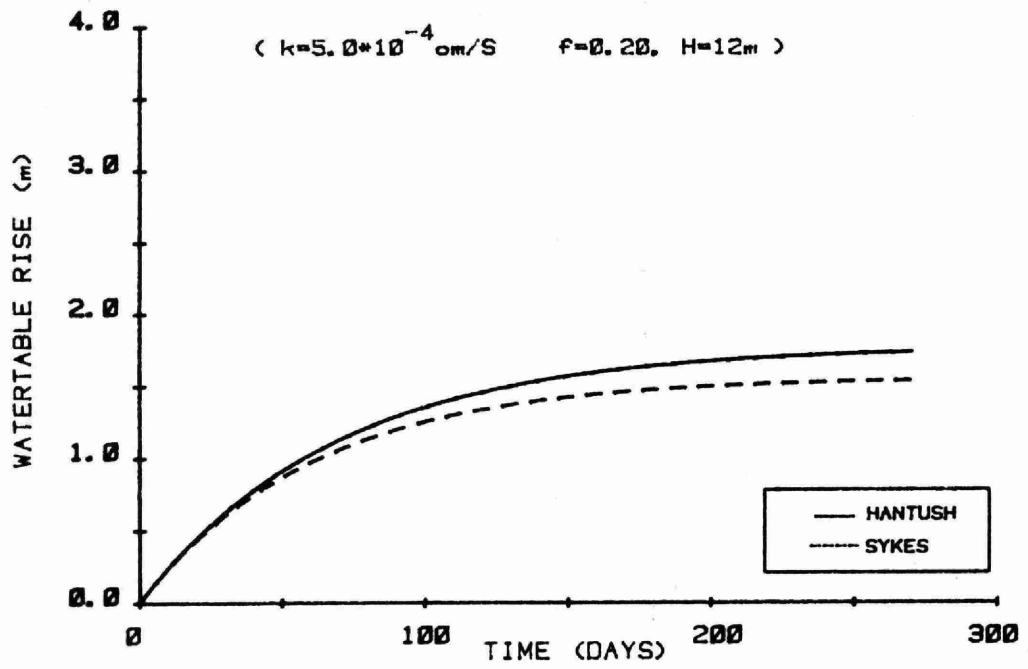

FIGURE 18 SYKES' COMPUTED RESULTS COMPARED TO HANTUSH (LOADING RATE 40900 L/day)

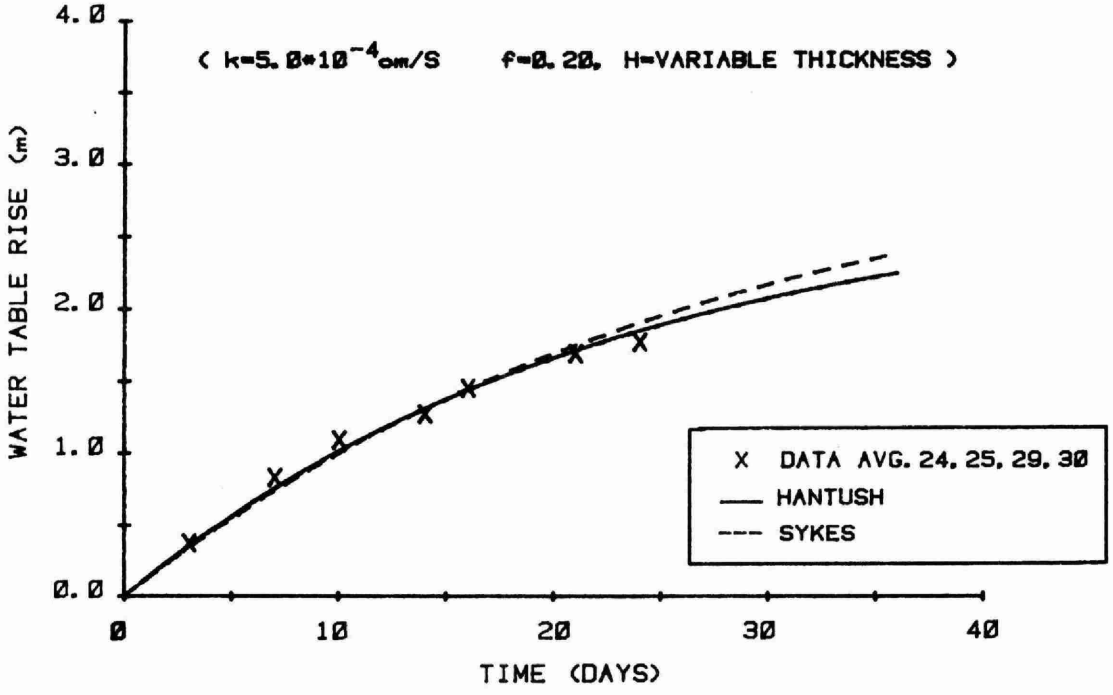

FIGURE 19 SYKES' COMPUTED RESULTS COMPARED TO HANTUSH (LOADING RATE 122700 L/day)

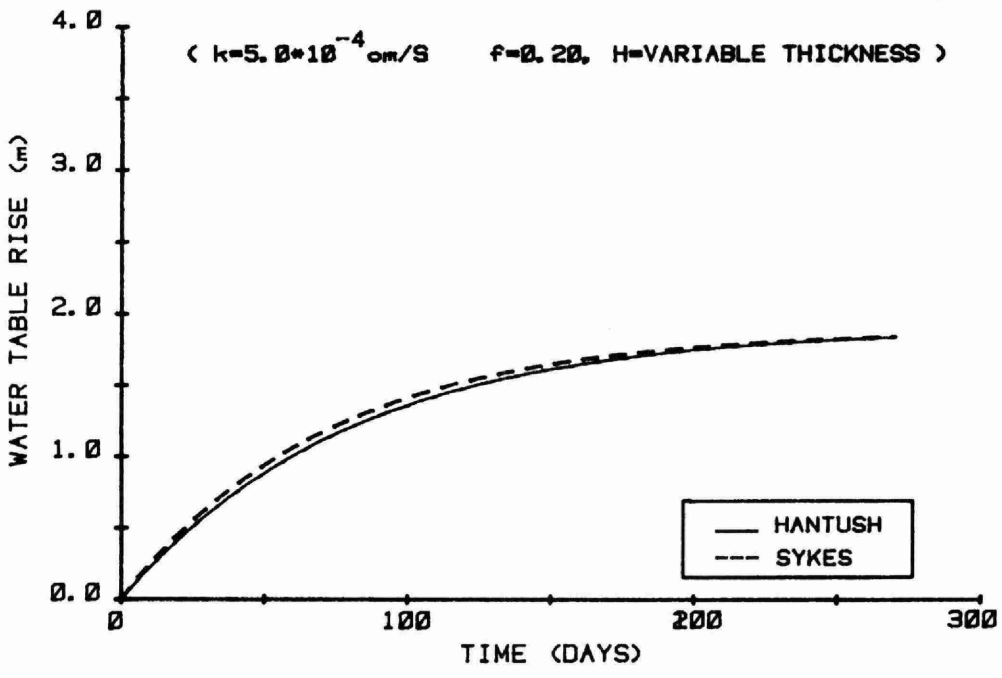

FIGURE 20 SYKES' COMPUTED RESULTS COMPARED TO HANTUSH (LOADING RATE 40900 L/day)

(ii) the practical use of two mathematical tools, (i.e. Hantush and Sykes) for the prediction of groundwater mounding beneath a recharge area or basin.

As discussed in sections 3.3 and 3.4, both the Hantush and Sykes methods gave reasonable, although conservative, predictions of the groundwater mounding under a large leaching bed provided that,

(i) the 'back-calculated' 'k' value or the right selection of the field-determined 'k' value was used, and

(ii) for the Hantush model, the rapid groundwater rise caused by a large quantity of infiltration at the time of spring thaw was not considered because of the model's requirement of a constant hydraulic loading rate.

These assumptions lead to a number of practical considerations in the prediction of the groundwater mounding under a recharge basin (or area) such as a leaching bed.

(i) In the calculation of the magnitude of the groundwater mound, values of soil (or aquifer) parameters are required. In this study, these values were obtained either by 'back-calculation' from the field data or by actual measurements in a number of boreholes made at the site. The mounding prediction was reasonable when the 'back-calculated' 'k' value or the 'k' value determined by the 'falling head' and the 'recovery' methods was used. As a result of this study, it is felt that the 'falling head' and the 'recovery' 'k' tests in piezometers are suitable for sandy silt soils. However, it is not certain whether these field tests would yield reasonable 'k' results for clayey soils for the groundwater mounding calculations. Perhaps, a model-scale field test or a field pumping test would give more meaningful 'k' and specific yield (s) results for fine-grained, cohesive soil deposits.

(ii) In this study, it was found necessary to consider the water table rise caused by the spring infiltration in order not to underestimate the maximum mounding. As indicated in Figure 10, the rise of the water table at various seasons was different. This was only reasonable because of the stochastic nature of climatic conditions. Therefore, in the design, it would be necessary to study weather data (precipitation, evaporation, temperature, etc.) at a potential site for as many years as practically feasible. In addition, prior to the installation of a leaching bed at a potential site, it is useful to install a number of piezometers at the site to monitor the natural fluctuations of the water table for a minimum of one year. The one-year water table fluctuation data, together with the weather data from past years can be used to make a reasonable estimate of the maximum rise of the water table at the potential site. A statistical approach may be used to predict the probability of the occurrence of the maximum rise in the water table due to spring thaw infiltration and the calculated mound caused by the design hydraulic loading in the leaching bed. In selecting the probable maximum rise of the water table due to spring infiltration, the designer should consider the chance for the occurrence of this maximum and the effect of surface flooding due to the excessive rise of the water table.

As a precautionary measure, a few piezometers may be installed near the centre of the leaching bed and the water table during the operation of the bed will be monitored. It may also be feasible to adjust the hydraulic loading rate in the leaching bed at the time of the spring thaw in order to avoid flooding of the bed.

(iii) In this study, both the Hantush and Sykes methods were used for the calculation of the groundwater mound. Because of the simplicity of the Hantush method, it would be a more practical tool for routine

calculations. Furthermore, at the present time, the inaccuracy in the prediction of mounding lies more in the inability to practically assess the overall soil properties.

However, it should be pointed out that the Sykes model has a number of flexible features which Hantush's method does not have. For example, in each element of Sykes' model, the soil properties, the infiltration rate and the thickness of the aquifer can be different. Therefore, Sykes' model can be used as a refined design tool if the soil properties at a potential site can be measured with reasonable accuracy. In addition, the Sykes finite-element model can more accurately represent the groundwater loading caused by seasonally varying infiltrations. For the Norwood site, the effect of spring infiltration was greater than that of the hydraulic loading of 40,900 L/d. As stated in the discussion of the Hantush model, the model assumes zero infiltration outside of the leaching bed. This assumption is not necessary with the finite-element analyses. Therefore, for sites in which natural infiltration or soil heterogenetics are important, a finite-element type analysis may be warranted.

GROUNDWATER CONTAMINATION

4.0 GROUNDWATER CONTAMINATION

The magnitude and extent of groundwater contamination due to subsurface sewage effluent disposal were investigated by conducting a regular and comprehensive sampling program to monitor the variation of contaminants concentration with time, distance and depth, under and in the vicinity of the leaching bed.

Type 'A' wells were used to monitor the contaminants concentration inside and outside the boundary of the leaching bed, while the multi-level Type 'B' wells were used to measure the concentrations at different depths within the perimeter of the leaching bed.

Since chemical pollutants travel farther and persist longer than bacterial pollutants (10), it was decided to restrict this investigation to chemical contamination of the groundwater. Because of the ease of monitoring and typical behaviour characteristics of certain chemicals to enter and move freely within an aquifer (2, 20, 21, 27, 28), this study is mainly focused on subsurface movement of chloride, nitrate, sulphate, sodium, calcium, hardness and conductivity. Concentration levels of other contaminants and parameters in the case of sewage effluent feed are included.

Chemical analyses of all the groundwater samples collected were performed using standard analytical methods (16, 33), in the Central Laboratories of the Ministry of the Environment, in Toronto.

All the statistical values and graphs that are presented were analyzed on an electronic computer (HP - 9825A) and are based on standard mathematical equations and statistical curves.

4.1 Variation in Chemical Concentration of Groundwater

In order to study the effect of the subsurface sewage effluent disposal on the quality of groundwater, variation in the chemical concentrations of the groundwater were monitored before and after the disposal of sewage effluent.

4.1.1 Background Concentration (C_b)

A 12 week sampling program of the groundwater was conducted in the project area to establish the natural quality of the groundwater before subsurface disposal. Because of a wide difference in the background concentration values between the north and south ends of the leaching bed, it was decided to use the lowest of the background values recorded at the individual sampling well locations for calcium, sulphate, hardness and conductivity. The field averages were used for chloride, sodium and nitrate. The analyses results of these samples are presented in Table 13.

4.1.2 Feed Concentration (C_o)

The chemical concentration of the feed (before subsurface disposal) during the total time of the study, could be grouped under three main periods.

Period 1, covered the time between October 5, 1976 and November 10, 1976 when the hydraulic loading rate was 122,700 L/d.

Period 2, was a rest period between November 10, 1976 and May 17, 1977 when the operation of the system was stopped due to bed failure. However, the quality of the plant effluent was monitored during this time.

Period 3, began on May 17, 1977 when the operation of the system was re-started and the loading was maintained at a reduced rate of 40,900 L/d to December 13, 1978.

TABLE 13

BACKGROUND CHEMICAL CONCENTRATION IN THE GROUNDWATER
BEFORE SUBSURFACE DISPOSAL

Well No.	Average Background Concentrations in mg/L						
	Nitrate	Chloride	Sodium	Calcium	Sulphate	Conductivity *	Hardness
1	0.10	2.1	1.2	14	5	89	38
2	0.11	2.7	1.9	11	7	144	74
3	0.17	4.7	4.0	40	19	200	111
4	0.70	4.4	3.8	28	17	230	101
5	0.10	4.4	2.8	14	5	57	23
6	0.32	4.2	1.6	11	4	61	25
7	0.10	3.3	2.5	14	11	82	35
8	0.15	4.4	2.0	15	11	85	35
9	0.40	4.3	2.7	29	9	160	88
10	0.18	4.5	6.2	38	14	208	114
11	0.10	5.8	5.7	44	25	280	147
12	0.14	4.4	4.8	44	13	256	160
13	0.10	4.3	4.2	25	17	220	100
14	0.14	5.0	1.5	19	9	75	55
15	0.40	4.6	4.4	17	11	117	46
16	0.73	5.8	4.2	62	23	335	194
17	0.18	3.7	6.5	103	20	578	366
18	0.10	4.6	4.8	49	20	307	165
19	0.10	6.2	2.8	42	19	255	135
20	0.13	7.3	2.3	25	20	220	120
21	0.10	7.1	1.9	25	17	215	100
22	0.40	5.8	6.5	20	16	133	54
23	0.13	2.8	6.1	120	30	564	328
24	0.10	3.1	4.7	32	16	209	107
25	0.43	3.9	2.9	35	21	208	109
26	0.18	3.8	2.8	45	25	265	144
27	0.10	5.5	6.8	89	18	438	258
28	0.10	3.0	7.8	94	21	549	306
29	0.10	3.3	10.0	91	26	527	297
30	0.15	5.9	7.1	67	26	392	210
31	0.12	5.6	4.8	39	21	240	124
32	0.99	4.0	3.7	23	15	164	78
33	0.10	2.8	4.5	27	12	195	103
34	0.17	5.5	3.9	28	16	195	90
35	0.10	4.8	3.3	32	11	355	185
36	0.30	3.0	2.7	26	7	210	81
Avg.	0.23	4.4	5.5	36	16	215	110

* Conductivity reported in µmhos/cm

TABLE 14

CHEMICAL CONCENTRATIONS IN THE FEED BEFORE SUBSURFACE DISPOSAL

Chemicals and Other Parameters *	PERIOD 1 Loading Rate 122 700 L/d			PERIOD 3 Loading Rate 40 900 L/d			Total for Loading Periods 1 and 3		
	No. of Samples	Range	Mean	No. of Samples	Range	Mean	No. of Samples	Range	Mean
BOD_5	6	4-12	6.5	60	1-30	8.7	66	1-30	8.5
Suspended Solids	6	5-15	6.8	58	<5-20	8.5	64	<5-20	8.3
Total Nitrogen (as N)	6	24-36	27.4	56	13-32	20.1	62	13-36	20.8
Nitrate (as N)	6	22-32	25.0	56	4-26	15.5	62	4-32	16.4
Sodium (as Na)	6	67-81	74	55	60-100	75	61	60-100	75
Potassium (as K)	6	11-15	12.2	54	6-15	9.7	60	6-15	10.0
Chloride (as Cl)	6	81-104	90	53	75-154	104	59	75-154	103
Calcium (as Ca)	6	100-116	105	53	101-139	116	59	100-139	115
Sulphate (as SO_4)	6	59-79	68	56	41-98	64	62	41-98	65
Conductivity (µmhos/cm)	6	850-1010	947	51	910-1120	1009	57	850-1120	1002
Hardness (as $CaCo_3$)	6	295-306	297	55	280-379	320	61	280-379	318
Alkalinity (as $CaCo_3$)	6	163-205	190	59	162-300	226	65	162-300	223
Magnesium (as Mg)	2	9-12	10.5	53	5-11	7.4	55	5-12	7.5
pH	6	7.3-7.9	7.6	58	6.4-8.6	7.7	64	6.4-8.6	7.7

* All concentrations are reported in mg/L except Conductivity and pH values.

Table 14 shows the range and mean values of the chemical concentrations and other parameters in the feed for periods 1 and 3 and for the total period, (period 1 and 3), of subsurface effluent disposal.

The variation in the quality of the Norwood Sewage Treatment Plant secondary effluent for the total study period is shown in Table 15 which indicates the concentration levels of the selected contaminants and parameters for 15%, 50% and 85% of the time.

TABLE 15

VARIATION IN QUALITY OF PLANT SECONDARY EFFLUENT FOR THE TOTAL STUDY PERIOD

Chemicals and Other Parameters (mg/L)	No. of Samples	Values % of Time Equal to or Less Than		
		15%	50%	85%
Total Nitrogen	82	16.9	20.8	25.7
Sodium	77	66.8	74.4	82.9
Chloride	80	81.2	99.7	122.3
Calcium	80	102.6	112.5	123.3
Sulphate	82	54.4	63.8	74.9
Conductivity *	78	945.7	974.6	1004.3
Hardness	83	282.0	311.5	344.2

* Conductivity reported in µmhos/cm

4.1.3 Chemical Concentration of Groundwater After Disposal (C)

Table 16 shows the maximum concentration level of the selected contaminants recorded at the sampling well locations in the project site. The highest of the maximum recorded concentrations of nitrate, chloride and sodium occurred at well location 25; of calcium, sulphate and hardness at well location 11 and conductivity at well location 27. The high concentrations of calcium, conductivity and hardness, indicated near the southern corner of the leaching bed, could probably be due to the deposits of limestone in that part of the site.

4.1.4 Concentration Variation with Time

Figures 21, 22, 23, 24, 25, 26 and 27 indicate contaminants concentration variation with time in relation to the natural background levels and feed concentrations for the loading period, at the sampling well locations where highest concentration of contaminants were recorded.

4.1.5 Concentration Variation with Distance

Figures 28, 29, 30, 31, 32, 33 and 34 show the concentration variations from C/C_o = 1.0 to 0.1, with respect to distance from the centre of the leaching bed, for selected weeks. In general, concentration of the contaminants decreased with an increase in distance away from the leaching bed.

The maximum displacement of contaminants in week 146 at the concentration level C/C_o = 0.1 was 85 m for chloride, 82 m for nitrate, 96 m for sulphate, 73 m for sodium, 104 m for hardness, 98 m for calcium and conductivity.

4.1.5 Concentration Variation with Depth

Figures 35, 36, 37, 38, 39, 40 and 41 show the concentration levels of the contaminants at selected depths. Each concentration value represents an average of some 40-46 samples collected at each sampling

TABLE 16

MAXIMUM CONCENTRATION LEVELS OF CONTAMINANTS RECORDED IN THE SAMPLING WELLS AFTER SUBSURFACE DISPOSAL

Well No.	Concentration of Contaminants in mg/L						
	Nitrate	Chloride	Sodium	Calcium	Sulphate	Conductivity *	Hardness
1	0.2	4	3	30	8	176	95
2	4.4	6	3	39	30	248	122
3	0.7	7	8	88	22	490	243
4	5.7	24	7	72	67	490	188
5	0.7	7	6	44	20	290	138
6	0.5	6	4	41	26	261	134
7	0.8	5	4	46	20	253	122
8	1.2	8	4	39	24	245	120
9	1.6	8	7	86	30	500	257
10	8.3	76	11	146	60	860	435
11	15.0	102	41	212	90	1070	532
12	10.0	45	5	92	34	580	288
13	5.4	31	7	91	33	490	296
14	2.7	11	4	50	24	320	158
15	4.2	6	7	54	28	394	174
16	1.4	19	7	115	41	650	345
17	6.4	39	15	118	57	710	372
18	17.0	96	54	130	72	900	400
19	24.0	100	69	141	70	970	414
20	21.0	96	53	154	69	1000	430
21	3.4	54	8	132	37	700	383
22	13.0	15	11	137	30	780	425
23	14.0	91	23	150	65	939	481
24	16.0	74	11	122	57	730	364
25	27.0	110	82	155	80	1060	466
26	22.0	97	73	136	70	1060	396
27	20.0	104	60	162	66	1110	480
28	13.0	88	13	162	69	970	491
29	16.0	85	38	149	63	960	460
30	18.0	87	20	148	63	910	429
31	22.0	88	45	180	70	1080	517
32	21.0	75	23	122	59	760	354
33	17.0	75	6	100	54	710	348
34	1.2	7	7	60	30	380	199
35	0.4	7	6	94	46	510	286
36	0.6	6	5	104	28	533	296
Highest Value	27	110	82	212	90	1110	532

* Conductivity reported in µmhos/cm

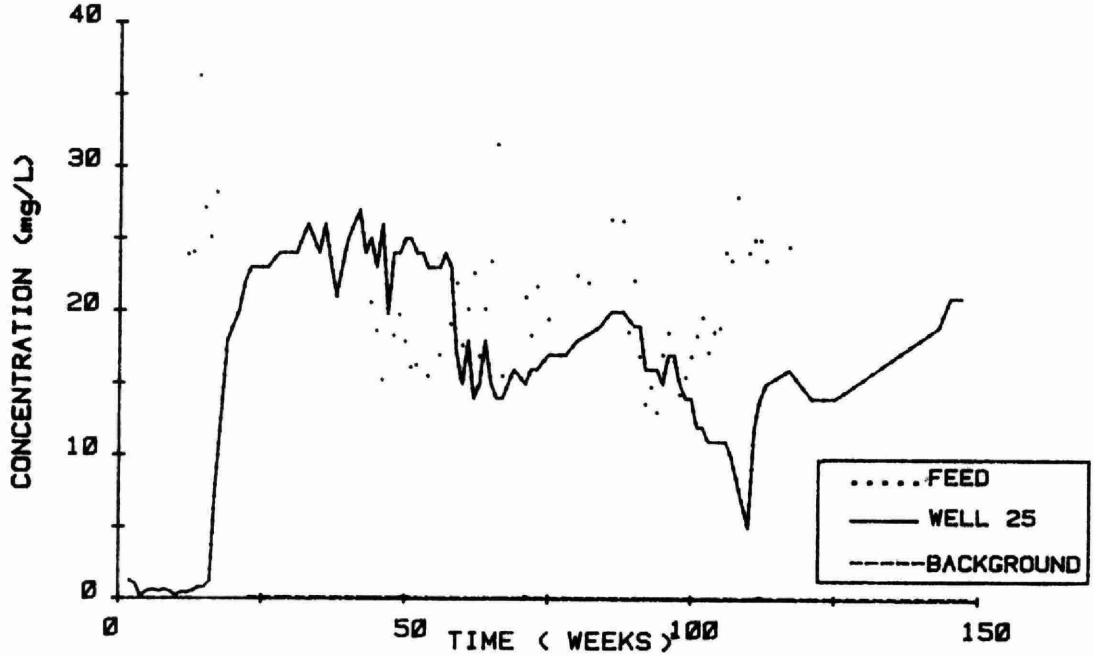

FIGURE 21 VARIATION OF NITRATE IN THE GROUNDWATER AFTER DISPOSAL AT SAMPLING WELL LOCATION INDICATING HIGHEST CONCENTRATION

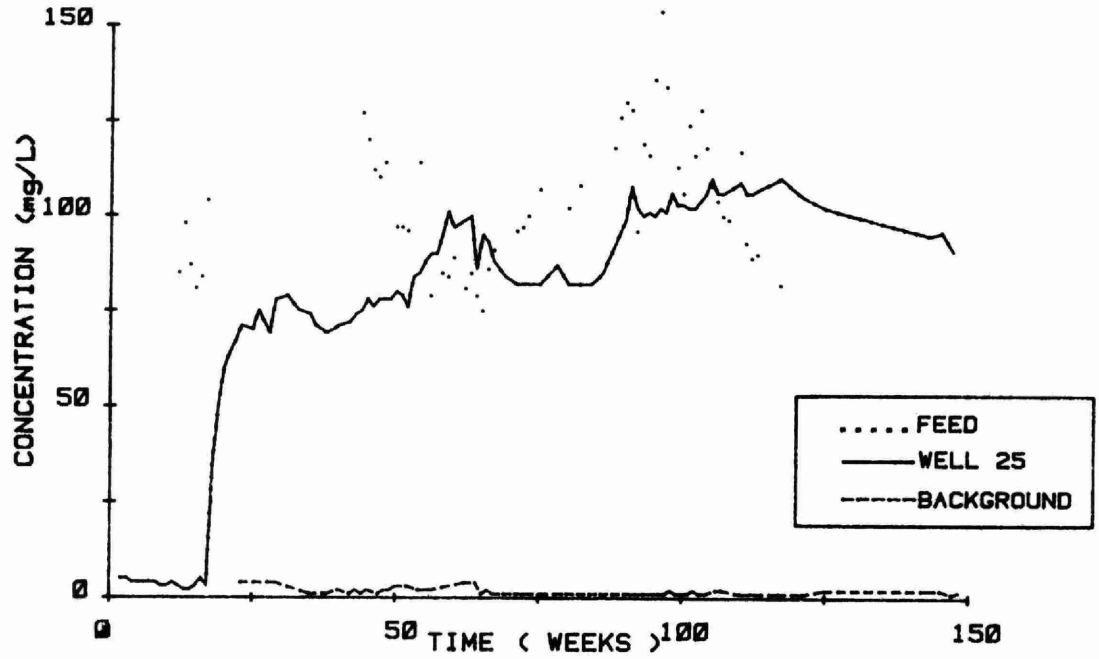

FIGURE 22 VARIATION OF CHLORIDE IN THE GROUNDWATER AFTER DISPOSAL AT SAMPLING WELL LOCATION INDICATING HIGHEST CONCENTRATION

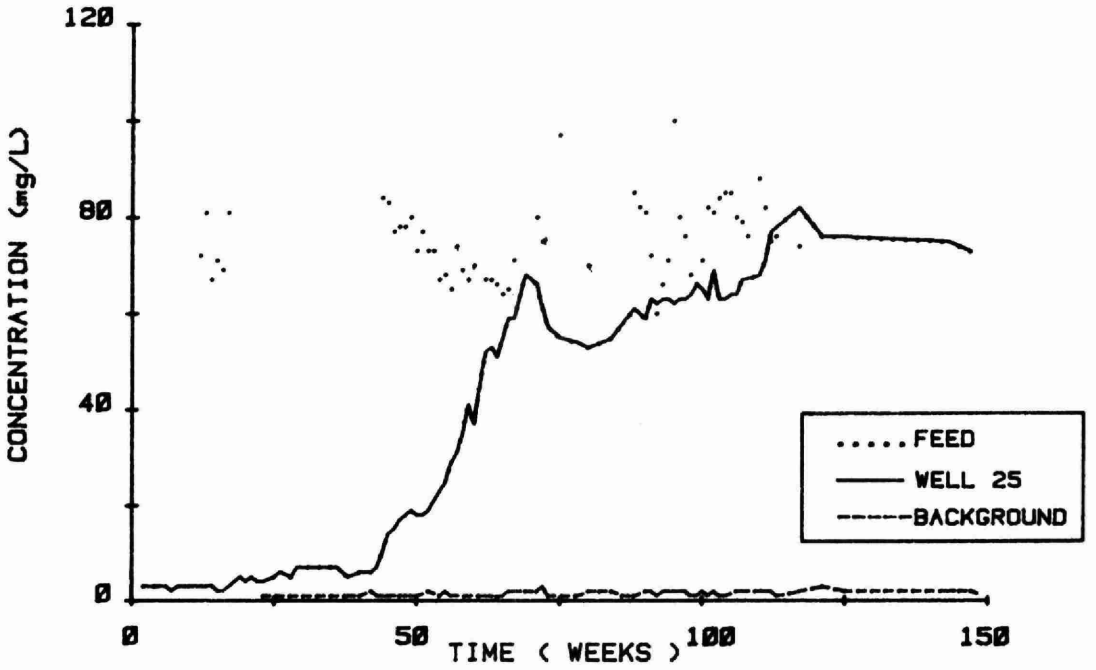

FIGURE 23 VARIATION OF SODIUM IN THE GROUNDWATER AFTER DISPOSAL AT SAMPLING WELL LOCATION INDICATING HIGHEST CONCENTRATION

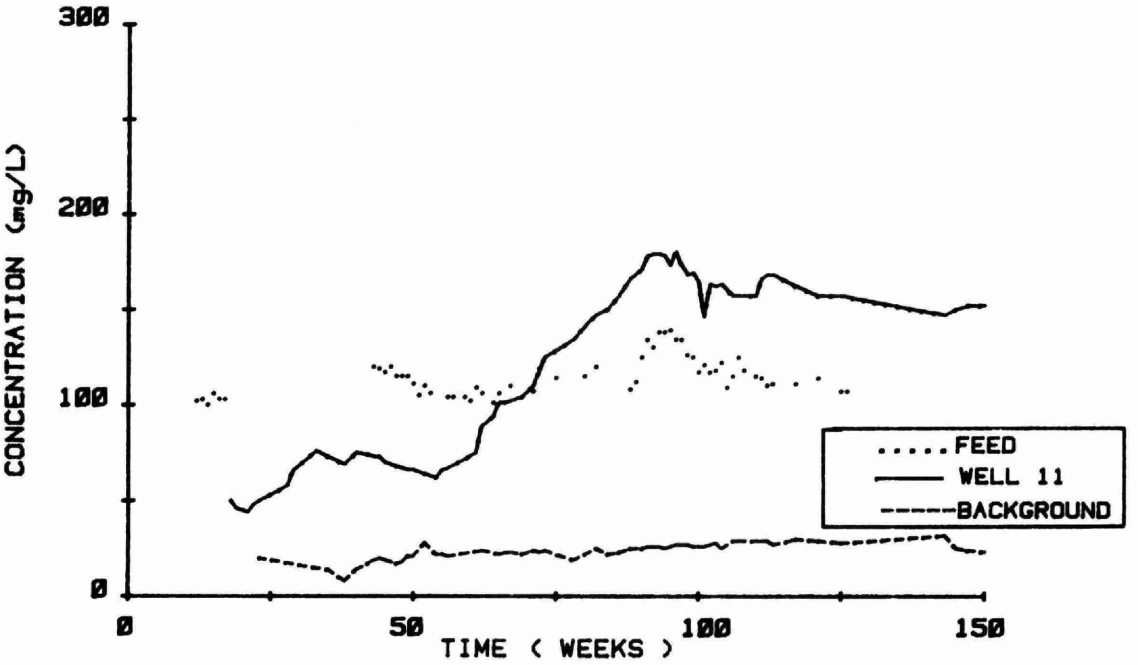

FIGURE 24 VARIATION OF CALCIUM IN THE GROUNDWATER AFTER DISPOSAL AT SAMPLING WELL LOCATION INDICATING HIGHEST CONCENTRATION

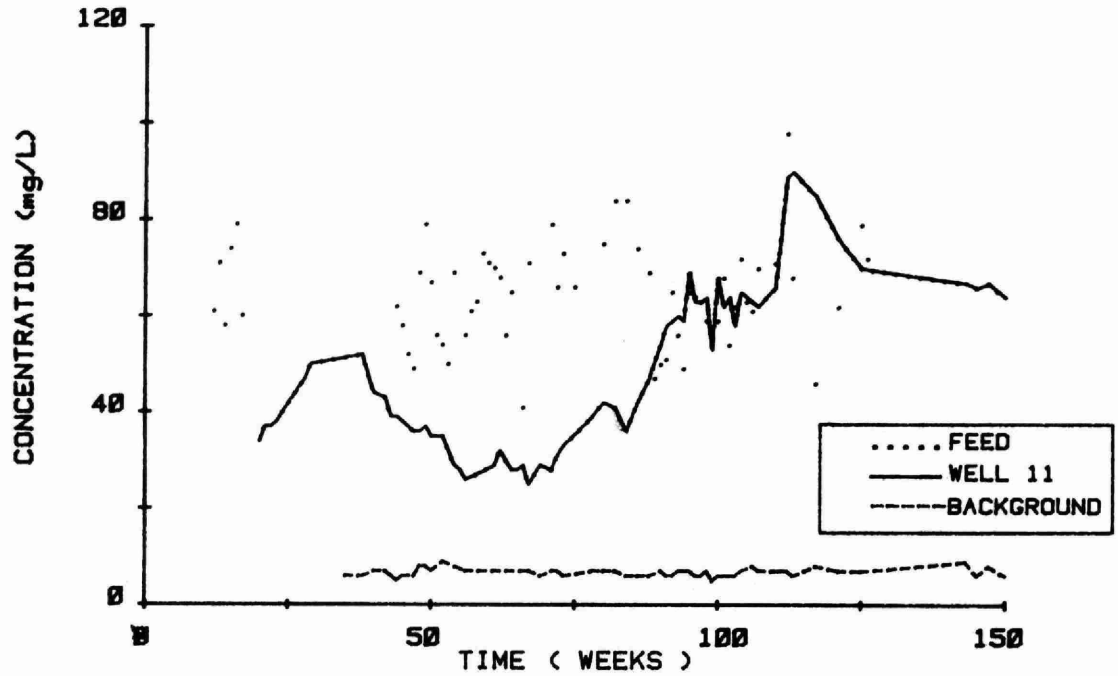

FIGURE 25 VARIATION OF SULPHATE IN THE GROUNDWATER AFTER DISPOSAL AT SAMPLING WELL LOCATION INDICATING HIGHEST CONCENTRATION

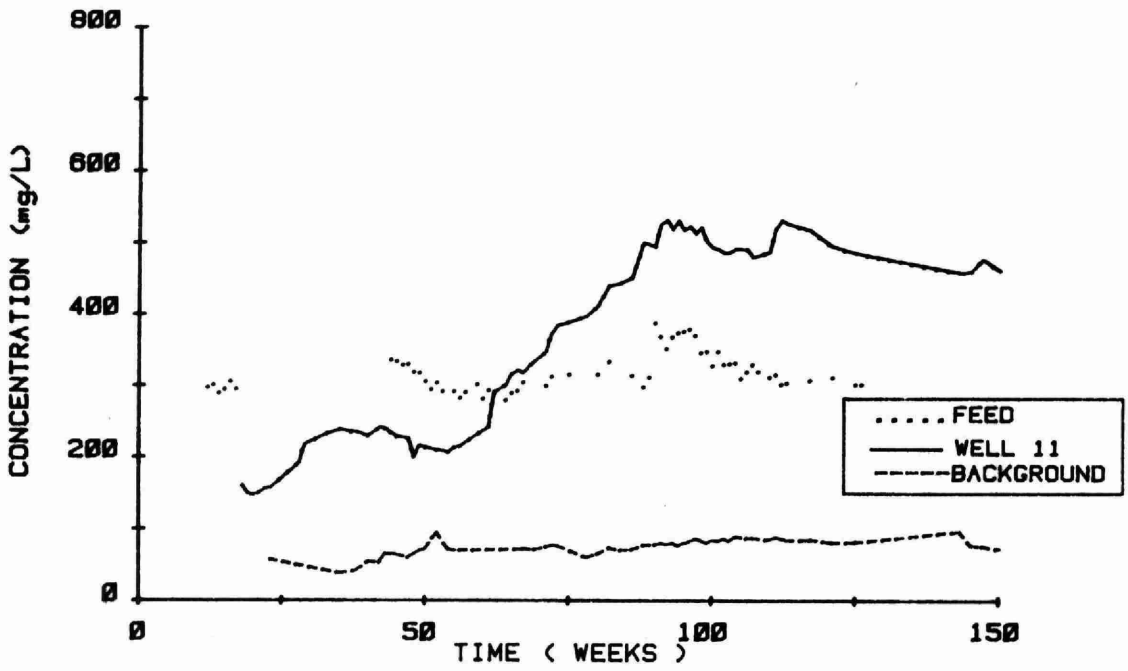

FIGURE 26 VARIATION OF HARDNESS IN THE GROUNDWATER AFTER DISPOSAL AT SAMPLING WELL LOCATION INDICATING HIGHEST CONCENTRATION

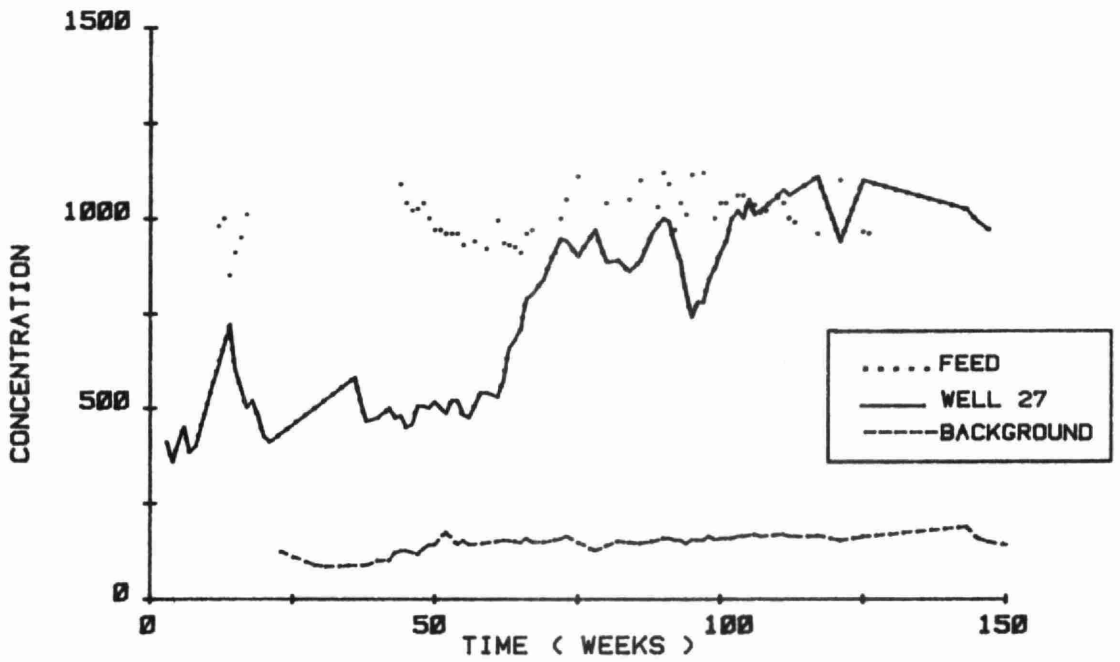

FIGURE 27 VARIATION OF CONDUCTIVITY IN THE GROUNDWATER AFTER DISPOSAL AT SAMPLING WELL LOCATION INDICATING HIGHEST CONCENTRATION

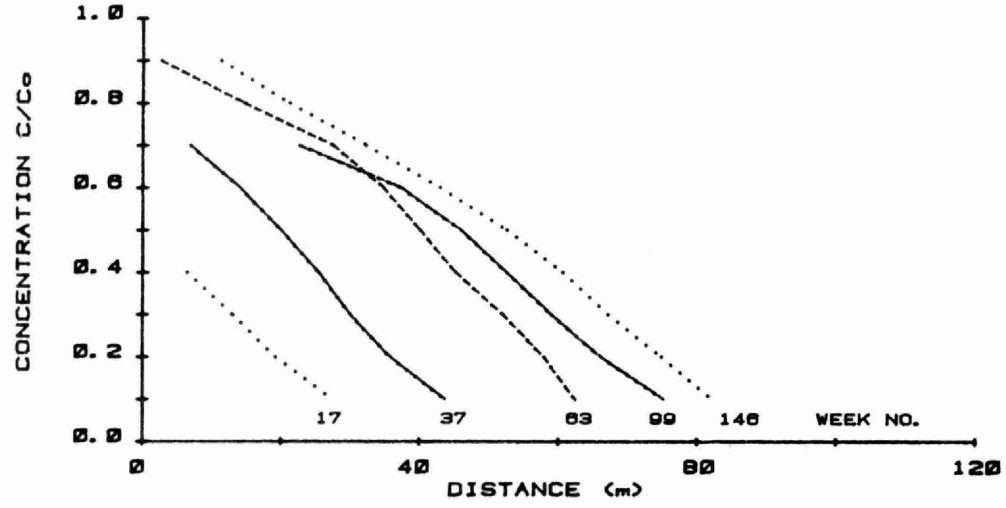

FIGURE 28 VARIATION OF NITRATE CONCENTRATION WITH DISTANCE FOR SELECTED WEEKS

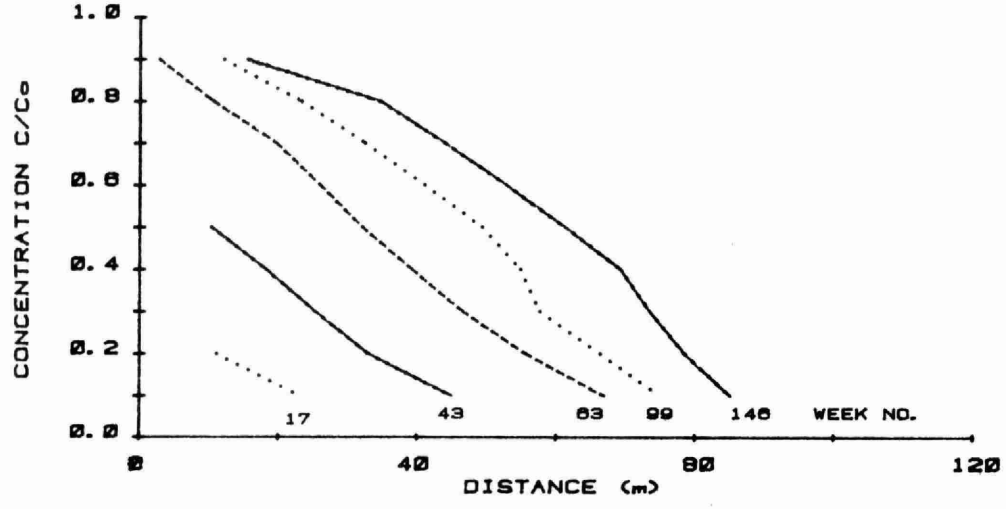

FIGURE 29 VARIATION OF CHLORIDE CONCENTRATION WITH DISTANCE FOR SELECTED WEEKS

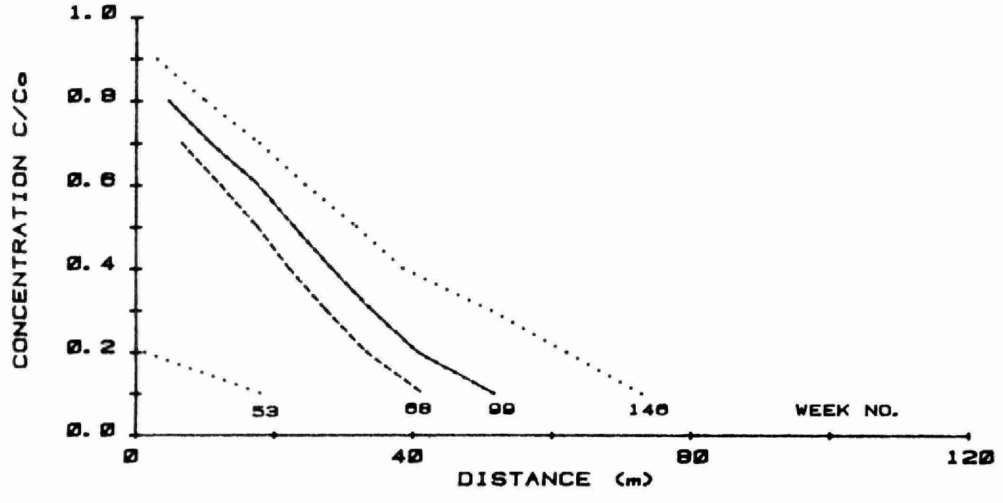

FIGURE 30 VARIATION OF SODIUM CONCENTRATION WITH DISTANCE FOR SELECTED WEEKS

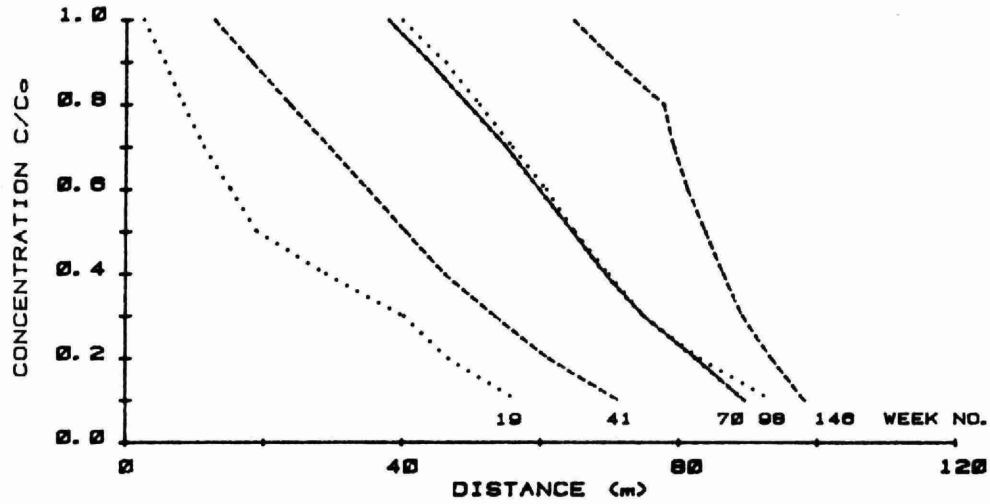

FIGURE 31 VARIATION OF CALCIUM CONCENTRATION WITH DISTANCE FOR SELECTED WEEKS

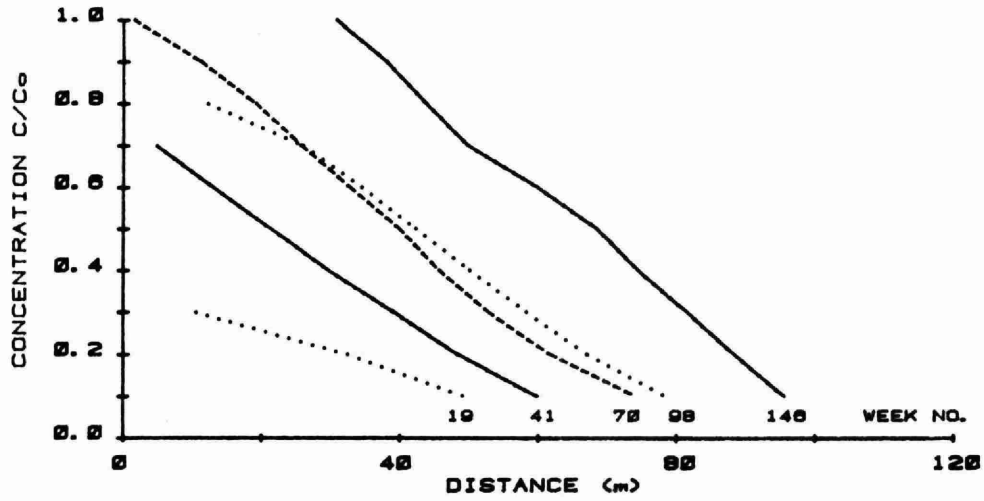

FIGURE 32 VARIATION OF SULPHATE CONCENTRATION WITH DISTANCE FOR SELECTED WEEKS

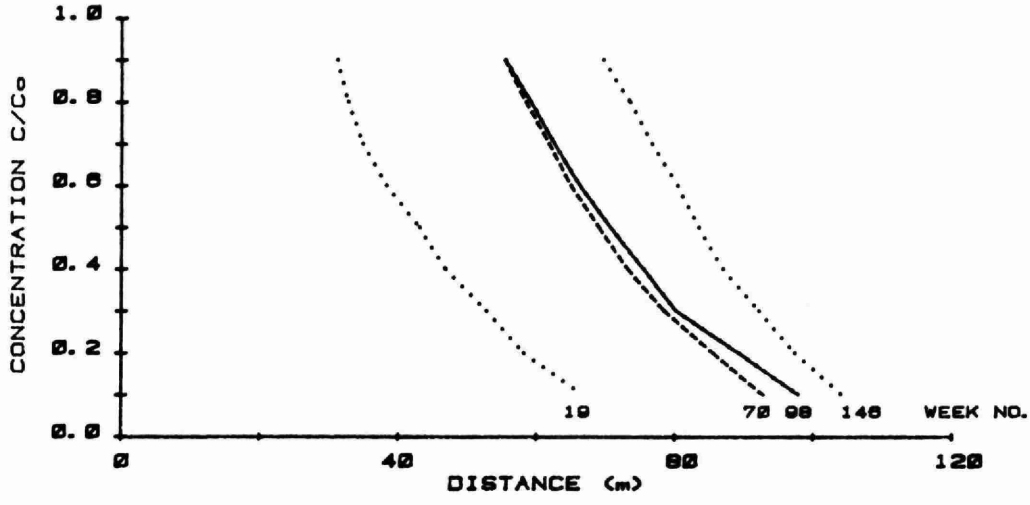

FIGURE 33 VARIATION OF HARDNESS CONCENTRATION WITH DISTANCE FOR SELECTED WEEKS

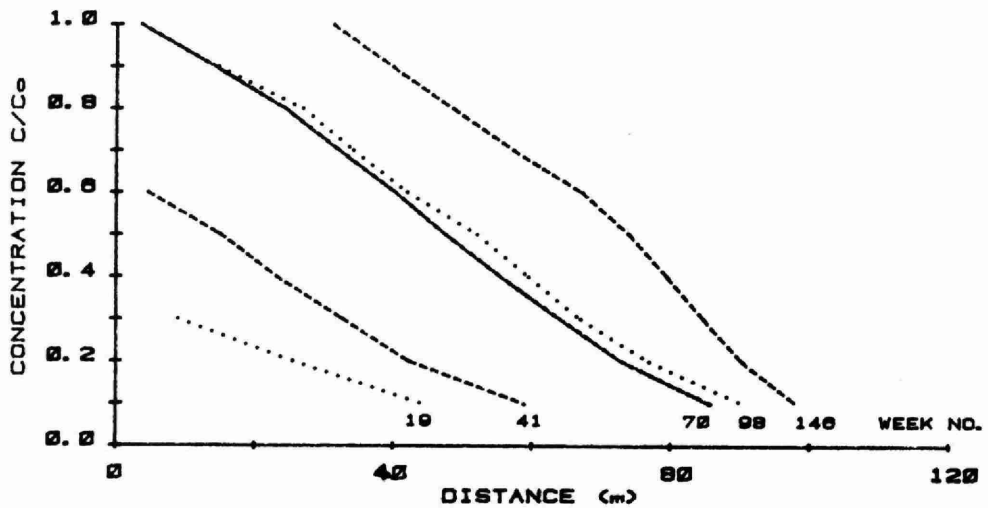

FIGURE 34 VARIATION OF CONDUCTIVITY CONCENTRATION WITH DISTANCE FOR SELECTED WEEKS

FIGURE 35 CONCENTRATION OF NITRATE AT SELECTED DEPTHS BELOW THE WATER TABLE (mg/L)

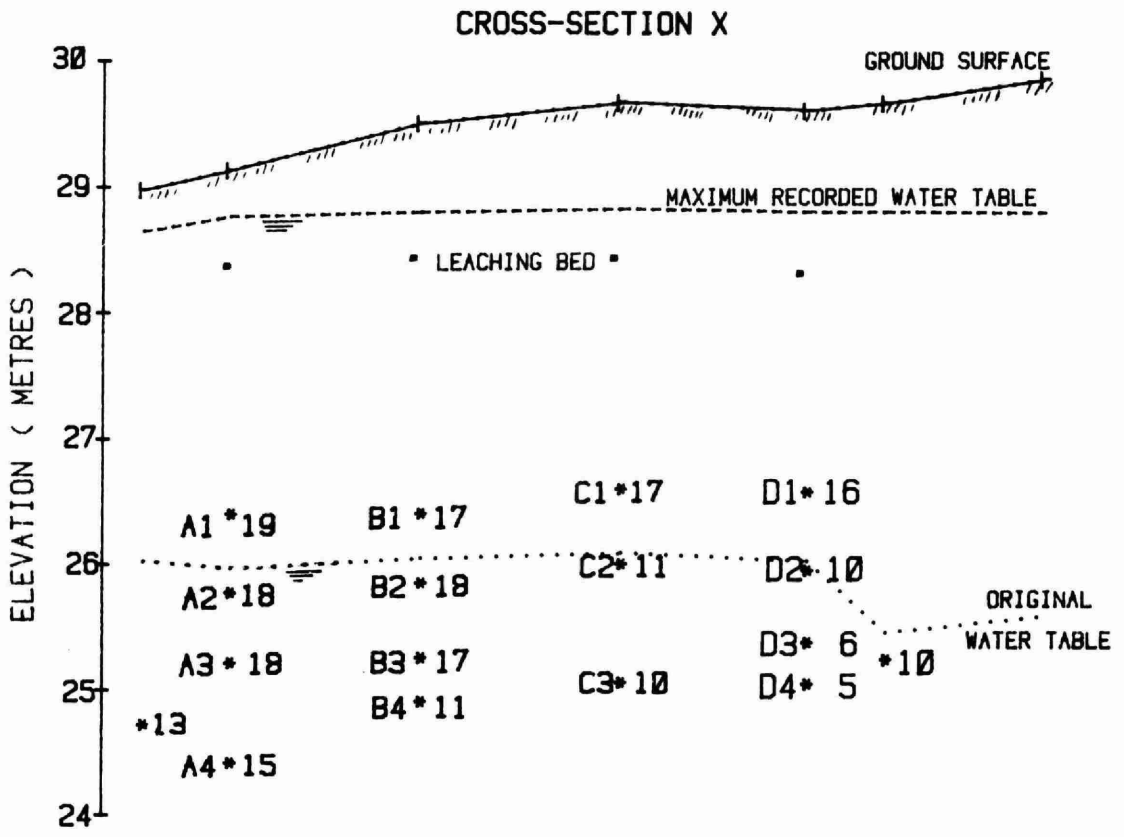

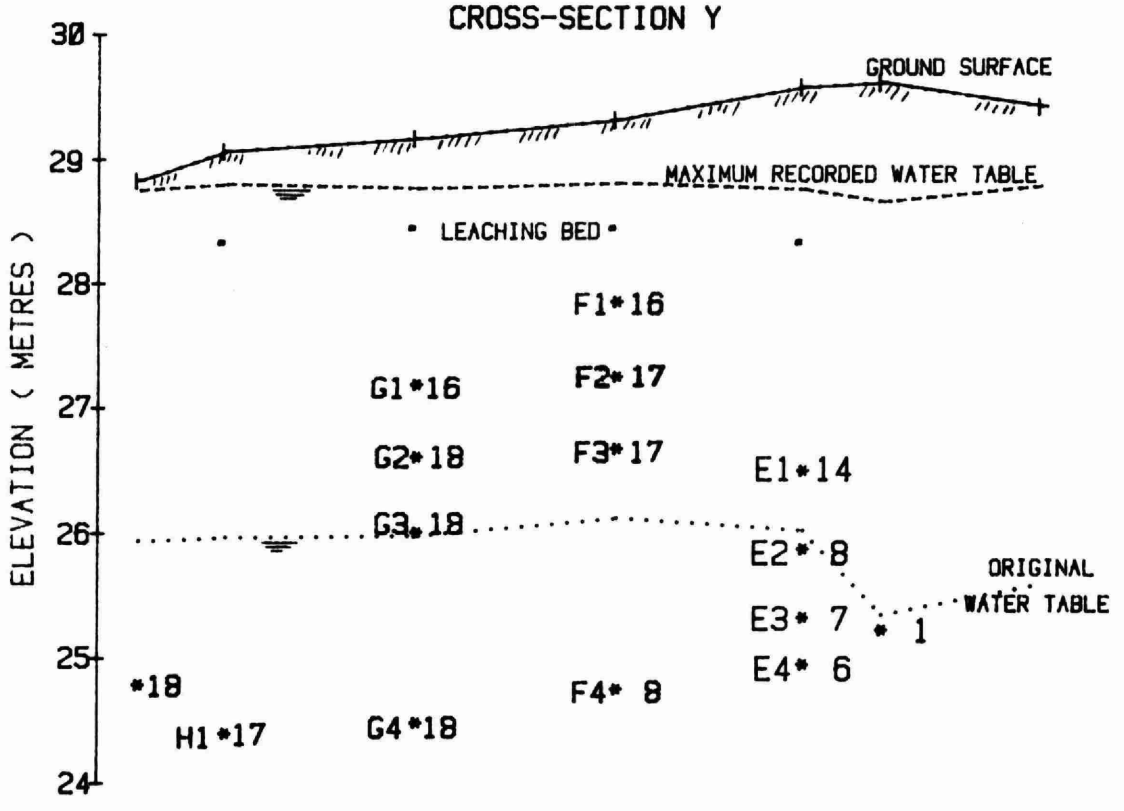

FIGURE 36 CONCENTRATION OF CHLORIDE AT SELECTED DEPTHS BELOW THE WATER TABLE (mg/L)

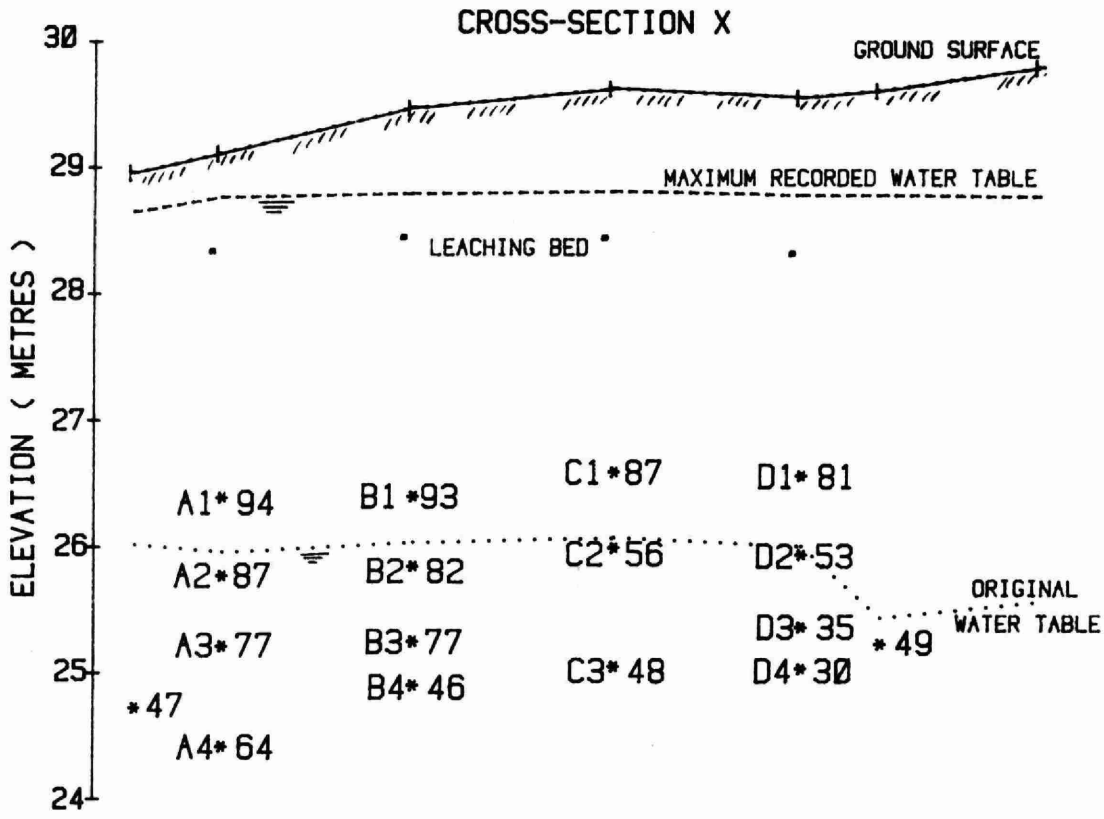

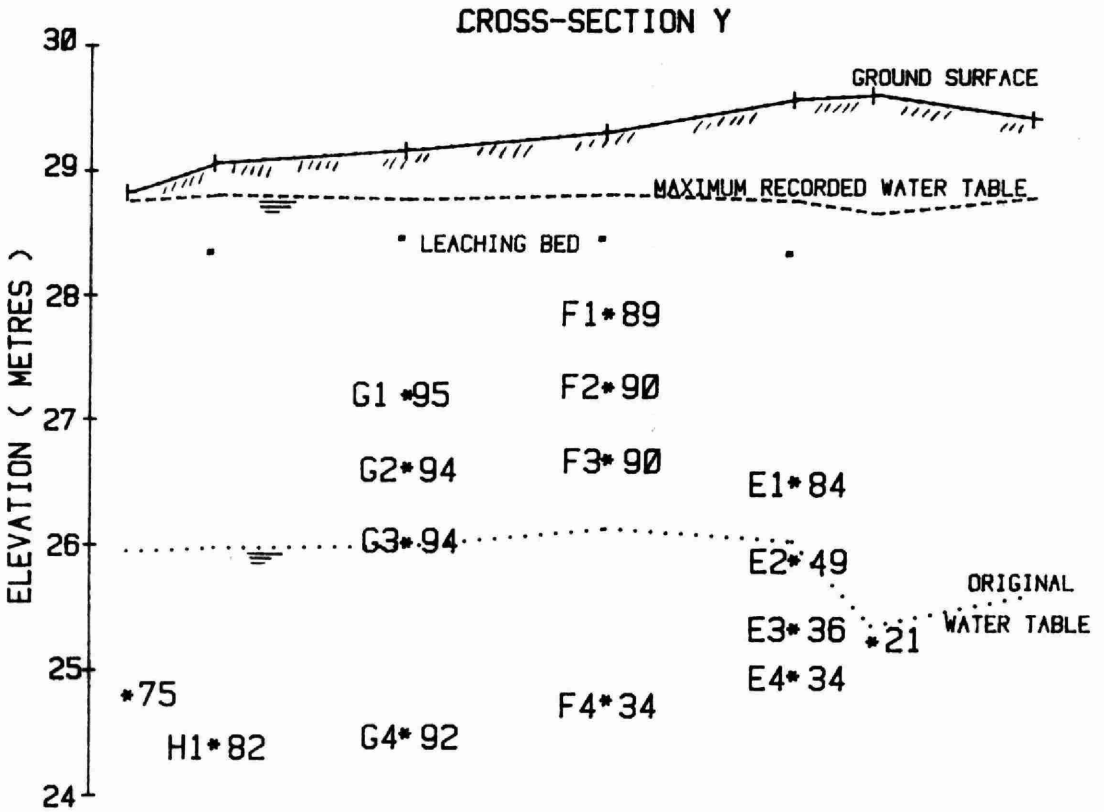

FIGURE 37 CONCENTRATION OF SODIUM AT SELECTED DEPTHS BELOW THE WATER TABLE (mg/L)

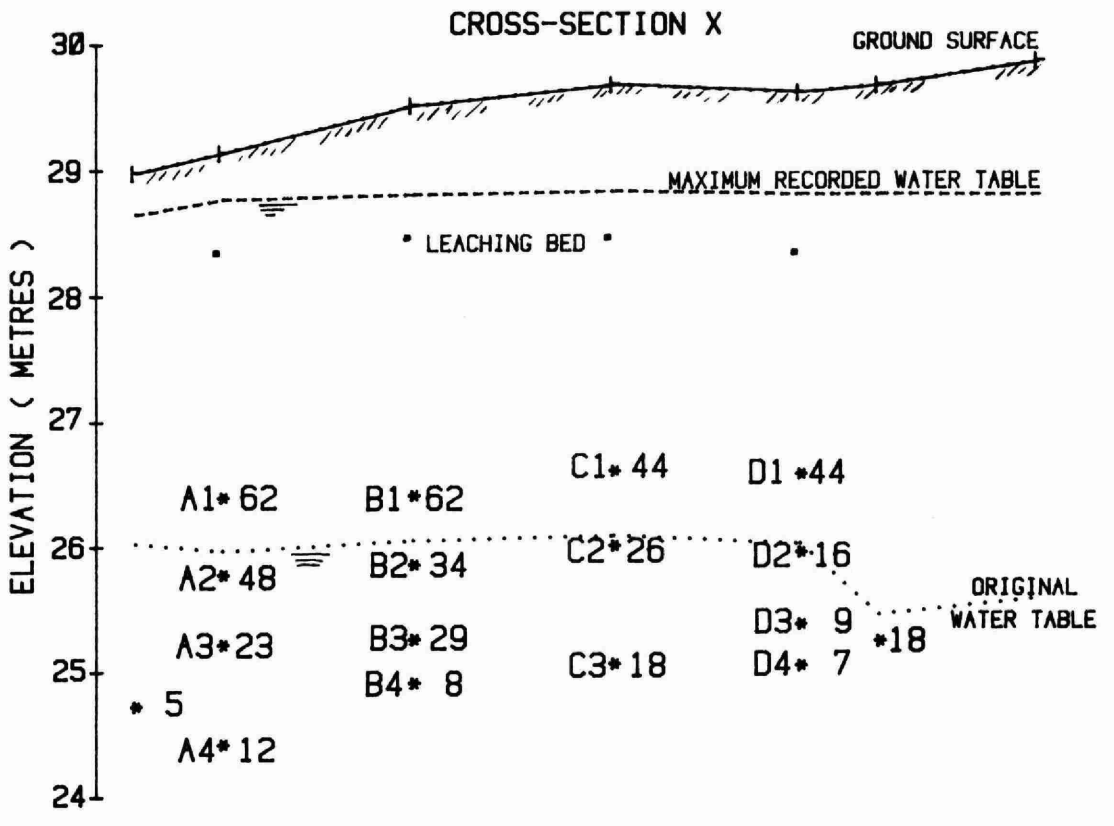

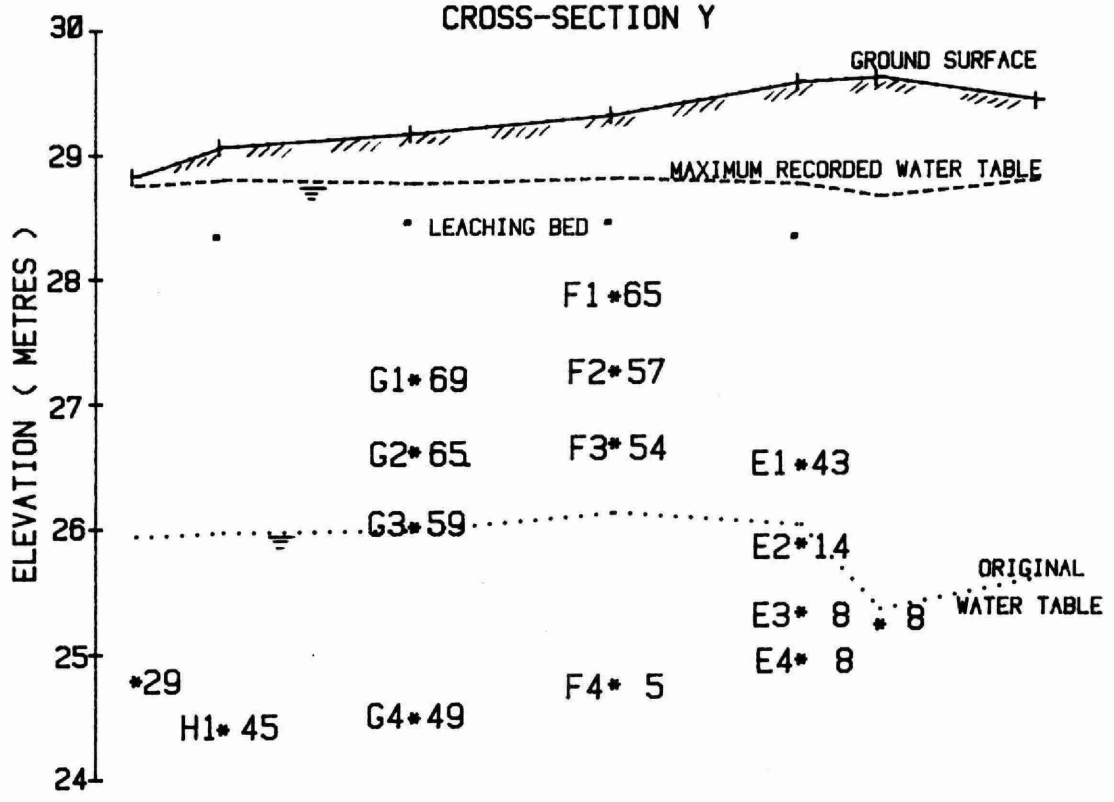

FIGURE 38 CONCENTRATION OF CALCIUM AT SELECTED DEPTHS BELOW THE WATER TABLE (mg/L)

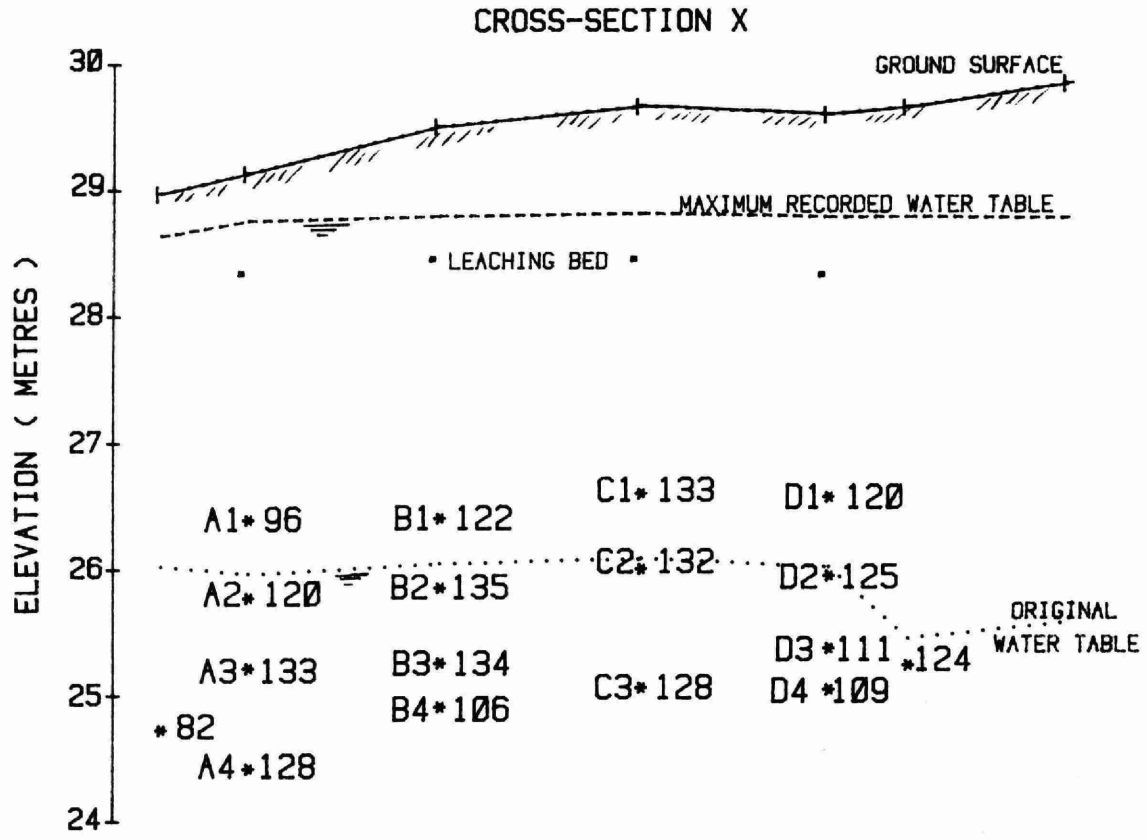

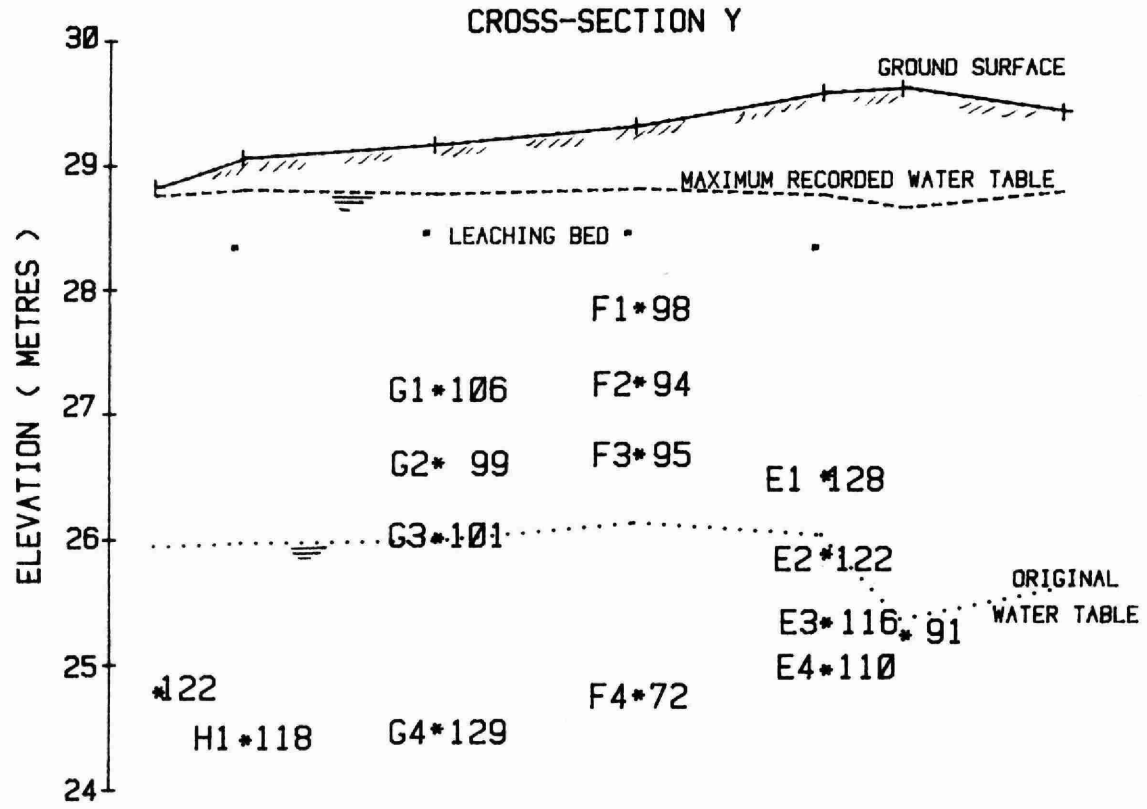

FIGURE 39 CONCENTRATION OF SULPHATE AT SELECTED DEPTHS BELOW THE WATER TABLE (mg/L)

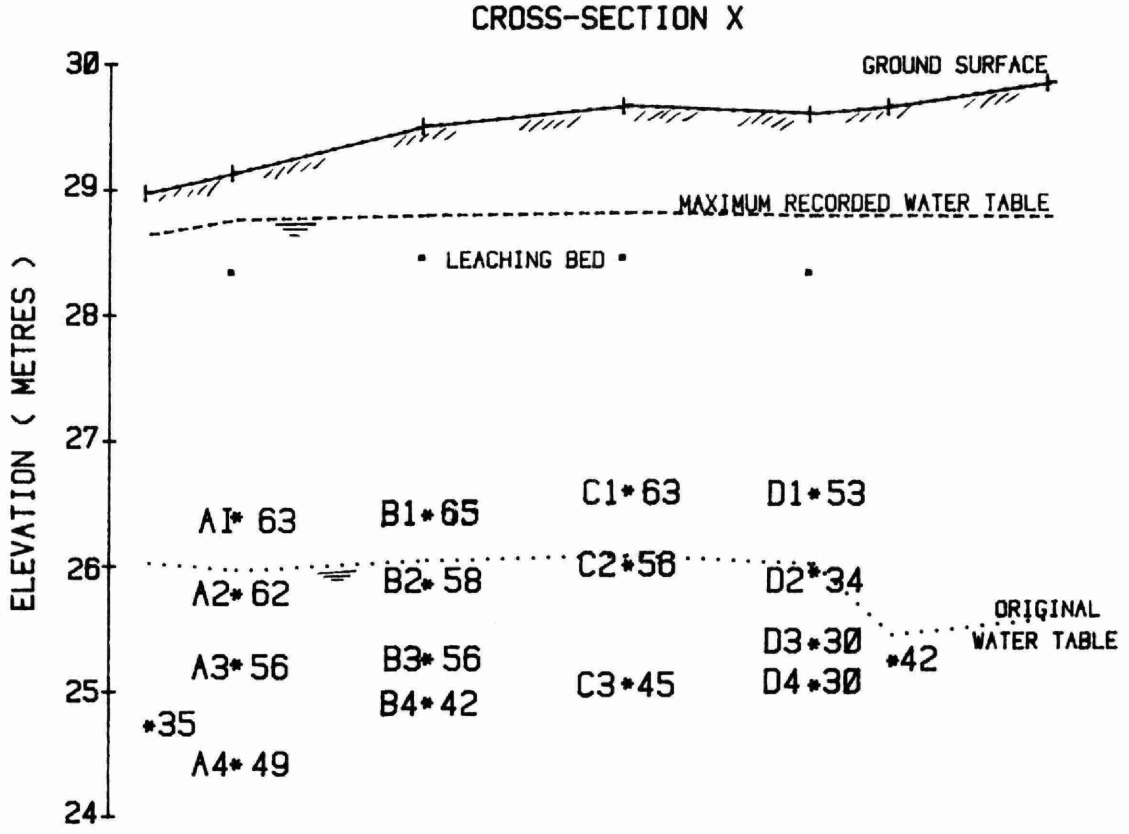

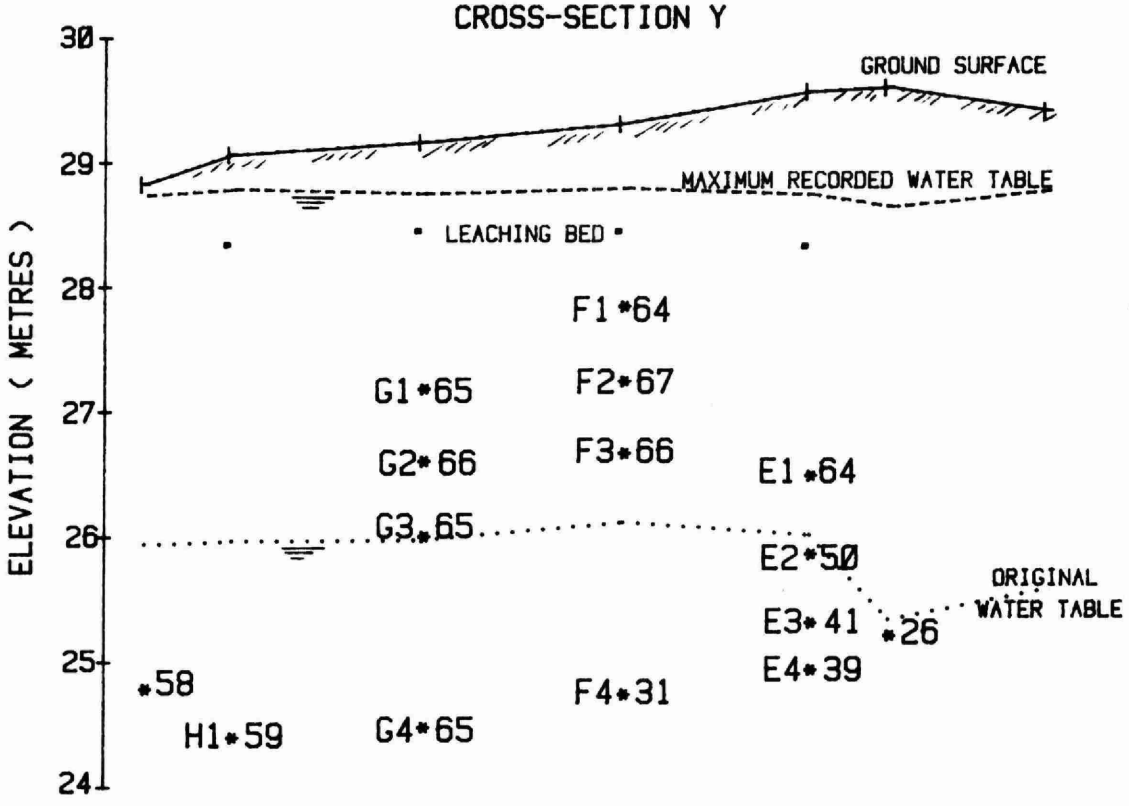

FIGURE 40 CONCENTRATION OF HARDNESS AT SELECTED DEPTHS BELOW THE WATER TABLE (mg/L)

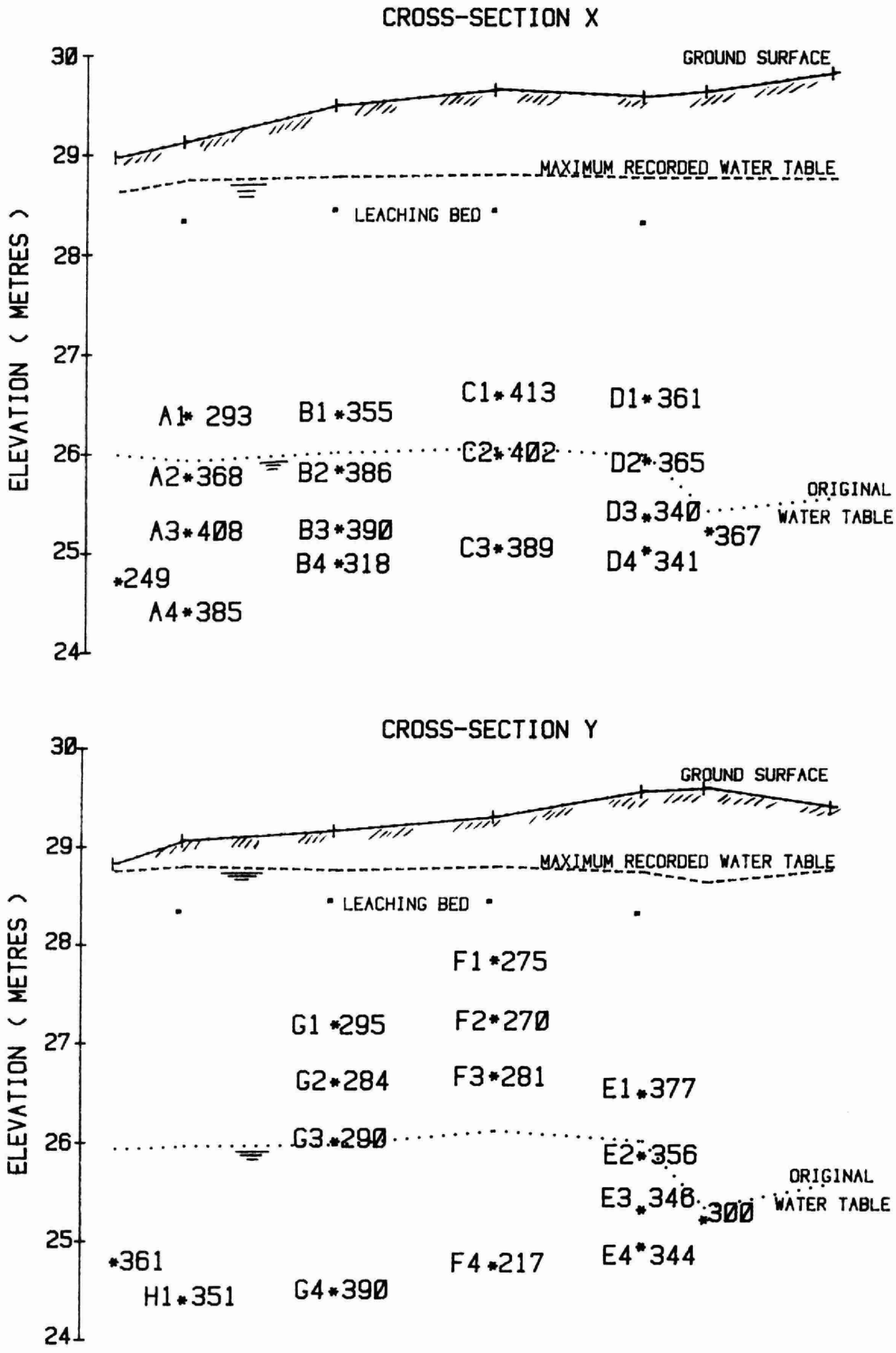

FIGURE 41 CONCENTRATION OF CONDUCTIVITY AT SELECTED DEPTHS BELOW THE WATER TABLE (μ mhos)

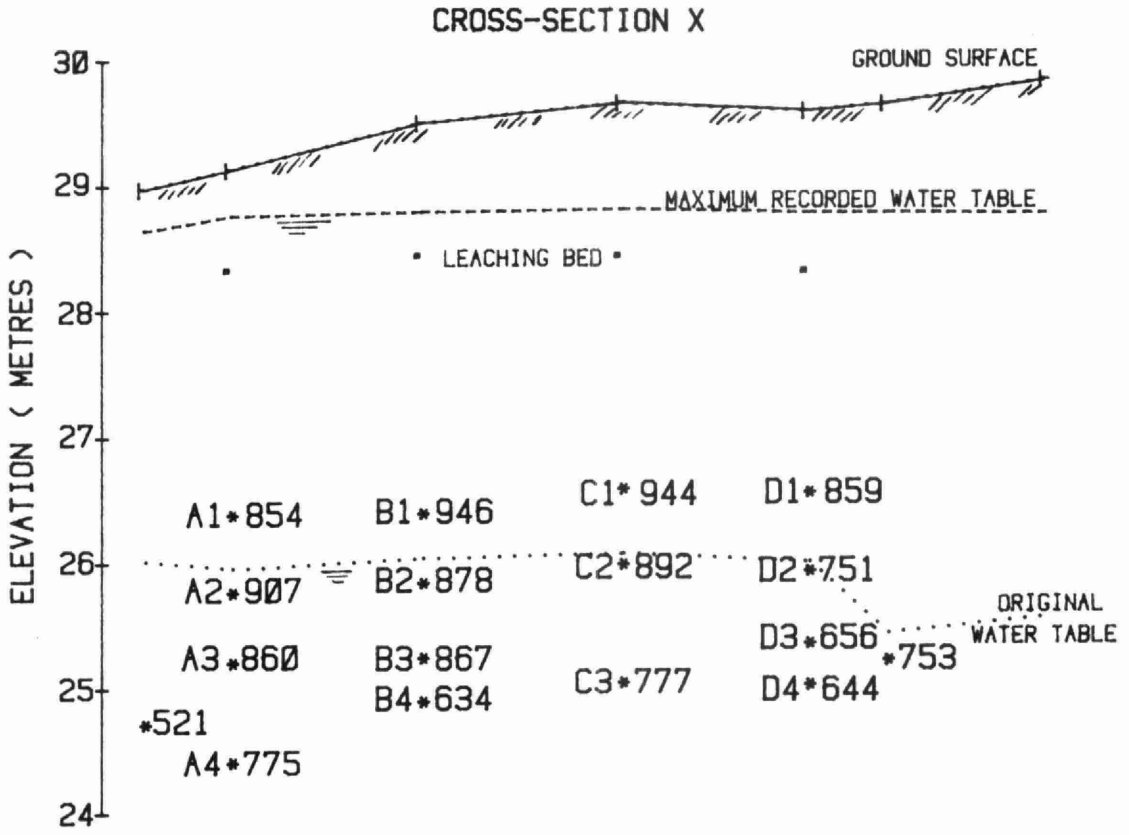

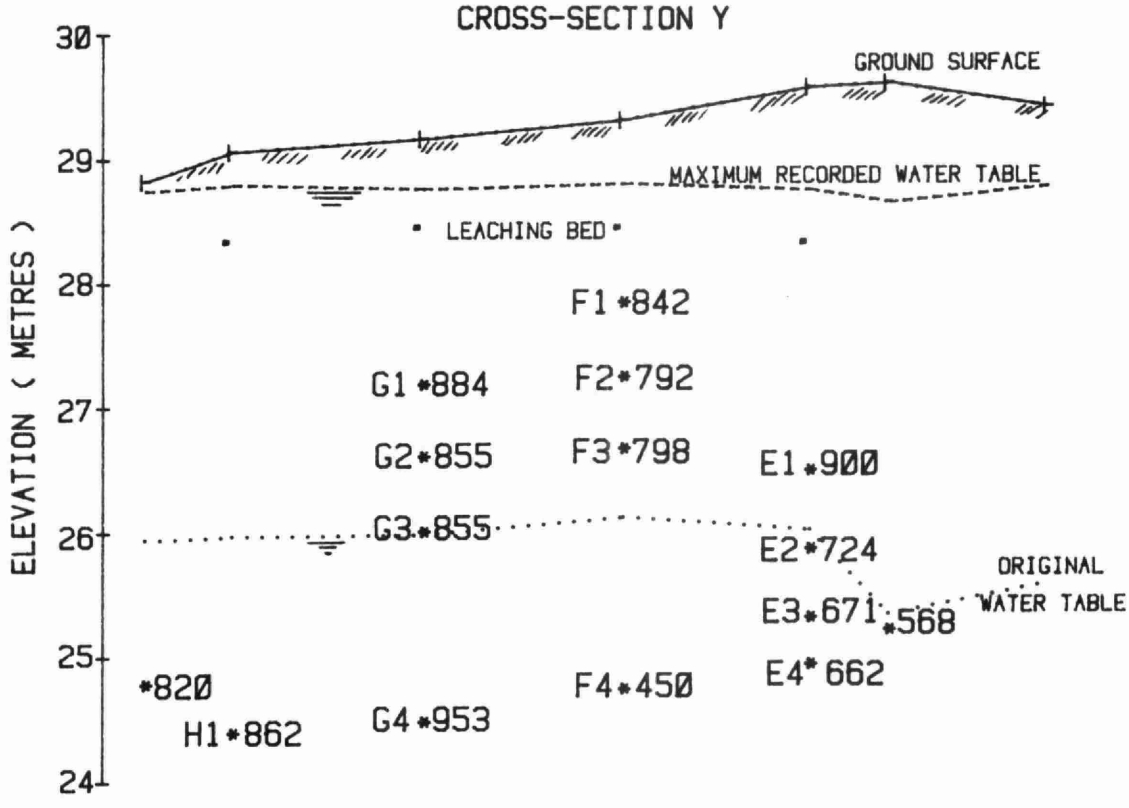

level of a multi-level well, between May 1977 and April 1979. The figures show two cross-sections x and y taken at the centre of the multi-level wells in bays A, B, D and G, F, E, respectively, parallel to the length of the leaching bed.

In general, the highest concentration of contaminants was found within one metre of depth below the groundwater table. The level of concentration decreased with increased depth below the water table. Some of the figures show a variation to the above statement in cases of concentrations above the original water table line. This could be due to the fluctuations of the water table between the original and maximum level of the groundwater, presence of clay lenses and changes in the density of the soil medium. In the case of calcium and hardness, the increase in concentration with depth could probably be due to ion exchange with sodium and potassium on the surfaces of clay particles. The decrease in concentration with depth of sodium could be due to ion exchange as well as dispersion and dilution.

4.2 Movement of Contaminants in Groundwater

The movement of contaminants in groundwater depends on various factors, such as, hydraulic loading, subsoil conditions, direction of groundwater flow and hydrogeological factors, etc. The travel and distribution patterns of the contaminants were the net result of the above-mentioned factors in each case.

4.2.1 Breakthrough Field Velocities

Breakthrough at a sample location occurs when the concentration level of the element or the dissolved salt in the groundwater increases above the background value at that location. The velocity is the rate at which a substance travels between two points in unit time. The equation used in this study for plotting contours and dispersion plumes was:

$$\text{Concentration} = \frac{C - C_b}{C_o - C_b} = <1$$

where C is contaminant concentration in the groundwater (after disposal)

C_b is background or natural concentration of contaminant in the groundwater

C_o is contaminant concentration in the feed

1 is taken as complete saturation

In this study, breakthrough is taken as the 0.1 concentration level. Breakthrough contaminant concentrations were plotted at 10 week intervals and velocities were calculated in relation to distance travelled in metres per day.

The breakthrough time and velocity were calculated from the contaminant front plotted in accordance with the data collected from the sampling well network, with regard to concentration variations from C/C_o = 1.0 to 0.1 of the contaminants, with respect to time and distance, as shown in Figures 42, 43, 44, 45, 46, 47, 48 and 49.

Table 17 shows the breakthrough field velocities of chloride, nitrate, sodium, calcium, sulphate, conductivity and hardness for a 10 week time interval.

4.2.2 Adsorption Capacity of Soil

Adsorption may be defined as the tendency exhibited by all solids to condense upon their surfaces a layer of any solute or a gas with which they are in contact.

Adsorption capacity of the soil, as used in this study, refers to the selective uptake and storage of contaminants (chemicals) present in the soil water, per unit weight of the soil.

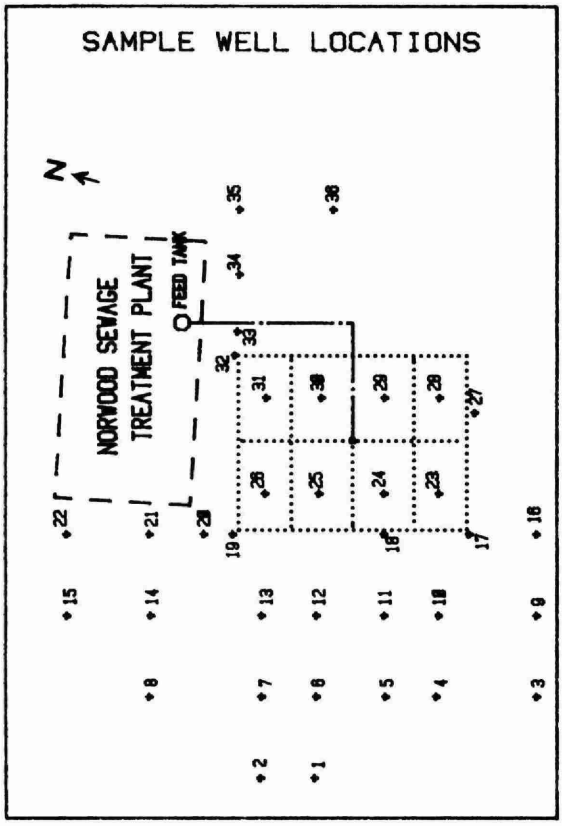

FIGURE 42

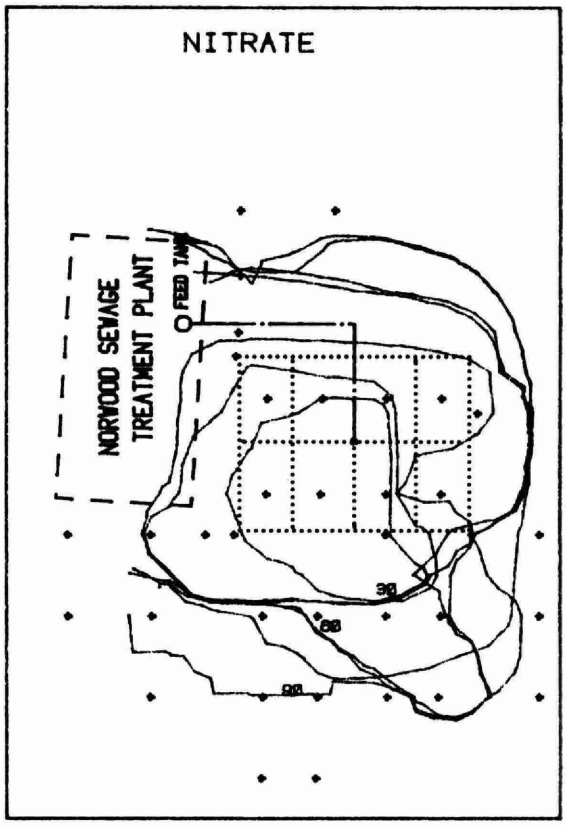

FIGURE 43

CONTAMINANT BREAKTHROUGH FRONT AT 10 WEEK INTERVALS

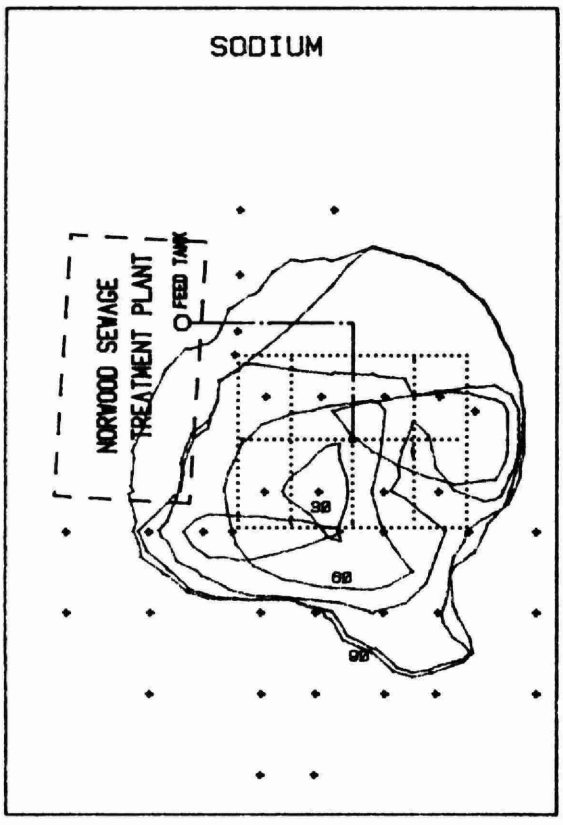

FIGURE 44

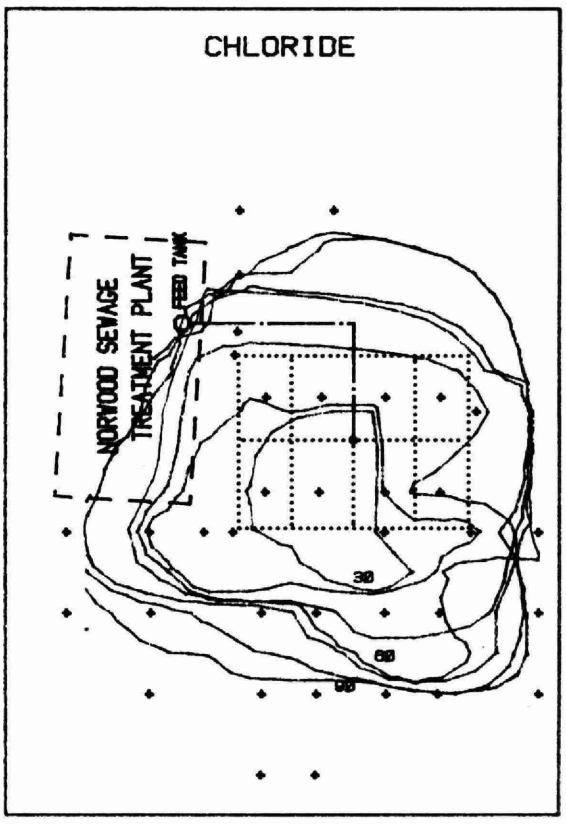

FIGURE 45

SCALE

0 METRES 90

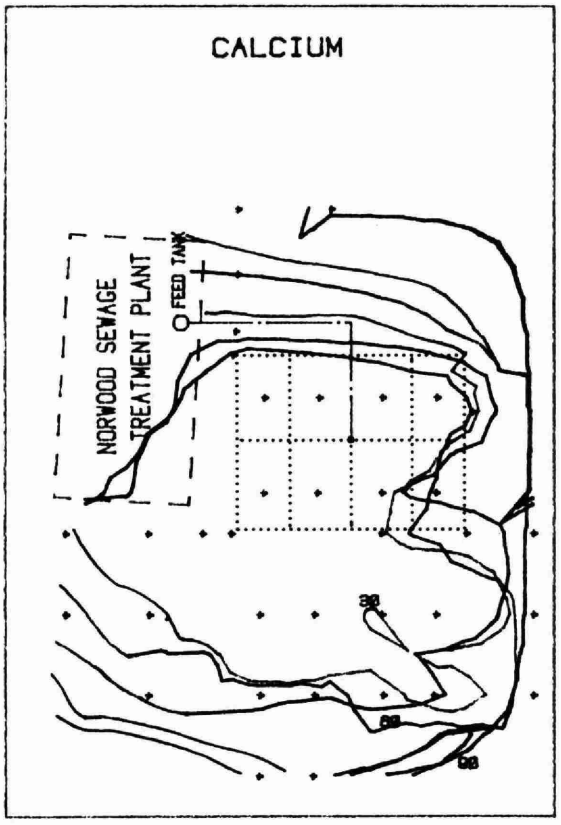

FIGURE 46

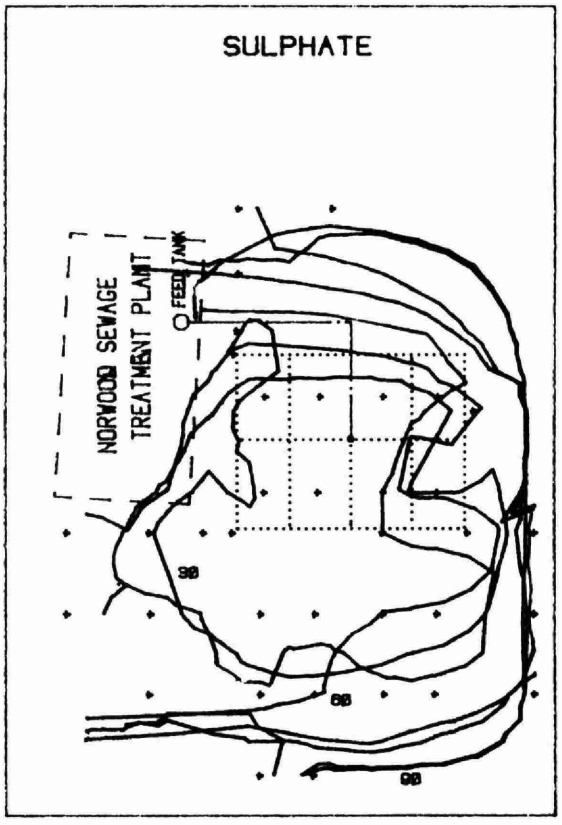

FIGURE 47

CONTAMINANT BREAKTHROUGH FRONT AT 10 WEEK INTERVALS

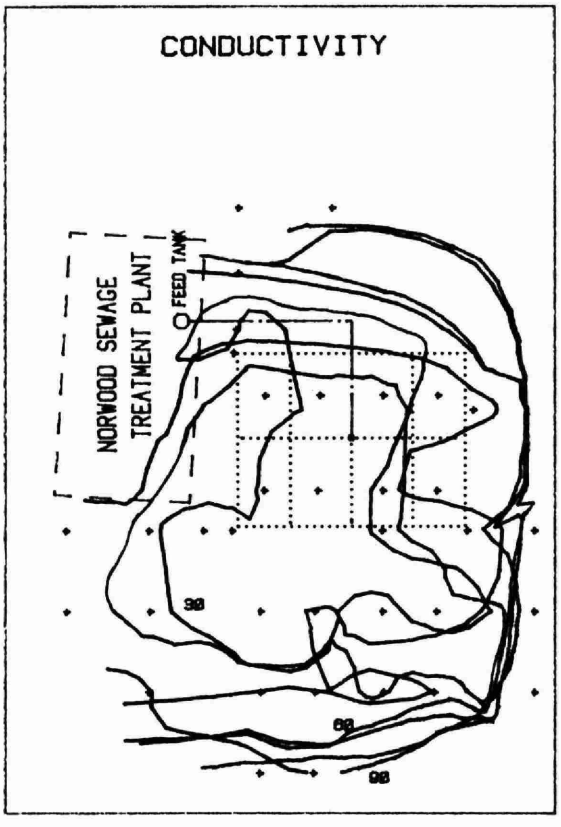

FIGURE 48

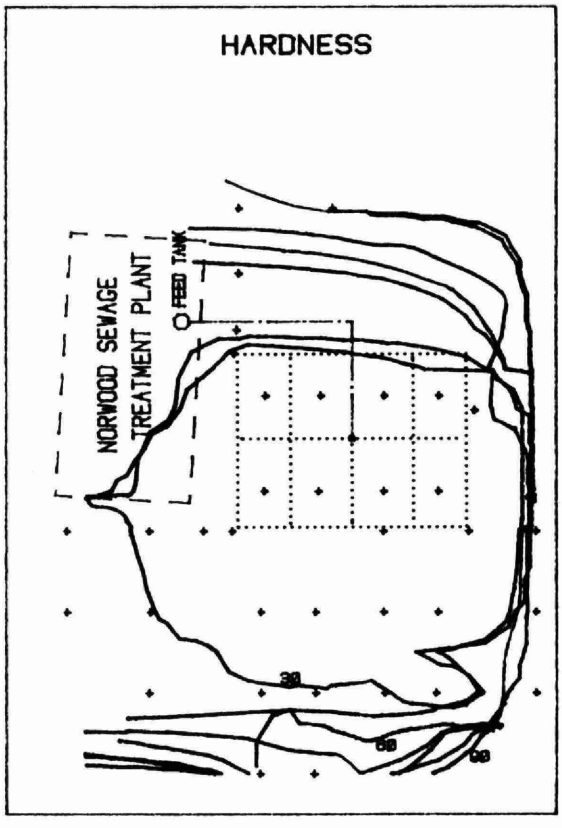

FIGURE 49

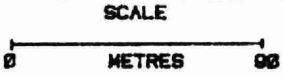

TABLE 17

BREAKTHROUGH FIELD VELOCITIES OF THE SELECTED CONTAMINANTS

Contaminants	Chloride	Nitrate	Sodium	Calcium	Sulphate	Conductivity	Hardness
Time in Weeks	Velocity (m/d)	Velocity (m/d)	Velocity (m/d)	Velocity (m/d)	Velocity (m/d)	Velocity (m/d)	Velocity (m/d)
10	0.100	0.117	-	0.104	-	0.113	0.108
20	0.155	0.152	-	0.201	0.033	0.171	0.159
30	0.162	0.157	0.042	0.186	0.089	0.179	0.158
40	0.163	0.160	0.076	0.169	0.095	0.172	0.155
50	0.158	0.156	0.086	0.155	0.096	0.157	0.149
60	0.147	0.145	0.094	0.141	0.103	0.145	0.138
70	0.140	0.135	0.098	0.132	0.102	0.134	0.128
80	0.132	0.128	0.096	0.123	0.100	0.125	0.121
90	0.123	0.122	0.097	0.116	0.099	0.118	0.114
100	0.115	0.117	0.096	0.111	0.097	0.112	0.109
Average Velocity	0.140	0.139	0.086	0.144	0.090	0.143	0.134

The adsorption capacity of soil could be calculated using an extension of the Langmuir equation (4, 14, 35, 38). The modified form of the equation is given as follows:-

$$\frac{V_w}{V_x} = 1 + \frac{A\rho_b}{C_o f} \qquad \text{.....(a)}$$

or $$A = \left(\frac{V_w}{V_x} - 1\right) \times \frac{f}{\rho_b} \times C_o \qquad \text{.....(b)}$$

where 'A' is the adsorption capacity of the soil in micrograms per gram

'V_w' is the velocity of the waterfront

'V_x' is the velocity of the contaminant front

'f' is the porosity of the soil

'ρ_b' is the bulk density of the soil in grams per cubic centimetre

'C_o' is the equilibrium concentration of contaminant discharge to the ground, in milligrams per litre.

In addition to the inherent assumptions in the derivation of Langmuir's equation, (4, 14, 35, 38), the following assumptions were made for calculation of adsorption capacity of the soil:

1. The chloride front (case 1) and conductivity front (case 2) were not affected by the soil. Hence, the adsorption capacity of the soil for chloride (case 1) and conductivity (case 2) = 0.
2. The velocity of the waterfront is equal to the velocity of the chloride front ($V_w = V_{cl}$ for case 1) and velocity of the conductivity front ($V_w = V_{con}$ for case 2).
3. The average breakthrough velocity of the contaminant is taken as the velocity of the contaminant front (V_x).

4. The mean concentration value of the contaminant in the feed is taken as the equilibrium concentration of the contaminant, discharged to the ground (C_o).

The estimated value of the bulk density (ρ_b) for the project site was 1.6 grams per cubic centimetre and the average bulk porosity (f) as measured from the saturated soil samples was 0.35.

The calculated velocity of the calcium front was highest most probably as a result of the desorption of the calcium from limestone deposits in the project area. After the calcium, the highest calculated value of the contaminant velocity front was that of conductivity. For the sake of comparison, two values of adsorption capacity of the soil in the project area were calculated based on the assumption that the soil adsorption capacity for chloride (case 1) and conductivity (case 2) was zero.

Case 1: When the adsorption capacity of the soil for chloride was assumed equal to zero, the velocity of the waterfront 'V_w' was equal to the velocity of the chloride front. The value of the calculated adsorption capacity 'A' in µg/g was 0 for chloride, 0.03 for nitrate, 3.21 for hardness, 8.15 for sulphate, and 10.75 for sodium.

Case 2: When the adsorption capacity of the soil for conductivity was assumed equal to zero, the velocity of the waterfront 'V_w' was equal to the velocity of the conductivity from 'V_{con}'. The value of the calculated adsorption capacity 'A' in µg/g was 0.49 for chloride, 0.14 for nitrate, 4.81 for hardness, 8.64 for sulphate, and 11.34 for sodium.

The calculated adsorption capacities of the selected contaminants based on the above-mentioned two assumptions are presented in Table 18. The difference between these two sets of adsorption capacity values is

TABLE 18

ADSORPTION CAPACITY OF NORWOOD SOIL FOR THE SELECTED CONTAMINANTS

Contaminants	C_o* Avg. Concentration in Feed (mg/L)	V_w** Velocity of Water Front (m/d)		V_x*** Velocity of Contaminant Front (m/d)	A Adsorption Capacity (µg/g)	
		V_{cl}	V_{con}		$V_w = V_{cl}$	$V_4 = V_{con}$
Chloride (as Cl)	99.7	0.140	0.143	0.140	0	0.49
Nitrate (as N)	20.8	0.140	0.143	0.139	0.03	0.14
Sulphate (as SO_4)	63.8	0.140	0.143	0.090	8.15	8.64
Sodium (as Na)	74.4	0.140	0.143	0.086	10.75	11.34
Calcium (as Ca)	112.5	0.140	0.143	0.144	-ve****	-ve****
Hardness (as $CaCo_3$)	311.5	0.140	0.143	0.134	3.21	4.81
Conductivity	974.6	0.140	0.143	0.143	-	0

* Mean value is used for Nitrate and Median value used for all other contaminants

** Velocity of the waterfront is assumed to be approximately that of chloride and conductivity

*** Breakthrough velocities of the contaminants are used

**** Negative value indicates desorption of containment.

negligible. The adsorption by the soil of chlorides, nitrates, hardness and conductivity is not very significant. The adsorption of sulphates and sodium is higher compared to chlorides, nitrates, hardness and conductivity values. In the case of calcium, a desorption is indicated.

4.2.3 Travel of Contaminants

Figures 50, 51, 52, 53, 54, 55 and 56 indicate the distance travelled by the selected contaminants at the concentration $C/C_o = 0.1$, with respect to time. Figure 57 shows the relative travel of all the selected contaminants.

Initially, except in the case of sodium, the distance of contaminant travel from the edge of the leaching bed increased with time. Later, the rate of increase in the distance gradually decreased until there was no further increase. The curve shown in the above figures became asymptotic and the distance of the contaminant travel at the concentration $C/C_o = 0.1$ became constant for the rest of the period.

Figures 50 and 57 initially indicate an increase in distance travelled by nitrate with time, at the concentration level $C/C_o = 0.1$. After reaching a distance of 82 m, the curve became asymptotic.

Figures 52 and 57 indicate an initial adsorption and then desorption of sodium until the curve becomes asymptotic at a distance of 73 m.

Figures 53, 55 and 57 indicate an increased travel distance of calcium and hardness due to desorption.

4.2.4 Spread of Contaminants

The concentration plumes of the selected contaminants were plotted, using the concentration levels from $C/C_o = 0.9$ to 0.1, with respect to time. In the case of Figures 62c, 62d, 63a, 63b, 63c, 63d and 64d, the contours near the edges of the diagram are artificially compressed as a result of boundary conditions of the computer plotter.

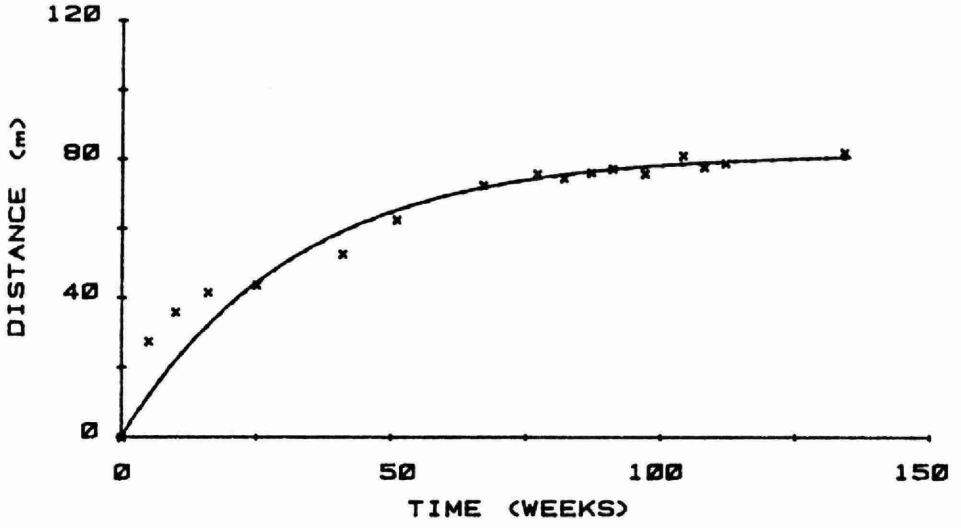

FIGURE 50 TRAVEL OF NITRATE AT CONCENTRATION C/Co=0.1

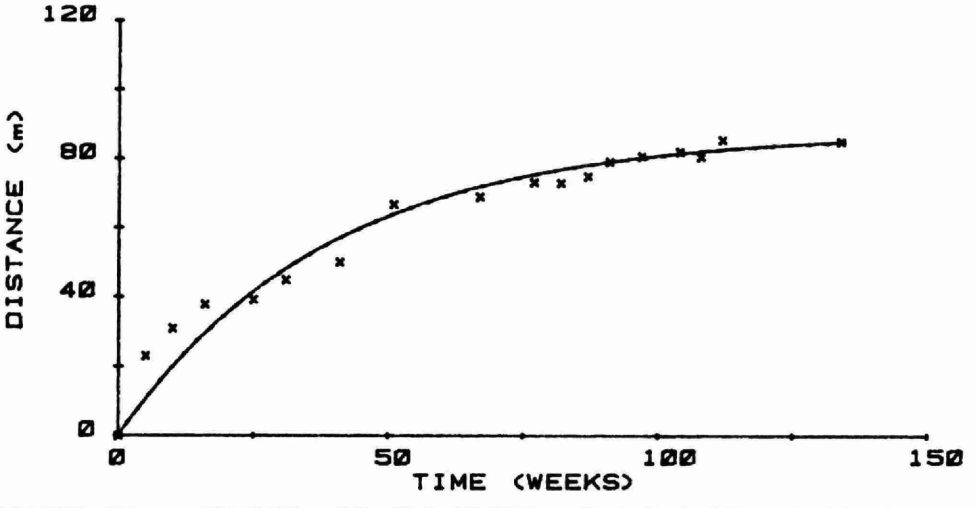

FIGURE 51 TRAVEL OF CHLORIDE AT CONCENTRATION C/Co=0.1

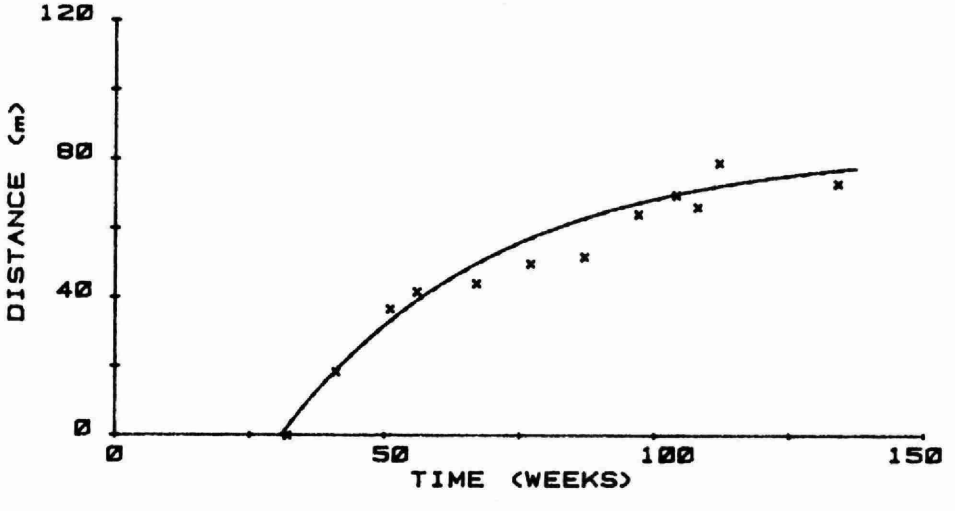

FIGURE 52 TRAVEL OF SODIUM AT CONCENTRATION C/Co=0.1

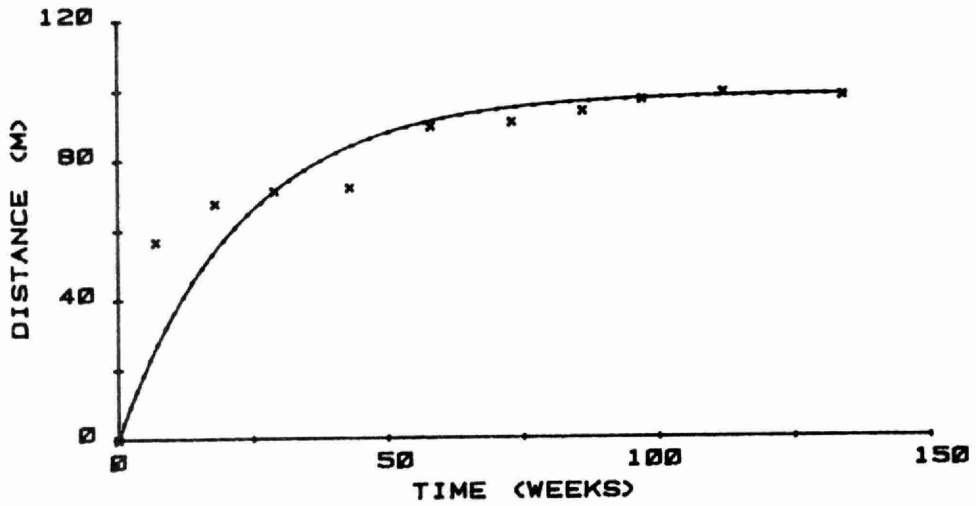

FIGURE 53 TRAVEL OF CALCIUM AT CONCENTRATION C/Co=0.1

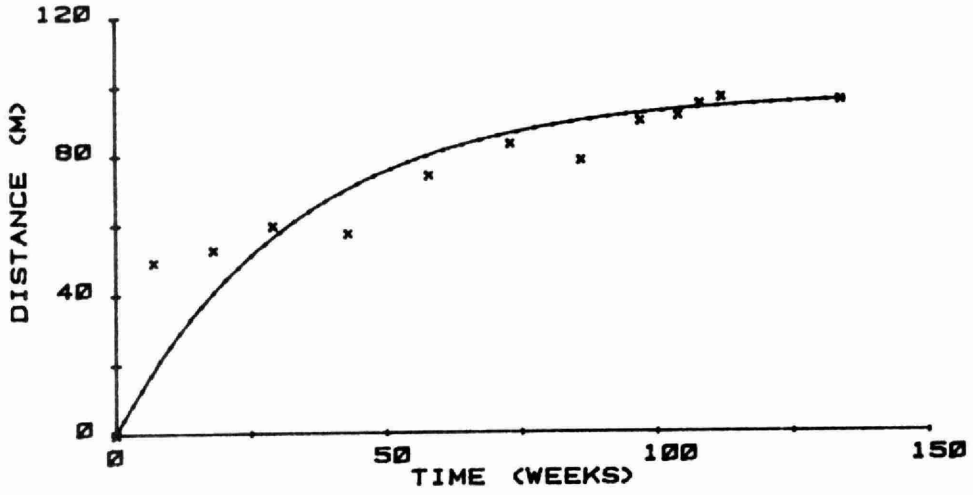

FIGURE 54 TRAVEL OF SULPHATE AT CONCENTRATION C/Co=0.1

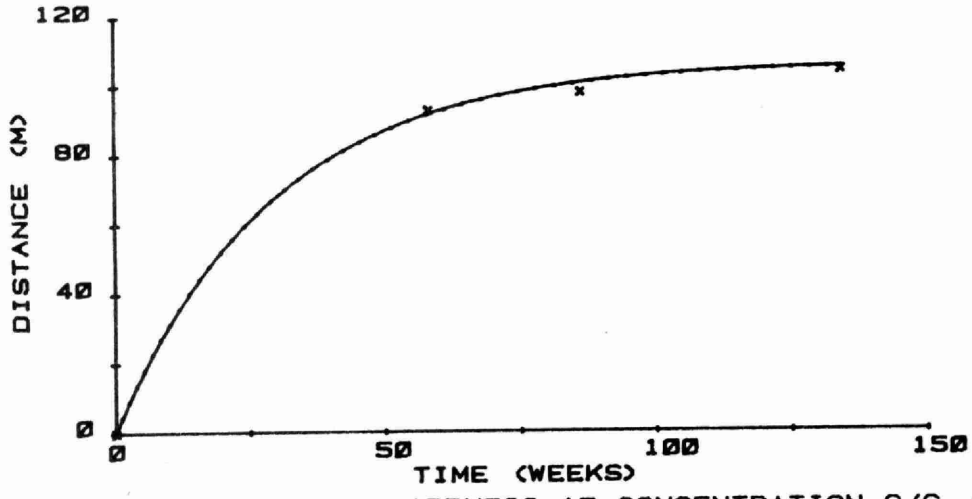

FIGURE 55 TRAVEL OF HARDNESS AT CONCENTRATION C/Co=0.1

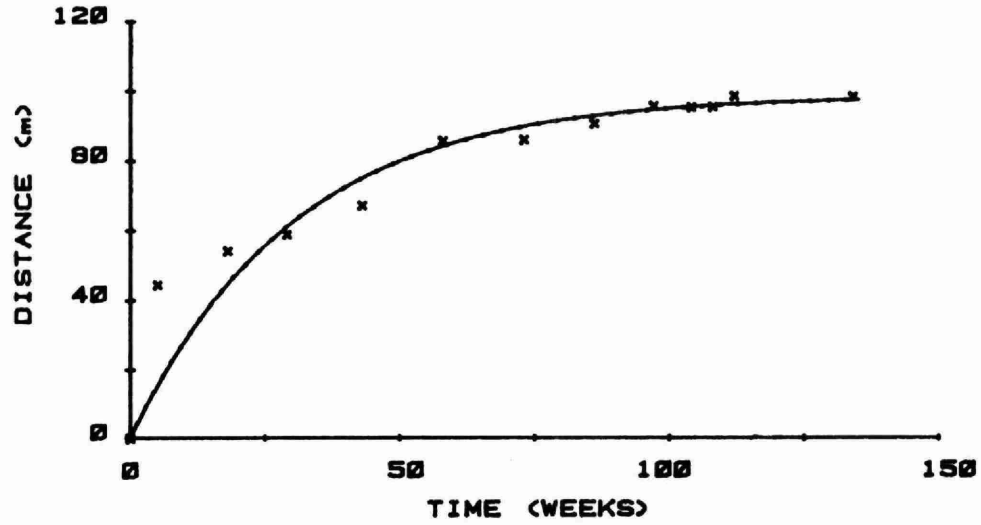

FIGURE 56 TRAVEL OF CONDUCTIVITY AT CONCENTRATION C/Co=0.1

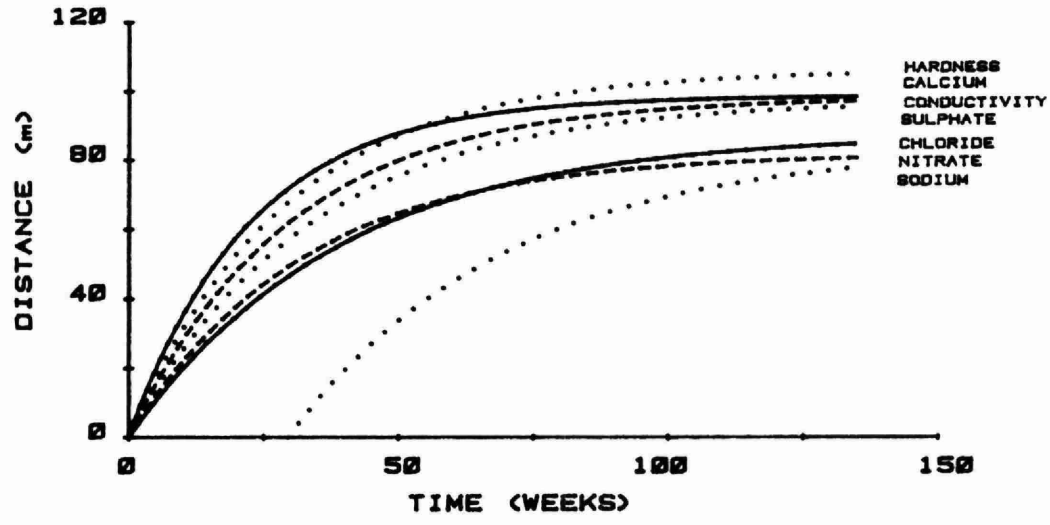

FIGURE 57 RELATIVE TRAVEL OF ALL SELECTED CONTAMINANTS AT CONCENTRATION C/Co=0.1

Chloride

Figures 58a, 58b, 58c and 58d indicate the distribution pattern of chloride for weeks 17, 63, 97 and 146, respectively, at various concentration levels. The chloride plume in the 17th week had its peak adjacent to well 25 and seemed to move in the southern direction. In week 63, the plume expanded in all directions and more in the southern direction. In week 97, the spread became more uniform and showed movement toward southern and western directions. In week 146, the spread was more in the northwestern direction, towards the river.

The breakthrough velocity of chloride at the concentration C/C_o = 0.1 ranged from 0.10 m/d to 0.16 m/d. The maximum distance travelled from the centre of leaching bed was 85 m. The maximum area of chloride spread in week 146 was 2.3 hectares.

Nitrate

Figures 59a, 59b, 59c and 59d indicate the movement pattern of nitrate in weeks 17, 63, 116 and 146, respectively. The nitrate plume in week 17 had its peak of concentration near well 25 and the direction of its movement was in the southern and southeastern directions. In week 63, the concentration peak was between wells 19 and 20. The spread covered a larger area and the direction of move was more in the southeastern and northeastern directions. In weeks 116 and 146, the spread of concentration contour C/C_o = 0.1 was more in the southwestern and northwestern directions.

The breakthrough velocity of nitrate ranged from 0.12 m/d to 0.16 m/d. The maximum distance travelled was 82 m. The maximum area of nitrate spread in week 146 was 2.1 hectares.

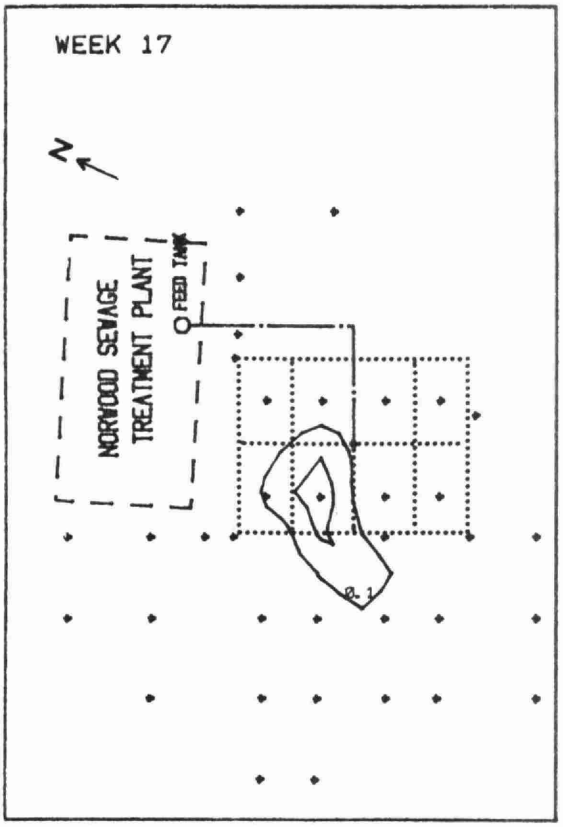

FIGURE 58a

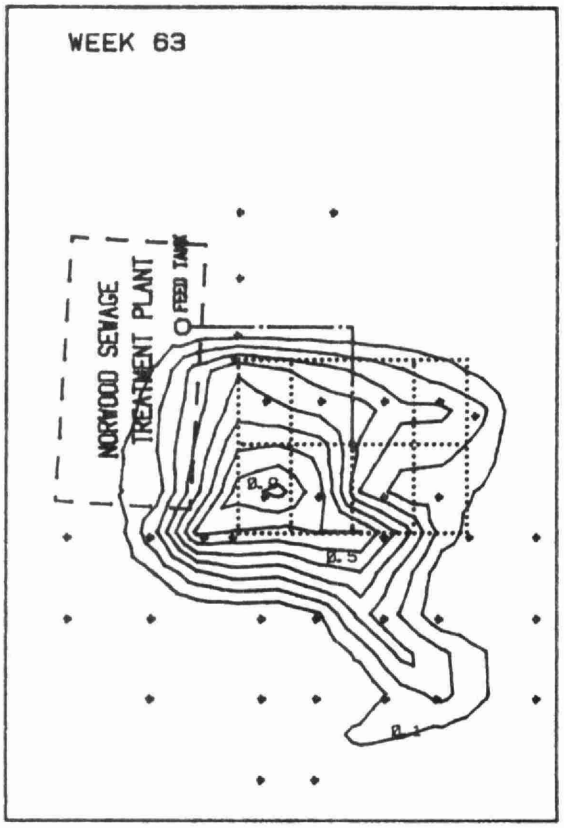

FIGURE 58b

CHLORIDE CONCENTRATION CONTOURS

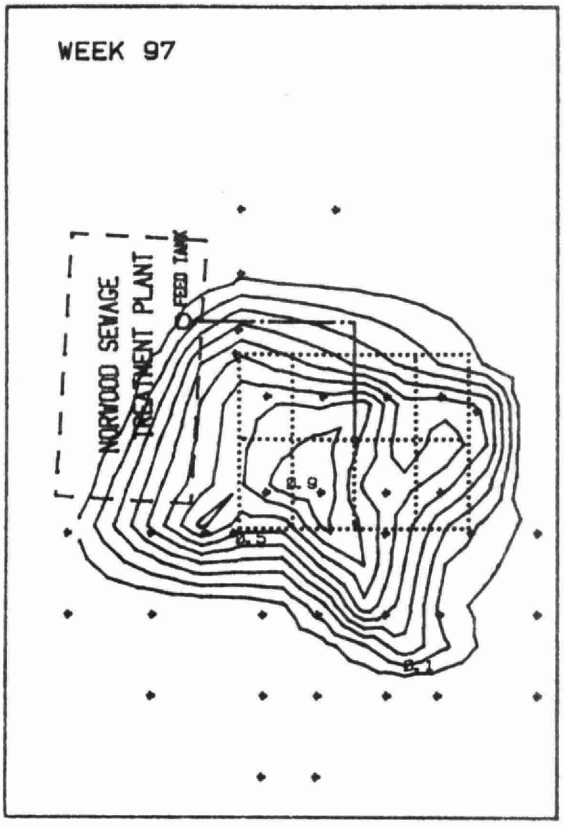

FIGURE 58c

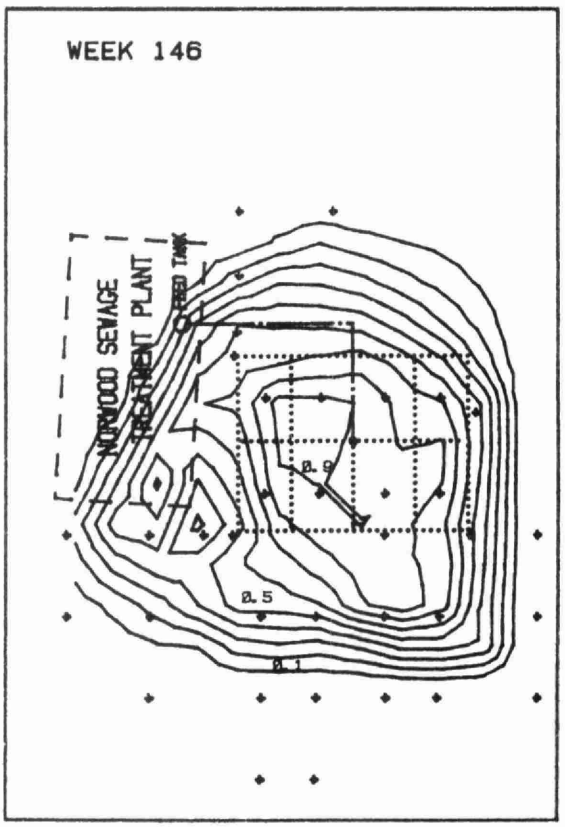

FIGURE 58d

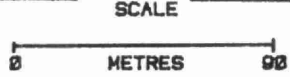

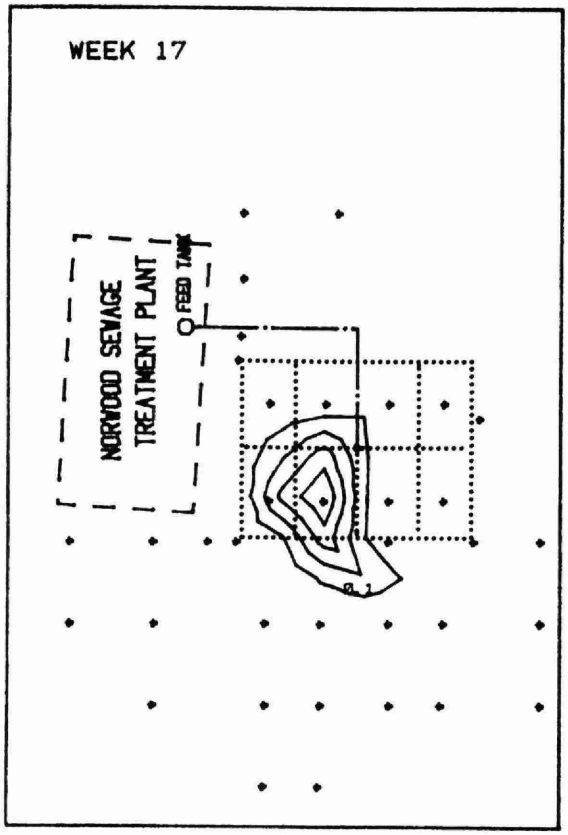

FIGURE 59a

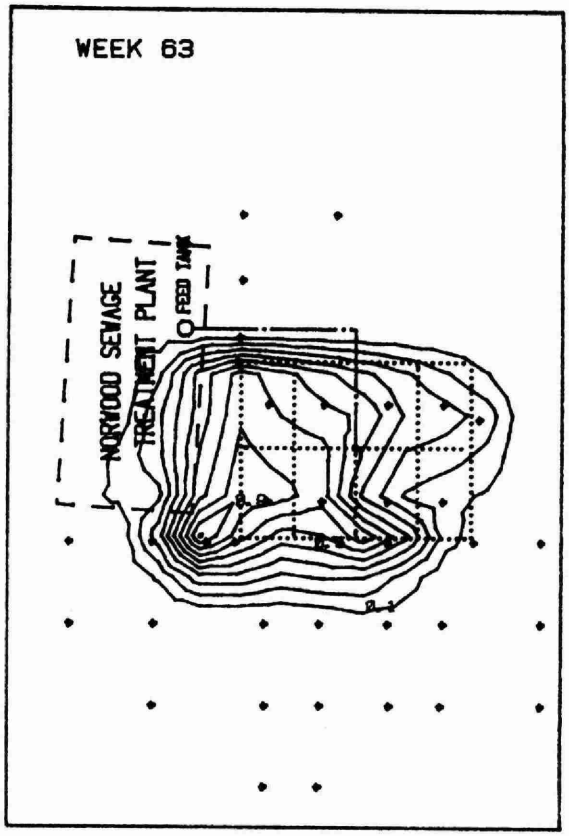

FIGURE 59b

NITRATE CONCENTRATION CONTOURS

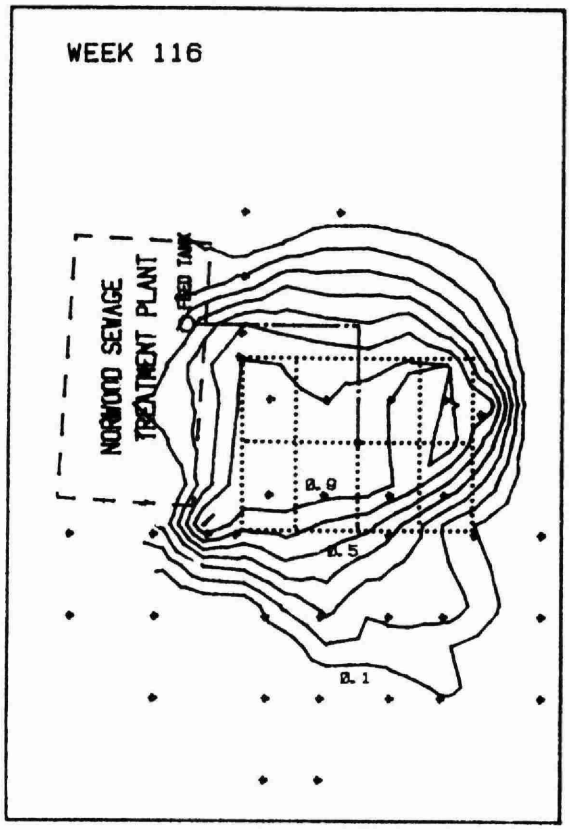

FIGURE 59c

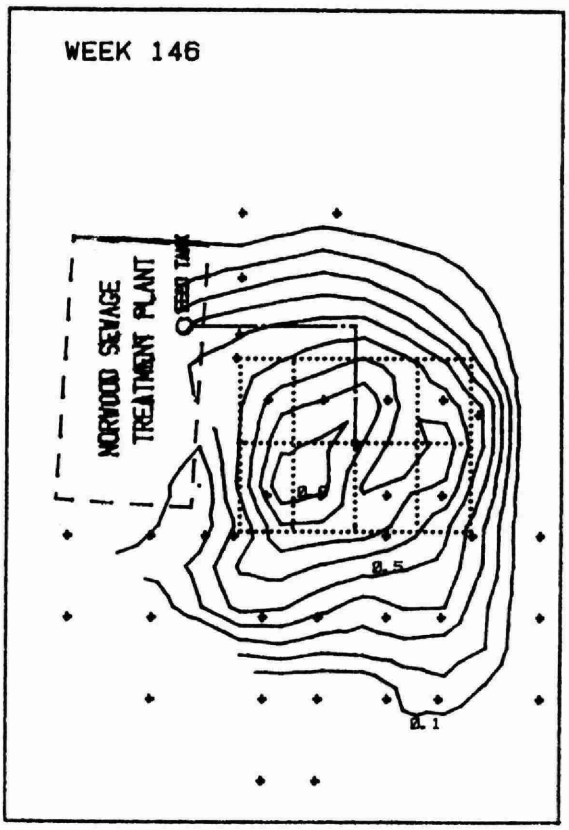

FIGURE 59d

Sulphate

Figures 60a, 60b, 60c and 60d indicate the distribution pattern of sulphate in weeks 19, 63, 85 and 146, respectively, with the peak of the concentration near well 25 in week 19. The concentration contour C/C_o = 0.1 of the sulphate plume seemed to move in southeastern and northeastern directions. In week 63, the movement was more in the southeastern and northwestern directions. In weeks 85 and 146, the distribution was more in the southern and western directions.

The breakthrough velocity of sulphate ranged from 0.03 m/d to 0.10 m/d. The maximum distance travelled was 96 m. The maximum area of sulphate spread in well 146 was 2.9 hectares.

Sodium

Figures 61a, 61b, 61c and 61d indicate the movement pattern of sodium in weeks 53, 85, 116 and 146, respectively. The concentration peak was near well 25 in week 53 and the concentration contour C/C_o = 0.1 seemed to move more in the southern direction. The plume expanded in all directions in weeks 85 and 116, and showed more spread in the western and southern directions in week 146.

The breakthrough velocity of sodium ranged from 0.04 m/d to 0.10 m/d. The maximum distance travelled was 73 m. The maximum area of sodium spread in week 146 was 1.7 hectares.

Calcium

Figures 62a, 62b, 62c and 62d show the distribution pattern of calcium in weeks 19, 63, 116 and 146. Four concentration peaks indicated in week 19, formed one peak, around wells 19, 20, 25 and 26, in week 63. The plume seemed to spread in all directions and moved in the southern direction. The plume expanded in weeks 116 and 146. In week 146, more movement was indicated in the southern direction.

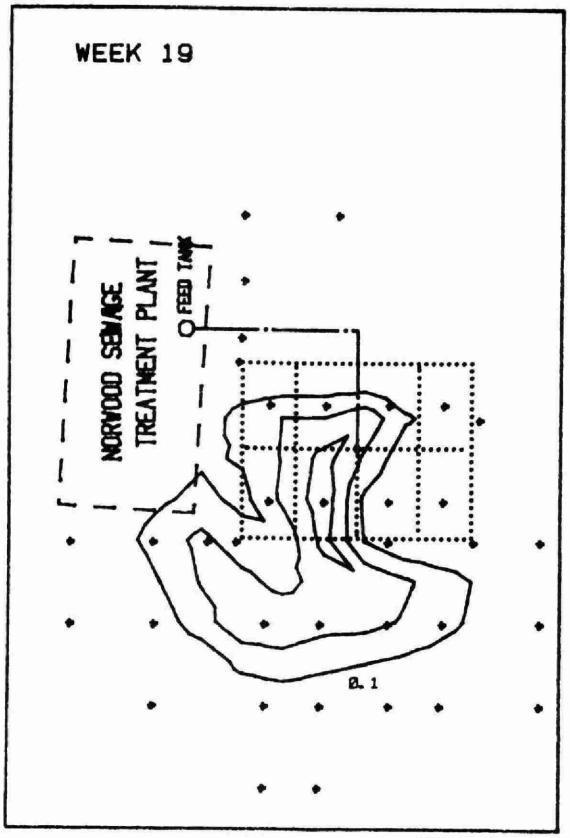

FIGURE 60a

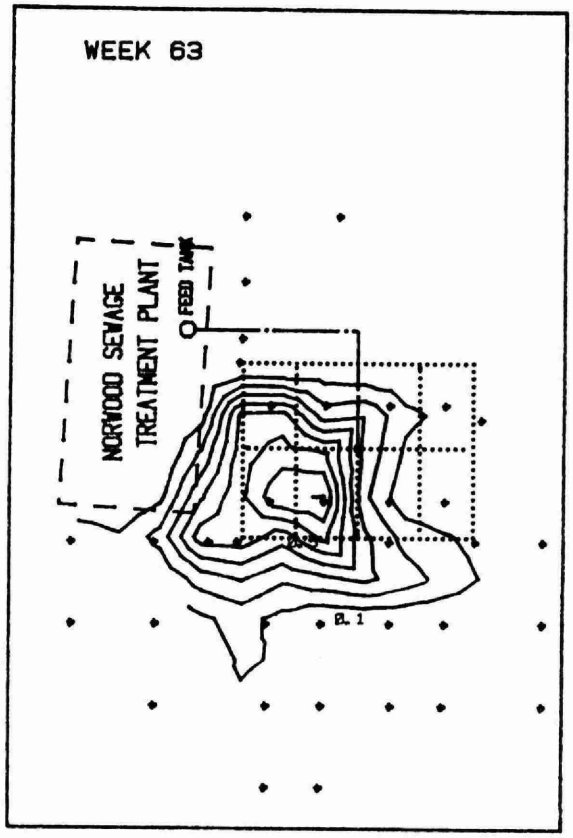

FIGURE 60b

SULPHATE CONCENTRATION CONTOURS

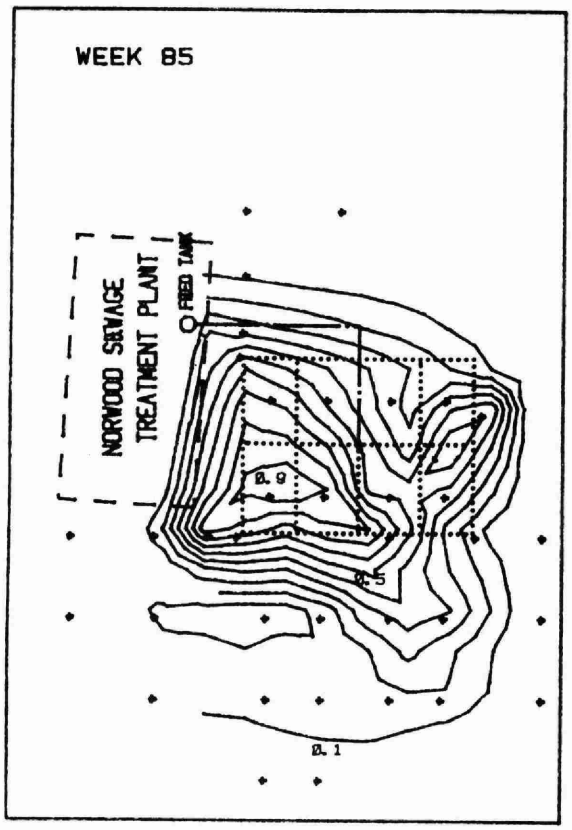

FIGURE 60c

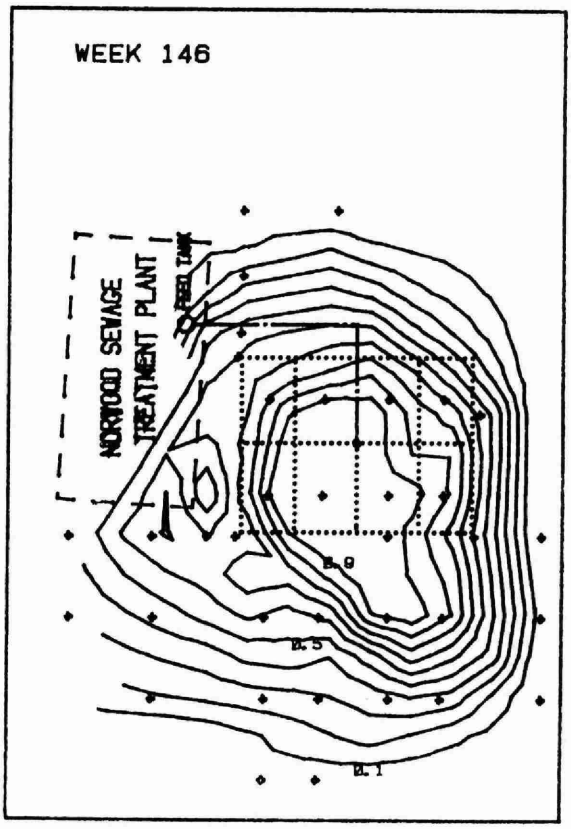

FIGURE 60d

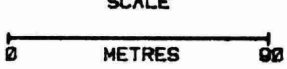

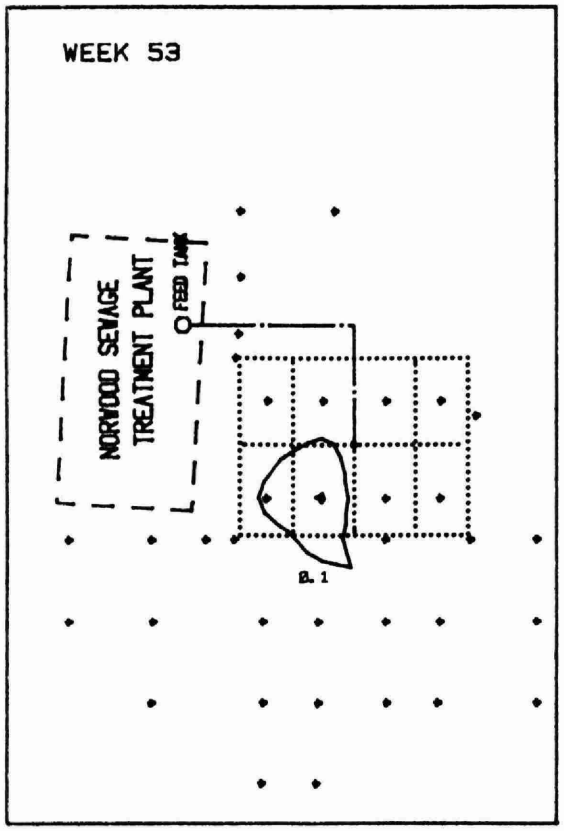

FIGURE 61a

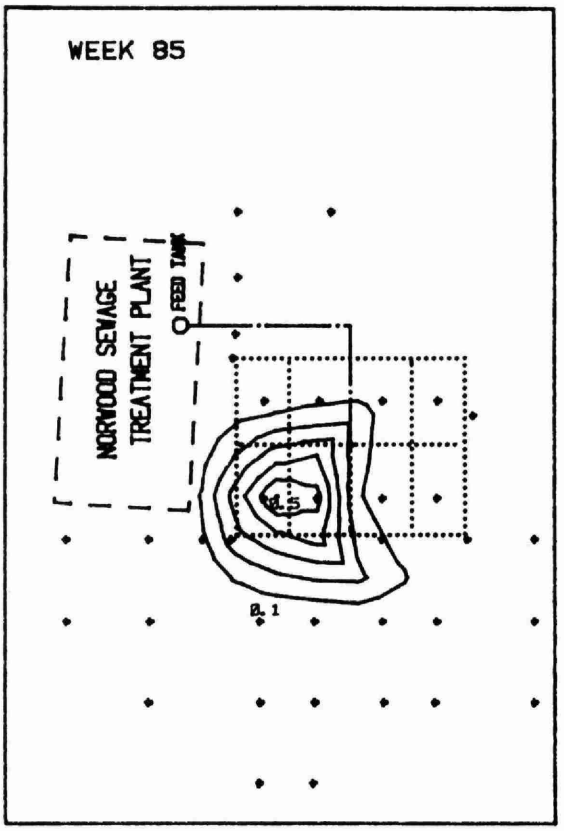

FIGURE 61b

SODIUM CONCENTRATION CONTOURS

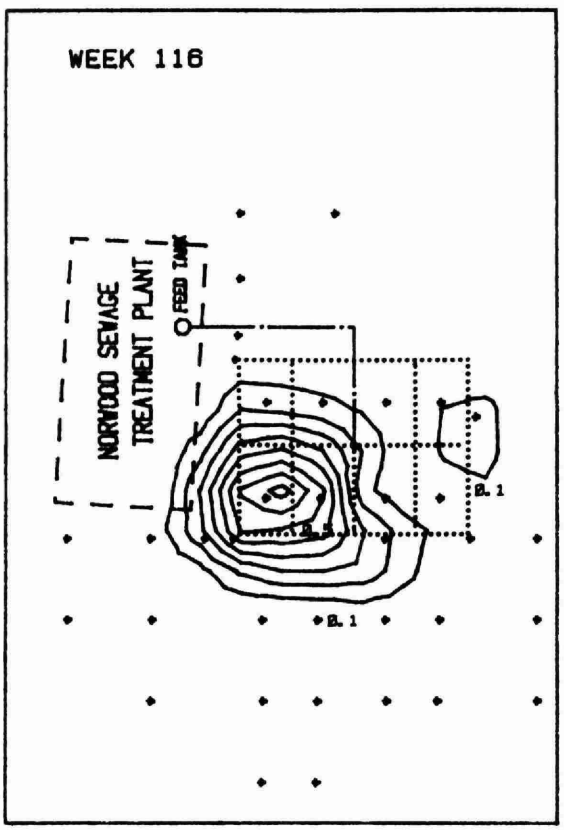

FIGURE 61c

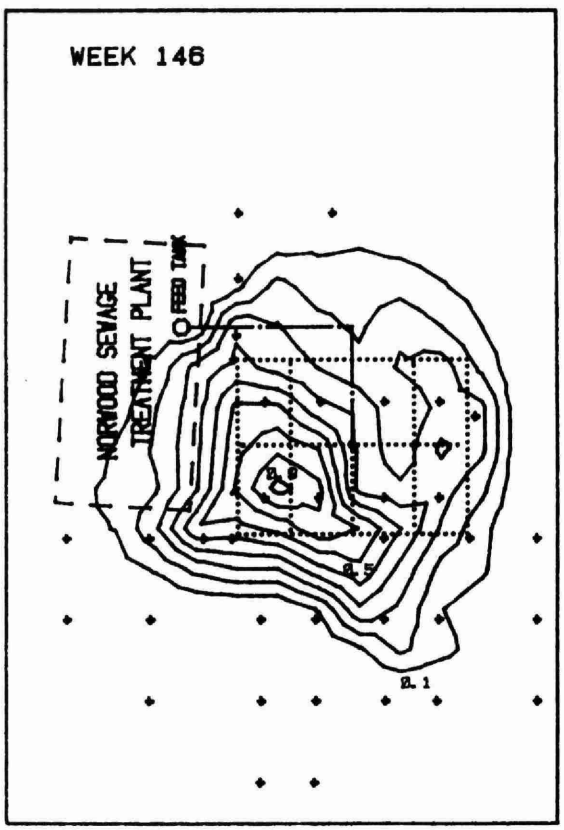

FIGURE 61d

SCALE

0 METRES 90

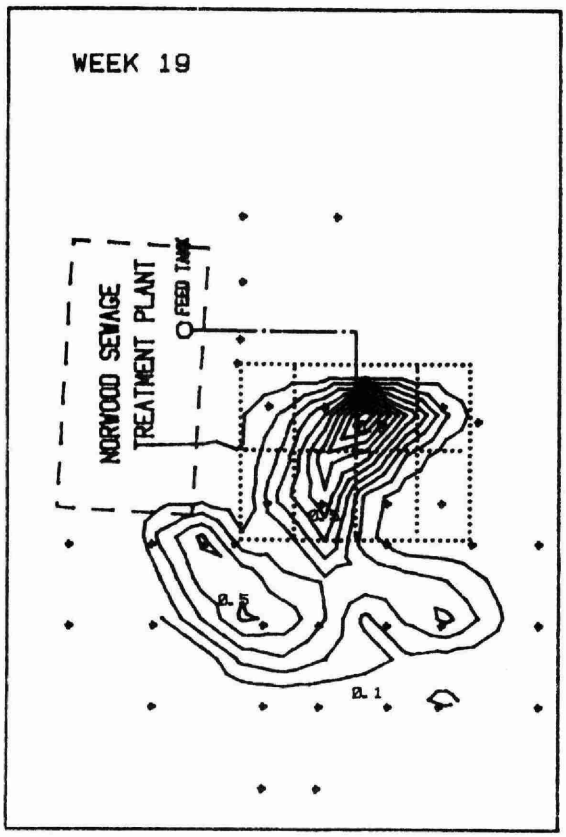

FIGURE 62a

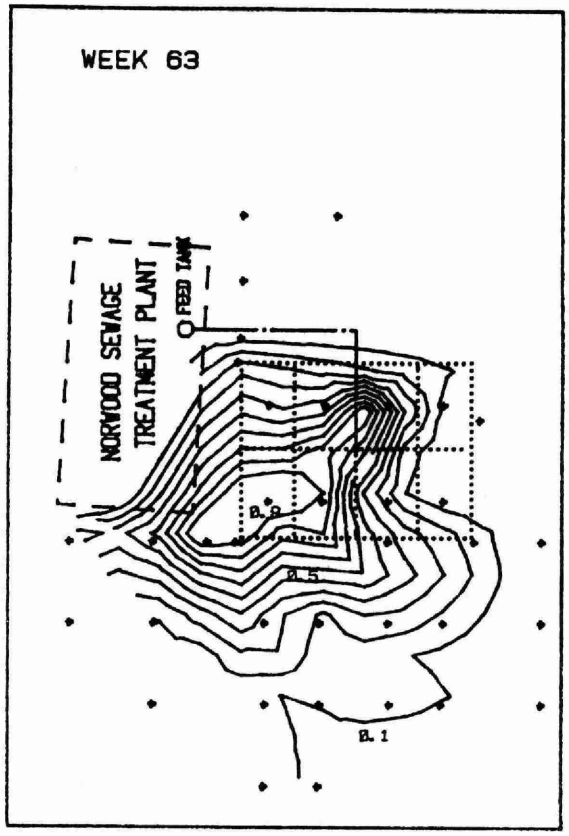

FIGURE 62b

CALCIUM CONCENTRATION CONTOURS

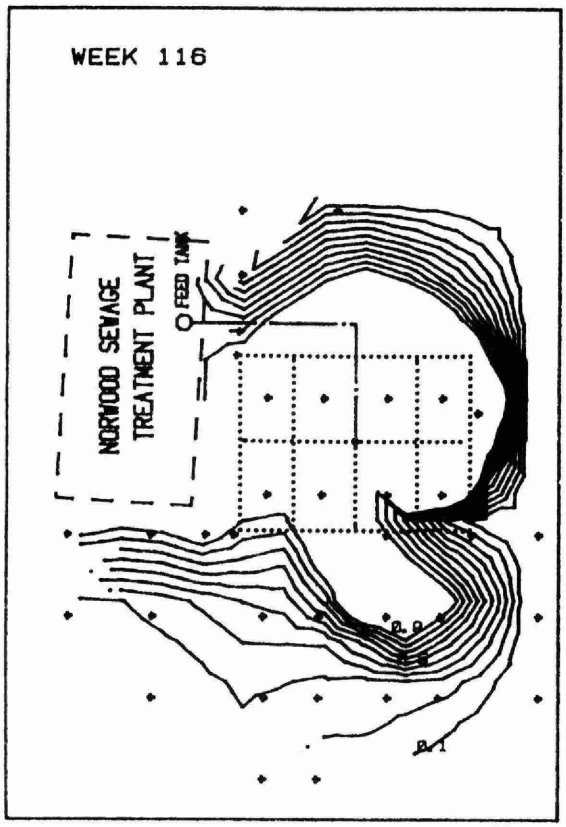

FIGURE 62c

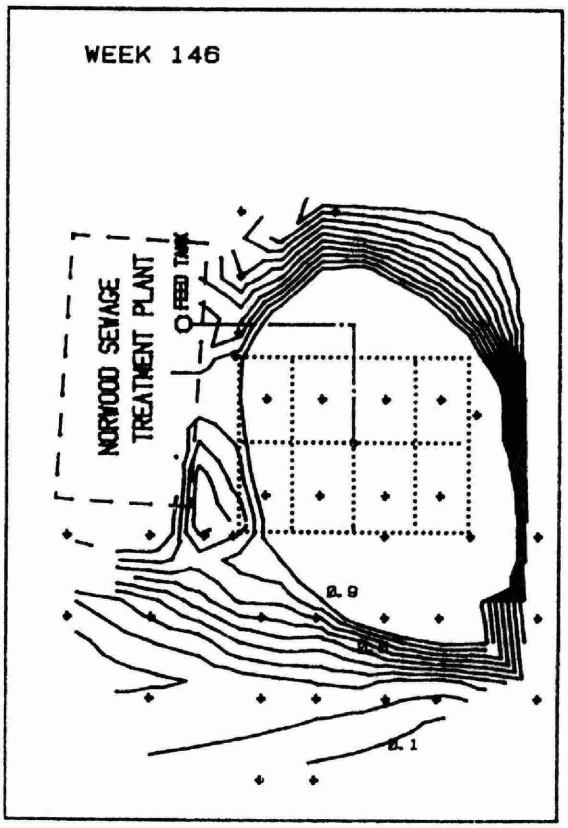

FIGURE 62d

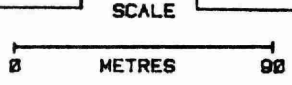

The breakthrough velocity of calcium ranged from 0.10 m/d to 0.20 m/d. The maximum distance travelled was 98 m. The maximum area of calcium spread in week 146 was 3.0 hectares.

Hardness

Figures 63a, 63b, 63c and 63d indicate the distribution pattern of hardness in weeks 19, 70, 98 and 146, respectively. Multiple concentration peaks indicated in week 19 formed one peak and the plume seemed to expand more in the southerly direction in weeks 70 and 98. In week 146, expansion of plume was in all directions and more dispersion in the southerly direction was indicated.

The breakthrough velocity of hardness ranged from 0.11 m/d to 0.16 m/d. The maximum distance travelled was 104 m. The maximum area of spread in week 146 was 3.4 hectares.

Conductivity

Figures 64a, 64b, 64c and 64d indicate the movement patterns of conductivity in weeks 19, 55, 116 and 146, respectively. Two peaks of conductivity values in week 19 were located near wells 19 and 25. The dispersion was more in the southern direction. In week 55, the peak of the concentration was around well 25 and the spread was more in the northwestern and southern directions. In weeks 116 and 146, the plume expanded in all directions and more in the southern direction.

The breakthrough velocity of conductivity ranged from 0.11 m/d to 0.18 m/d. The maximum distance travelled was 98 m. The maximum area of conductivity spread in week 146 was 3.0 hectares.

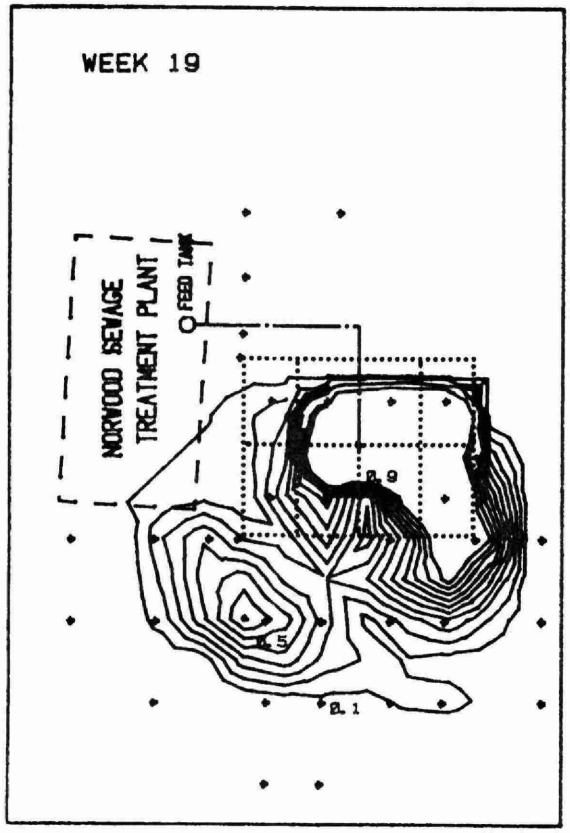

FIGURE 63a

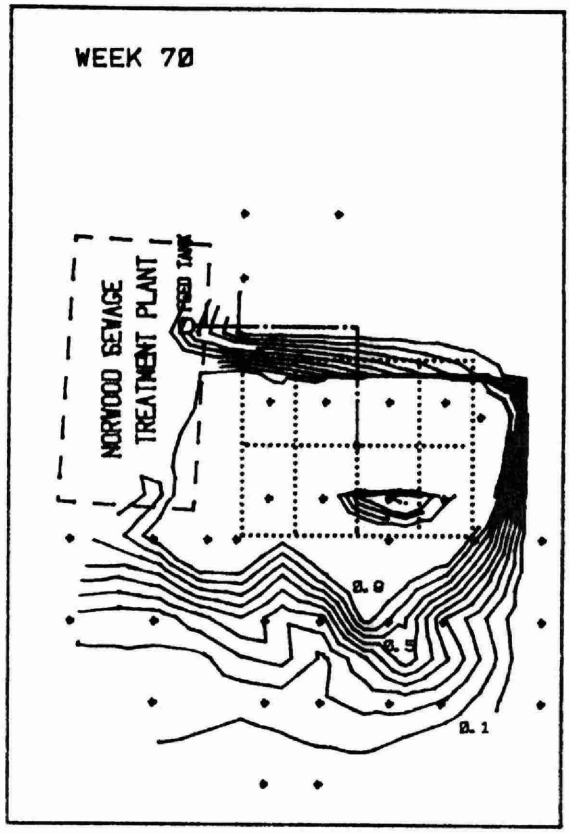

FIGURE 63b

HARDNESS CONCENTRATION CONTOURS

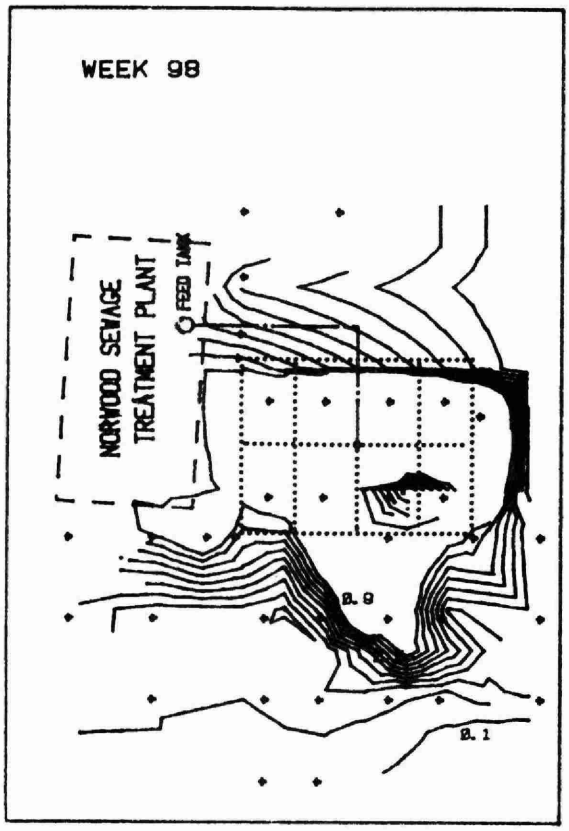

FIGURE 63c

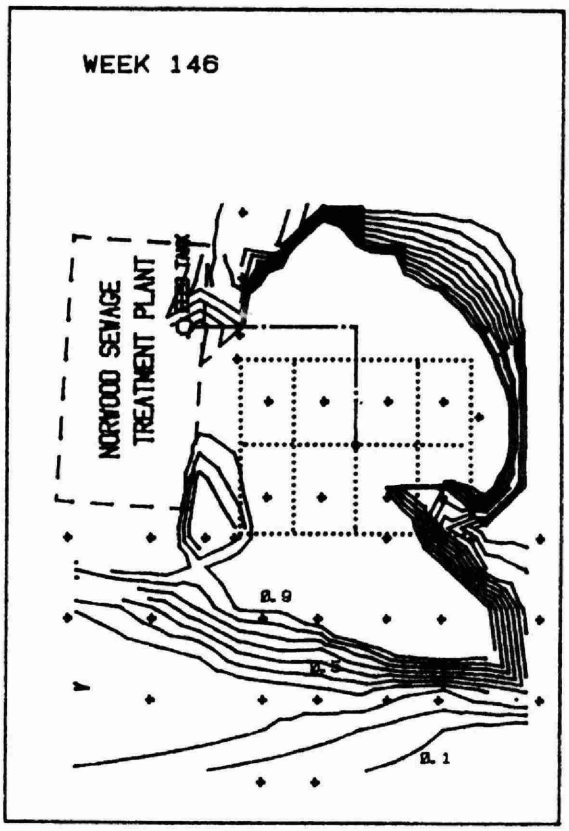

FIGURE 63d

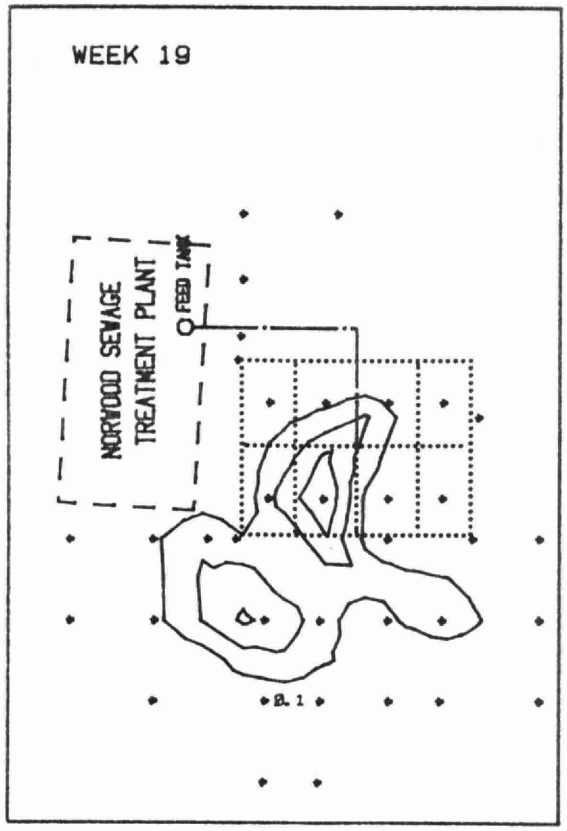

FIGURE 64a

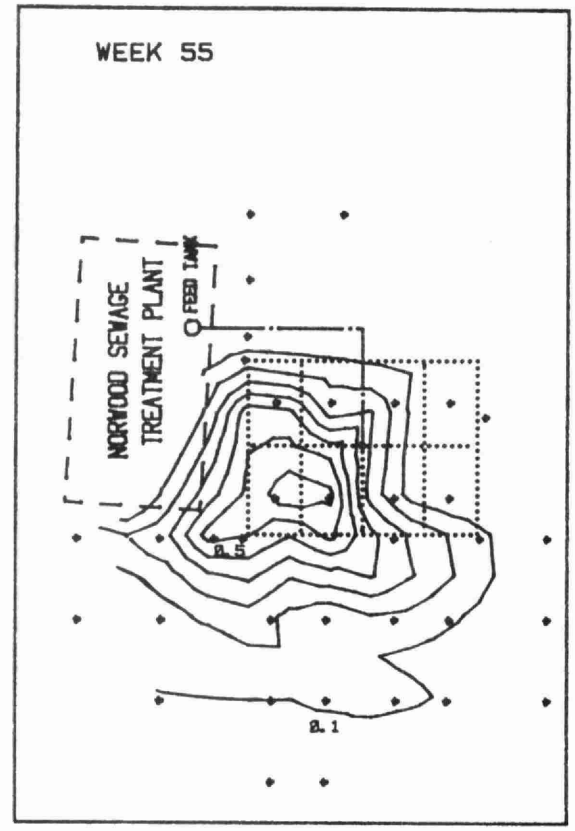

FIGURE 64b

CONDUCTIVITY CONCENTRATION CONTOURS

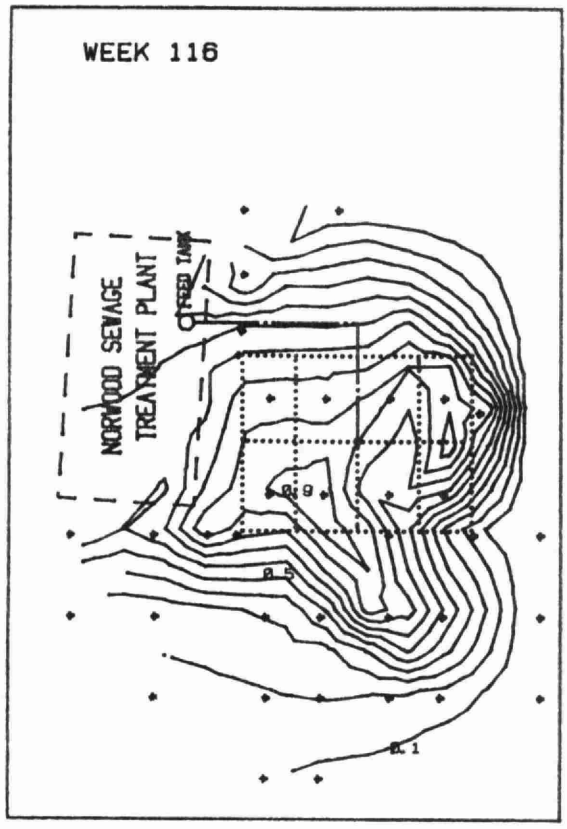

FIGURE 64c

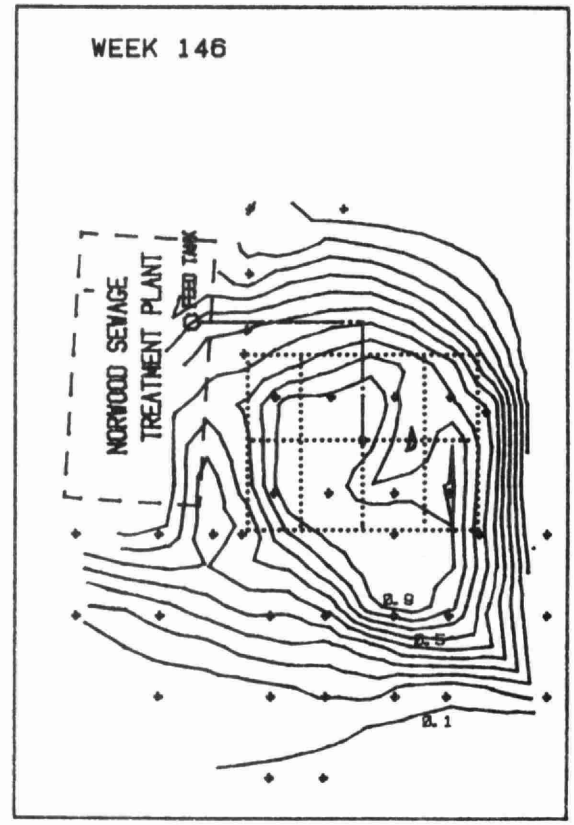

FIGURE 64d

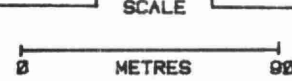

4.3 Discussion on Groundwater Contamination

The groundwater contamination in the study area, due to subsurface disposal of sewage effluent from a large size leaching bed, may be considered from two main points: magnitude and extent.

1. Magnitude of the Problem

Comparing the concentrations of the selected contaminants before and after subsurface disposal, it could be seen that the maximum increase in the level of the selected contaminants concentration in the groundwater was approximately within one metre below the water table, under and in the vicinity of the leaching bed. It may be assumed that with time, the concentrations in the vicinity of the bed would eventually become equal to the concentrations of the chemicals in the feed. Hence, the groundwater in this area is not safe for human consumption due to the high level of the contaminants concentration.

2. Extent of the Problem

Considering the movement of the selected contaminants at the concentration $C/C_o = 0.1$, the maximum distance travelled and the area of spread of the contaminants by week 146, were as shown in the Table 19.

The velocities of the selected contaminants, over the period of the study, ranged from 0.4 - 0.2 m/d, due to the many factors that affected the movement of contaminants in the groundwater, such as, the fluctuations in the level of groundwater due to mounding as a result of hydraulic loading, precipitation and evapotranspiration losses, soil characteristics, presence of rock or clay lenses, attenutation reactions, etc.

In accordance with Darcy's law, the velocity of the contaminants increased with the rise in the groundwater level due to mounding. With an increase in distance from the peak of the mound, the velocities tended to decrease with time.

TABLE 19

SPREAD OF THE SELECTED CONTAMINANTS AT THE CONCENTRATION $C/C_o = 0.1$

Contaminants/ Parameters	Breakthrough Field Velocity* (m/d)	Maximum Distance Travelled from the Centre of the Bed (m)	Area of Spread in Hectares
Nitrate	0.139	82	2.1
Chloride	0.140	85	2.3
Sodium	0.086	73	1.7
Calcium	0.144	98	3.0
Sulphate	0.090	96	2.9
Hardness	0.134	104	3.4
Conductivity	0.143	98	3.0

*Average Value

The average Breakthrough Field velocities of the contaminants are indicated in Table 19. For the period of 134 weeks (938 days), after subtracting the initial 12 week time lapse before the actual sub-surface disposal of sewage effluent began, the maximum radius of the contaminants spread from the centre of the leaching bed at the concentration level $C/C_o = 0.1$ was calculated to be 104 m. The maximum area of the contaminants spread at the concentration $C/C_o = 0.1$ was 33,975 m^2 or 3.4 ha as indicated in Table 19.

Besides the hydraulic loading and hydrogeological factors (9), the concentration of the contaminants reaching the groundwater is a function of the quality and quantity of the effluent discharge (1, 22, 34). If the quality of the effluent disposed deteriorates or the quantity of the effluent increases in relation to groundwater, the contamination would spread over a larger area.

Installation of large subsurface sewage disposal systems, hence, should only be allowed in aquifers of such soil and hydrogeologic conditions that will provide sufficient attenuation and/or dilution to the contaminants, for protection to public health, especially from nitrate contamination (2, 20, 26).

SUMMARY

5.0 SUMMARY

An extensive field investigation was conducted to determine the environmental impact of a large subsurface sewage disposal system on groundwater mounding and contamination.

The data concerning the fluctuation of the water table beneath a large leaching bed were obtained for a period of approximately 2½ years from August 1976 to April 1979. The mounding of the water table was influenced by the soil conditions, the hydraulic loading rate, natural environmental factors, such as, precipitation, evapotranspiration, and the quantity of infiltration attributed to the spring thaw.

At the high loading rate of 122,700 L/d, the groundwater mound reached 1.99 m in 35 days. For the hydraulic loading rate of 40,900 L/day, the height of the mound was 1.54 m averaged over 26 weeks during the summer and fall seasons in 1978. At the spring thaw period in 1978, the maximum rise of the mound as a result of both the hydraulic loading and the spring thaw infiltration was 2.75 m.

Two mathematical models, (Hantush's and Sykes'), were used to make predictions of the groundwater mound. Reasonable comparison of experimental data and theoretical results were obtained for the following values of input parameters:

$k \simeq 5 \times 10^{-4}$ cm/s, $f = 0.2$ and $H = 12$ m.

From the mathematical modelling exercise, some design guidelines were suggested for the prediction of the groundwater mounding beneath a leaching bed.

In order to study the groundwater contamination due to subsurface sewage effluent disposal from a large leaching bed, seven chemical parameters, namely: nitrate, chloride, sodium, calcium, sulphate, hardness and conductivity were selected.

The concentration of contaminants under and in the vicinity of the leaching bed increased significantly after effluent disposal.

The highest contaminant concentration with respect to depth was found within one metre below the groundwater table. A decrease in concentration levels with depth was indicated.

Contaminants concentration tended to decrease with an increase in distance away from the leaching bed. The maximum distance travelled at week 146, at the concentration $C/C_o = 0.1$ was 85 m for chlorides, 82 m for nitrates, 96 m for sulphates, 73 m for sodium, 98 m for calcium, 104 m for hardness and 98 m for conductivity. The distance and time curves of the contaminants became asymptotic after reaching the above distances.

The velocity of the contaminants at the concentration $C/C_o = 0.1$ varied from 0.14 m/d for chloride and nitrate, 0.09 m/d for sulphate and sodium, 0.14 m/d for calcium and conductivity, and 0.13 m/d for hardness.

A modified version of the Langmuir Equation was used to determine the adsorption capacity of the soil. The adsorption capacity of the soil in µg/g, for the case $V_w = V_{cl}$, was 0 for chlorides, 0.03 for nitrates, 3.21 for hardness, 8.15 for sulphates and 10.75 for sodium. The adsorption capacity of the soil in µg/g, for the case $V_w = V_{con}$, was 0.49 for chlorides, 0.14 for nitrates, 4.81 for hardness, 8.64 for sulphates and 11.34 for sodium.

In general, the contaminants seemed to spread in all directions in the beginning and more distribution was indicated toward the river in the later stages.

CONCLUSIONS

6.0 CONCLUSIONS

A. Conclusions related to the groundwater mounding portion of the study are as follows:-

1. Many factors affected the fluctuations of the water table beneath a large leaching bed including precipitation, evapotranspiration, and the hydraulic loading rate. The relative significance of these factors on the movement of the water table depends on the site and on the seasons. In the case of Norwood, the influence of the infiltration at the spring thaw period in 1978 was more significant than the effect of the hydraulic loading (40,900 L/d).

2. Two mathematical models (Hantush's and Sykes'), were used to predict the extent of the groundwater mounding. For identical values of input parameters similar results were given by the two models. Because of the relative simplicity in the use of the Hantush method, it is more suitable as a routine design tool. However, the flexibility of Sykes' finite-element model should not be overlooked, and the numerical method may be used for more complicated site conditions if the soil characteristics can be measured with greater accuracy.

3. In using Hantush's solution, it is recommended that the 'falling head' and the 'recovery' tests be used to measure the 'k' (permeability) values of sandy silt soils. In addition to the measurements of 'k' and specific yield (s), at individual locations, a detailed study of the soil stratigraphy at the proposed site should be carried out so that a proper interpretation of the soil test data can be made.

4. The Hantush method can be used to predict the mounding due to a constant hydraulic loading and it cannot be used to predict the mounding caused by the spring thaw infiltration. From this study, it is concluded that an estimate of the rise in water table due to the infiltration of surface water can be made on a statistical basis

according to the weather data and a minimum of one year's observational data on the natural fluctuations of the water table. The magnitude of the maximum water table rise should be equal to the sum of the rise caused by the hydraulic loading and due to surface infiltration.

B. Conclusions related to the groundwater contamination section of the study are as follows:-

1. Comparing the concentration of chemicals in the groundwater before and after subsurface disposal, the groundwater under and in the vicinity of leaching bed approached the chemical concentrations of the feed.

2. The maximum concentration of the contaminants with respect to depth was within one metre below the water table. The concentrations tend to decrease with an increase in depth.

3. Groundwater mounding increased the contaminant velocity due to increased hydraulic gradient.

4. The maximum distance travelled by the contaminants at the concentration C/C_o = 0.1 observed for 134 weeks was 104 m from the centre of the leaching bed; the maximum area of the contaminants spread was approximately 3.4 ha.

5. The time and distance curves plotted for the selected contaminants at the concentration level C/C_o = 0.1 became asymptotic after reaching the maximum distances as indicated in week 146.

6. The magnitude and extent of the groundwater contamination depended on several factors such as the hydraulic loading rate, quantity and quality of sewage disposed, climatic and hydrogeological factors, subsoil conditions and size of the aquifer.

RECOMMENDATIONS

7.0 RECOMMENDATIONS

Based on the above conclusions, it is recommended that:

1. Large subsurface sewage disposal systems should only be installed in aquifers of such soil and hydrogeologic conditions that will provide sufficient attenuation and/or dilution to the groundwater contaminants to keep their concentration levels within safe federal and provincial limits.

2. These systems should be designed with due regard to the hydrogeological factors of the site (as mentioned in this report) so that hydraulic failure due to groundwater mounding does not occur.

REFERENCES

REFERENCES

1. Ali, M. M., "Effect of Pretreatment on Groundwater Contamination from Leaching Beds", Research Publication No. 83, Pollution Control Branch, Ministry of the Environment, July 1980.

2. Ali, M. M., "Unlined Sewage Storage Ponds as Sources of Groundwater Contamination", Masters Thesis, Texas Technological University, Lubbock, Texas, U.S.A., December 1970.

3. Ballentine, R. K., Raznek, S. R., and Hall, C. W., "Subsurface Pollution Problems in the United States", U.S.E.P.A., Report No. TS-00-72-02, 1972.

4. Banerzi, S. K., "Effect of Biological Slime on the Retention of ABS on Granular Media", San. Engnr. Series, No. 10, University of Illinois, 1963.

5. Bauman, P., "Groundwater Movement Controlled Through Spreading", Transactions A.S.C.E., Vol. 117, 1952.

6. Bouwer, H., "Groundwater Hydrology", published by McGraw-Hill Book Co., Chapter 8, 1978.

7. Brandes, M., "Effect of Precipitation and Evapotranspiration on the Filtering Efficiency of a Wastewater Disposal System", published by Journal Water Pollution Control Federation, Washington D.C., U.S.A., pp. 59, Vol. 52, January 1980.

8. Brown, D. M., McKay, G. A., Chapman, L. J., "The Climate of Southern Ontario", Climatological Study No. 5, Canada Department of Transport, Meteorological Branch, 1968.

9. Brown, R. H., "Hydrologic Factors Pertinent to Groundwater Contamination", Technical Report W61-5, Robert A. Taft Engnr. Centre, Proceedings of Groundwater Contamination Symposium, 1961.

10. Butler, R. G., Orlob, G. T., and McGauhey, D. H., "Underground Movement of Bacterial and Chemical Pollutants", Journal of A.W.W.A., Vol. 46, No. 2, February 1954.

11. Chan, H. T., and Kenney, T. C., "Laboratory Investigation of Permeability Ratio of New Liskeard Varved Soil", Canadian Geotechnique Journal, Vol. 10, pp. 453-472, 1973.

12. Deutsh, M., "Groundwater Contamination and Legal Controls in Michigan", U. S. Dept. of the Interior, Geological Survey, Water Supply Paper 1961, (1963).

13. Environment Canada, "Meteorological Observations in Eastern Canada", Monthly Record, Vol. 62, 63, 64, Nos. 1-12, 1976-1979.

14. Ewing, B. B., et al, "Synthetic Detergent in Soil and Groundwaters", San. Engnr. Series No. 8, University of Illinois, 1961.

15. Glover, R. E., "Groundwater Movement", U. S. Bur. Reclamation Engnr. Monog., pp. 31 and 67.

16. "Handbook of Analytical Methods for Environmental Samples", Vol. 1 and 2, Laboratory Services Branch, Ontario Ministry of the Environment, November 1975.

17. Hantush, M. S., "Growth and Decay of Groundwater Mounds in Response to Uniform Percolation", Water Resources Research, Vol. 3, No. 1, 1967.

18. Hunt, B. W., "Vertical Recharge of Unconfined Aquifer", Journal of the Hydraulic Division A.S.C.E., Vol. 97, No. HY 7, July 1971.

19. Hvorslev, M. T., "Time Lag and Soil Permeability in Groundwater Observations", Bull. No. 36. Waterways Experiment Station, U. S. Army Corps of Engineerings, Vicksburg, Mississippi, U.S.A., 1951.

20. Kaufman, W. J., "Chemical Pollution of Groundwaters", Journal A.W.W.A., March 1979.

21. Kwitz, L. T., and Melsted, S. W., "Movement of Chemicals in Soils by Water", Agronomy Department, University of Illinois, Urbana, Illinois, 1972.

22. Laak, R., "The Effect of Aerobic and Anaerobic Household Sewage Pretreatment on Seepage Beds", Ph.D. Thesis, University of Toronto, 1960.

23. Lambe, T. William, "Soil Testing for Engineers", John Wiley & Sons, Inc., 1960.

24. Marino, M. A., "Artificial Groundwater Recharge, I. Circular Recharging Area", Journal of Hydrology, Vol. 25, 1975.

25. Marino, M. A., "Artificial Groundwater Recharge, II. Rectangular Recharging Area", Journal of Hydrology, Vol. 26, 1975.

26. Miller, D. W., Deluca, F. A., and Tessier, T. H., "Groundwater Contamination in the Northeast States", E.P.A. - 600/2 - 74-056, June 1974.

27. Pitt, W. A., Jr., Mattraw, H. C., and Klien, H., "Groundwater Quality in Selected Areas Serviced by Septic Tanks", Dade County, Florida, U. S. Geol. Survey Open File Report, 1975.

28. Polowski, L. B., and Boyle, W. C., "Groundwater Quality Adjacent to Septic Tank-Soil Absorption System", Department of Natural Resources, State of Wisconsin, 1970.

29. Rao, N. H., and Sarma, P.B.S., "Growth of Groundwater Mound in Response to Recharge Groundwater", Vol. 18, No. 6, November to December 1980.

30. Schmid, W. E., "Field Determination of Permeability by the Infiltration Test", A.S.T.M., S.T.P. 417, pp. 142-159, 1966.

31. Singh, R., "Prediction of Mound Geometry Under Recharge Basins", Water Resources Research, Vol. 12, No. 4, August 1976.

32. Solomon, S. S., "Relationship Between Precipitation, Evaporation and Runoff in Tropical Equatorical Regions", Water Resources Research, Vol. 3, No. 1, 1967.

33. "Standard Methods for Examination of Water and Wastewater", 13th Edition, American Public Health Association, Inc., 1015 Eighteen Street, N.W., Washington D.C. 20036.

34. Stockton, E. L., "Disposal of Treated Sewage Effluent", Paper presented at Waste Disposal Conference at Michigan State University, 1960.

35. Suess, M. J., "Retardation of A.B.S. in Different Aquifers", Journal of A.W.W.A., 1964.

36. Sykes, J. F., "Transport Phenomena in Variably Saturated Porous Media", Ph.D. Thesis, Civil Engnr., University of Waterloo, Waterloo, Ontario, 1975.

37. Wilkinson, W. B., "Constant Lead in situ Permeability Tests in Clay Strata", Geotechnique, Vol. 18, No. 2, pp. 172-194, June 1968.

38. Zarnett, G. D., "Sorption Capabilities of Soils for Phosphorus Removal", Publication No. S58, Pollution Control Branch, Ontario Ministry of the Environment, 1976.

APPENDIX

FINITE ELEMENT MODEL FOR

GROUNDWATER MOUNDING

Prepared by:

Professor J. F. Sykes
Department of Civil Engineering
University of Waterloo
Waterloo, Ontario

1. INTRODUCTION

To model the secondary effluent discharge from a leaching bed located in the unsaturated zone and the groundwater mounding that results, the governing flow equation for a three dimensional spatial domain is:

$$(C + \frac{\theta}{n} S_s) \frac{\partial \Psi}{\partial t} = \frac{\partial}{\partial x_i} [k_{ij}(\theta) \frac{\partial \psi}{\partial x_j} + k_{i3}(\theta)] \quad i, j = 1, 3 \qquad (1)$$

where C is the specific moisture capacity, a function of the moisture content θ and the pressure head ψ; n is the porosity; S_s is the specific storage; and $k_{ij}(\theta)$ is the hydraulic conductivity tensor given here as a function of the moisture content. For the saturated zone, $k_{ij}(\theta)$ yields the saturated hydraulic conductivities. Equation (1) is nonlinear, in that the parameters C and $k_{ij}(\theta)$ are functions of the solution set. The specific storage coefficient S_s accounts for the compressibility of both the pore fluid and the formation itself with vertical consolidation being assumed for the latter.

The use of equation (1) to model the flow system results in the discharge from the leaching bed being modelled via either the boundary conditions associated with the equation or point source terms. Infiltration and evapotranspiration at the air-soil interface is also included in the model through boundary conditions.

To solve equation (1) and the associated initial conditions and boundary conditions, numerical solution techniques are required with the finite difference method and the finite element methods being commonly used. (Freeze, 1971; Dillon et. al., 1978; Segol, 1976). For three dimensional analyses, such models are both difficult and expensive to use. In addition, it is often the case that parameter uncertainty and a lack of complete spatial definition results in the

fact that three dimensional phenomena can often be modelled in two dimensions with little or no loss of information. For systems in which vertical effects do not predominate, areal models can be developed for the saturated zone by suitably integrating equation (1) over the vertical domain yielding an equation of the form:

$$S \frac{\partial h}{\partial t} = \frac{\partial}{\partial x_i} \left(T_{ij} \frac{\partial h}{\partial x_j}\right) + Q(x_i) \quad i, j = 1, 2 \tag{2}$$

where $T_{ij} = K_{ij} * b$ is the transmissivity tensor; K_{ij} is the saturated hydraulic conductivity tensor averaged over the aquifer thickness b; h is the head; S is the storativity and $Q(x_i)$ is a source term. The boundary conditions associated with the equation are:

$$h(x_i) = \hat{h}(x_i) \qquad \text{on} \quad \Gamma_1 \tag{3a}$$

and

$$q(x_i) = \hat{q}(x_i) \qquad \text{on} \quad \Gamma_2 \tag{3b}$$

where $h(x_i)$ is a prescribed head on boundary Γ_1 and $\hat{q}(x_i)$ is a prescribed flux on boundary Γ_2 where $\Gamma_1 + \Gamma_2 = \Gamma$ is the external boundary to the modelled domain. In the use of equation (2), the source/sink term $Q(x_i)$ can vary spatially and can represent infiltration, evapotranspiration or recharge loading from a leaching bed. For mounding of phreatic aquifers, the aquifer thickness as modelled by b is a measure of the height between the water table and the underlying confining bed. As such, it is a function of the solution set $h(x_i, t)$.

Equation (2) and its governing boundary and initial conditions can be solved both exactly and numerically. For the former, simplifying assumptions are commonly made and, in fact, are often necessary. Generally, the transmissivity is assumed to be constant. In addition, solutions are often available for regular spatial domains only.

2. SYKES FINITE ELEMENT MODEL

As is the case with the three-dimensional equation (1), the numerical solution of equation (2) is generally based on either the finite difference or the finite element methods. The literature abounds with such models and in this study, a finite element model developed by Sykes (1975) is used. The model is highly flexible and can investigate contaminant transport as well as flow in either two-dimensional variably saturated cross-sections. A wide range of boundary conditions is available in the model.

To solve equation (2), the Galerkin method of weighted residuals is used to replace the given differential equation by a set of integral equations which are solved numerically. In this sub-section, the Galerkin equation for fluid flow in two-dimensional areal spatial domains is developed. Details of the finite element method used to solve the equation are also presented.

Galerkin Flow Equation

In the Galerkin procedure, the general approach is to assume a trial solution whose functional dependence on position is chosen, but which includes undetermined functions of time. For equation (2), the trial solution assumed has the form:

$$h \doteq h^e = \langle n \rangle \{h\} \qquad (4)$$

where $\langle n \rangle$ is a set of prescribed non-dimensional spatial interpolation functions satisfying the boundary condition associated with equation (2) and h^e is the set of undetermined time dependent heads defined at the nodel points at a discretized continuum defining the solution domain. The sets $\langle n \rangle$ and $\{h\}$ must have the same number of ordered members.

Differentiation of equation (4) with respect to the spatial co-ordinates yields the pressure head gradients.

$$\frac{\partial h^e}{\partial x_i} = <\frac{\partial n}{\partial x_i}> \{h\} \tag{5}$$

in which $<\frac{\partial n}{\partial x_i}>$ is the transform vector giving the gradients in terms of the set of nodal point variables.

To develop the Galerkin equation, the flow equation (2) is expressed in terms of the partial differential operation L(h) giving

$$S \frac{\partial h}{\partial t} = \frac{\partial}{\partial x_i} (T_{ij} \frac{\partial h}{\partial x_j}) + Q(x_i) = L(h) \tag{6}$$

where i, j = 1, 2. In this equation, S and Q remain constant within an element of the subdivided continuum while T_{ij} is expressed as a functional coefficient utilizing the same set of non-dimensional interpolation functions as that used in equation (4).

To determine a solution set at the nodal points at time $t + \Delta t$ given the solution set at the nodal points of the discretized system at time t, a finite difference approximation for the time derivative is introduced. Thus, equation (6) is written as:

$$\frac{h^{t+\Delta t} - h^t}{\Delta t} = \alpha L(h)^{t+\Delta t} + (1 - \alpha) L(h)^t \tag{7}$$

where the recurrence parameter α is such that $0 \leq \alpha \leq 1$.

The use of the trial solution (4) in equation (6) results in a residual

$$R(h^e) \equiv L(h^e) - \frac{S \partial h^e}{\partial t} \tag{8}$$

As the number of members in the set {h} increases, the residual will become smaller, with the exact solution being obtained when the residual is identically zero. As an approximation to this ideal the integrals of the weighted residuals are set equal to zero giving:

$$\int_A \{n\}\, R(\langle n\rangle \{h\})\ dA = 0 \tag{9}$$

where following the Galerkin procedure the weights are selected as the interpolation function {n}.

In the manner of equation (9), the Galerkin flow equation can thus be developed as:

$$\frac{1}{\Delta t}\left[[A] + \alpha[B]\right]\{h\}^{t+\Delta t} = \left[\frac{1}{\Delta t}[A] + (1-\alpha)[B]\right]\{h\}^{t} + \{c\} + \{D\} \tag{10}$$

where

$$[A] = \sum_{e=1}^{m} \int \{n\}\, S\langle n\rangle\, dA \tag{11a}$$

$$[B] = \sum_{e=1}^{m} \int \{\frac{\partial n}{\partial x}\}\langle n\rangle \{T_{xx}\}\langle \partial n/\partial x\rangle + \{\frac{\partial n}{\partial y}\}\langle n\rangle \{T_{yy}\}\langle \partial n/\partial y\rangle\, dA \tag{11b}$$

$$\{c\} = \sum_{e=1}^{m} \int \{n\}\, Q(x_i)\, dA \tag{11c}$$

$$\{d\} = \sum_{e=1}^{m} \oint_{\Gamma_2} \{n\}\, T_{xx} \langle\frac{\partial n}{\partial x}\rangle\, dy - \{n\}\, T_{yy}\, \frac{\partial n}{\partial y}\, dx \tag{11d}$$

The vector {D} of equation (10) results from the application of Green's theorem in a plane to the second order term of equation (6), thus reducing it to a first order term and a surface integral. In so doing, the Neumann boundary condition of (3b) is incorporated in the

Galerkin equation. The nonlinear transmissivities, a function of the aquifer thickness b, are evaluated at time $t + \Delta t/2$ and are assumed to remain constant over a time step.

Finite Element Algorithm

To discretize the spatial domain and to develop the non-dimensional interpolation function introduced in equation (4), this study uses a mixed isoparametric quadrilateral element. The element contains between 4 and 12 degrees of freedom with the sides being either linear, quadratic or cubic. The integration of equation (11) is accomplished using a Gausslegendre Quadrature. With such a procedure, the functional coefficients (in this study Ti_j) are evaluated at the Gauss points. Two, three or four Gauss points are used in a given direction depending on whether the higher order polynomial of the two sides in that direction is linear, quadratic or cubic respectively.

In the Galerkin flow equation, the matrix $\{B\}$ is a function of the dependent variable h. To obtain an initial estimate of the head at time $t + \Delta t$, thus allowing the evaluation of $\{B\}$, a linear interpolation scheme is used such that for the nodal variable h

$$h^{t+\Delta t} = h^t + (h^t - h^{t-\Delta t_1}) \frac{\Delta t}{\Delta t_1} \tag{12}$$

The Newton Raphson technique (Sykes, 1975) is used to improve these estimates of head. In this method, for a nonlinear finite element equation of the form:

$$[A(h)]\{h\} - F = 0 \tag{13a}$$

Improvements to the estimate of $h^{t + \Delta t}$ are obtained from:

$$\{h_{new}\} = \{h_{old}\} + [A(h_{old})]^{-1} (-R) \qquad (13b)$$

where $$R = [A(h_{old})]\{h_{old}\} - F \qquad (13c)$$

Rapid convergence is achieved by incorporating an Aitken accelerator with the Newton-Raphson technique (Sykes, 1975).

To evaluate the matrix form $[A(h_{old})]^{-1} (-R)$ of the Newton-Raphson technique, an upper banded Gaussian elimination solver is used.

The finite element algorithm is programmed in fortran and run on an IBM 370.145 machine.

Information Required for Analysis

- mesh (nodes and elements)
- porosity
- elevation of confining layer
- permeability (hydraulic conductivity)
- hydraulic loading
- boundary conditions